INFORMATION TO USERS

This manuscript has been reproduced from the microfilm master. UMI films the text directly from the original or copy submitted. Thus, some thesis and dissertation copies are in typewriter face, while others may be from any type of computer printer.

The quality of this reproduction is dependent upon the quality of the copy submitted. Broken or indistinct print, colored or poor quality illustrations and photographs, print bleedthrough, substandard margins, and improper alignment can adversely affect reproduction.

In the unlikely event that the author did not send UMI a complete manuscript and there are missing pages, these will be noted. Also, if unauthorized copyright material had to be removed, a note will indicate the deletion.

Oversize materials (e.g., maps, drawings, charts) are reproduced by sectioning the original, beginning at the upper left-hand corner and continuing from left to right in equal sections with small overlaps.

Photographs included in the original manuscript have been reproduced xerographically in this copy. Higher quality 6" x 9" black and white photographic prints are availabie for any photographs or illustrations appearing in this copy for an additional charge. Contact UMI directly to order.

Bell & Howell Information and Learning
300 North Zeeb Road, Ann Arbor, MI 48106-1346 USA

UMI®
800-521-0600

Downloaded from SHAREOK. Persistent Handle URL: https://hdl.handle.net/11244/5897

UNIVERSITY OF OKLAHOMA

GRADUATE COLLEGE

IMPACTS OF HETEROGENEOUS SEDIMENTARY ORGANIC MATTER ON PHENANTHRENE SORPTION AND FATE PROCESSES

A Dissertation

SUBMITTED TO THE GRADUATE FACULTY

In partial fulfillment of the requirements for the

Degree of

Doctor of Philosophy

By

HRISSI KASSIANI KARAPANAGIOTI
Norman. Oklahoma
1999

UMI Number: 9952414



UMI Microform9952414

Copyright 2000 by Bell & Howell Information and Learning Company.
All rights reserved. This microform edition is protected against
unauthorized copying under Title 17, United States Code.

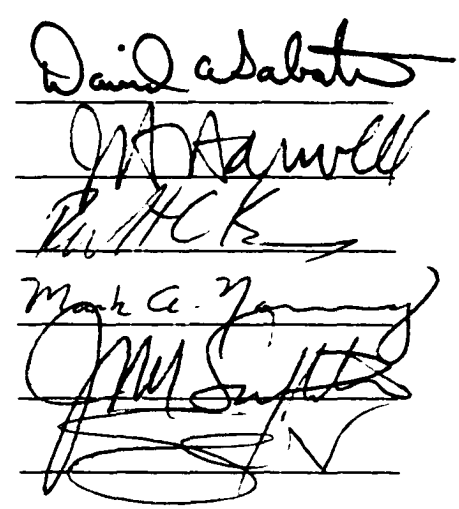
Bell & Howell Information and Learning Company
300 North Zeeb Road
P.O. Box 1346
Ann Arbor, MI 48106-1346

©Copyright by HRISSI KASSIANI KARAPANAGIOTI 1999
All Rights Reserved

IMPACTS OF HETEROGENEOUS SEDIMENTARY ORGANIC MATTER
ON PHENANTHRENE SORPTION AND FATE PROCESSES

A Dissertation APPROVED FOR THE
DEPARTMENT OF CIVIL ENGINEERING AND ENVIRONMENTAL SCIENCE

BY



DEDICATION

This dissertation is dedicated to my husband Manolis and our child yet to join us.
Also, to my parents, Andreas and Ntina and my brother Dimitrios.

ACKNOWLEDGEMENTS

There are not enough words to thank Dr. Sabatini for his valuable advice and support while I was a doctorate student. He is a real teacher and mentor. I have learned the most important things from him regarding both research and life. I wish every student could have a teacher like him once in his or her life. I would like to express my gratitude to my committee members: Dr. Strevett for always finding time through his busy schedule to answer my questions and his valuable input throughout my work. Dr. Suflita and Dr. Nanny for their valuable comments during my general exams. Dr. Knox and Dr. Harwell for agreeing to serve on my committee and for their support thoughout my course of study. I would like to thank Dr. Kolar for his valuable advice in modeling and Dr. Grathwohl from the University of Tübingen for his valuable input during my research. I would also like to thank Dr. Laguros for always being there for me. He gave me strength all these years with his discrete and powerful presence on Carson 3rd floor and I have learned a lot from him.

I wish to express special thanks to Bin Wu, Joe Grego, Ben Shiau, Joe Rouse, Chetan Goudar, Chris Gossard, Carrie Evenson, Tuan Van Doan for their advice and assistance. I must also mention my fellow graduate students: Delta Cseak, Micah Goodspeed, Torez Kasnavia, Jeff Childs, Cheng Hefa, Edgar Acosta, Gavin James. I would like to thank the CEES staff for their assistance.

I would also like to thank the students and staff from Dr. Grathwohl's hydrogeology lab in Tübingen, Germany and especially Sybille Kleineidam, Christoph Schüth, Hermann Rügner, and Bertrand Ligouis for their input on my research. I would also like to thank Brian Cardott from OKGS for his guidance.

TABLE OF CONTENTS

		Page
DEDICATION		iv
ACKOWLEDGEMENT		v
TABLE OF CONTENTS		vi
LIST OF TABLES		ix
LIST OF ILLUSTRATIONS		x
PREFACE		xii
CHAPTER 1	Phenanthrene Sorption with Heterogeneous Organic Matter in a Landfill Aquifer Material	1
	Abstract	1
	Introduction	2
	Materials and Methods	4
	Data Modeling	6
	Results and Discussion	9
	Soil Analysis	9
	Equilibrium Sorption Isotherms	11
	Sorption Kinetics	14
	Summary	22
	Acknowledgement	22
	References	23
CHAPTER 2	Impacts of Heterogeneous Organic Matter on Phenanthrene Sorption: Equilibrium and Kinetic Studies with Aquifer Material	26
	Abstract	26
	Introduction	27
	Materials and Methods	29
	Data Modeling	34
	Results and Discussion	36
	Soil Analysis	36
	Equilibrium Sorption Isotherms	41
	Sorption Kinetics	47
	Acknowledgement	57
	Nomenclature	57
	References	59
CHAPTER 3	Impacts of Heterogeneous Organic Matter on Phenanthrene Sorption: Different Aquifer Depths	62
	Abstract	62
	Introduction	63
	Materials and Methods	66
	Organic Petrology Methods	68

Data Modeling..... 71
Results and Discussion..... 75
Site Description / Fluvial History and Aquifer Profile..... 75
Sediment Analysis..... 79
Equilibrium Sorption Isotherms..... 80
Koc predictions..... 87
Kd predictions..... 90
Sorption Kinetics..... 91
Contaminant Transport and Fate..... 96
Acknowledgement..... 98
Nomenclature..... 98
References..... 100

CHAPTER 4 Model Coupling Intraparticle Diffusion/Sorption, Nonlinear Sorption and Biodegradation Processes..... 103
Abstract..... 103
4.1 Introduction..... 104
4.2 Methods..... 106
4.2.1 Experimental..... 106
4.2.2 Modeling..... 111
4.3 Results and Discussion..... 114
4.3.1 Sorption Kinetic Behavior..... 114
4.3.2 Phenanthrene Biodegradation..... 116
4.3.3 Model Validation..... 119
4.3.4 Sensitivity Analysis..... 125
4.3.5 Linear versus Nonlinear..... 129
4.4 Conclusions..... 133
Acknowledgement..... 133
References..... 134

APPENDICES..... 137

A: Preliminary Batch and Column Studies – Chapters 1 and 2... 138

B: Supplement to Chapter 1 – Tables 1.2 and 1.3: Naphthalene Equilibrium and Kinetic Sorption Properties..... 139

C: Supplement to Chapter 1 – Figure 1.4: Hot Methanol Extraction 140

D: Supplement to Chapter 1 – Tables 1.3 and 1.4: Model Error.. 141

E: Supplement to Chapter 2 – Table 2.2: Elemental Analysis..... 142

F: Supplement to Chapter 3 – Tables 3.1 and 3.4: Weight distribution, elemental analysis, and organic carbon in grain size fractions..... 143

G: Collaborative Information provided by Dr. Lyon as a supplement to Chapter 3 – An attempt to further characterize the organic matter properties presented in Table 3.2 and 3.3..... 144

H: Preliminary coupled sorption and biodegradation studies – Chapter 4..... 149

I: Collaborative Information provided by Chris Gossard as a supplement to Chapter 4 – Section 4.2.2..... 151

J: Collaborative Information provided by Dr. Strevett as a supplement to Chapter 4 – Section 4.3.2..... 154

K: Supplement to Chapter 4 – Calculations proposed by Chung et al. (1993) discussed in section 4.3.4..... 156

L: Independent research contacted on surfactant modified sorbents..... 157

LIST OF TABLES

		Page
Table 1.1:	Soil Analysis	10
Table 1.2:	Isotherm Results	13
Table 1.3:	Kinetic Sorption Properties based on Numerical Solution	16
Table 1.4:	Percent of Fast Sorption Sites and Time to Reach Equilibrium	19
Table 2.1:	Soil Subsamples and Organic Matter Characteristics	31
Table 2.2:	Soil Analysis	40
Table 2.3:	Isotherm Results	43
Table 2.4:	Kinetic Sorption Properties based on Numerical Solution	49
Table 2.5:	Qualitative Comparison of Organic Matter Sorption Characteristics	55
Table 3.1:	Aquifer Profile – Core Samples Taken South of Well 80	77
Table 3.2:	Isotherm Results	82
Table 3.3:	Organic Petrology of the Four Different Depth Samples	84
Table 3.4:	Sample Properties Important for Their Kinetic Sorption Behavior	92
Table 3.5:	Kinetic Sorption Properties	95
Table 4.1:	Important Sediment Sample and Sorption Properties	107
Table 4.2:	Experimental Variables for the Different Systems	110
Table 4.3:	NMO/S: Parameters of Sorption Kinetic Experiment	112
Table 4.4:	Lag time and first order biodegradation rate constant	118
Table 4.5:	Sensitivity Analysis	126
Table 4.6:	Sensitivity Analysis: Linear versus Nonlinear Sorption	130

LIST OF ILLUSTRATIONS

Page

Figure 1.1: Size fraction subsample isotherms..... 12

Figure 1.2: Size fraction subsample kinetic experiments..... 15

Figure 1.3: Size fraction subsample kinetic experiments..... 18

Figure 1.4: CRA composite sample kinetic experiment..... 20

Figure 2.1: Photomicrographs illustrating the different organic matter present in the samples: (a) overview of different particulate organic matter (POM), (b) coal particle (POM_{CL}), (c) charcoal particle (POM_{CH}), (d) phytoclast particle (POM_{PH}), (e): quartz aggregates cemented with clay matrix, (f): strong yellowish fluorescing AOM within the clay matrix (M_{AOM}), (g): isolated quartz mineral, and (h): strong yellow fluorescing organic coating (C_{AOM})..... 37

Figure 2.2: Phenanthrene sorption isotherms for three subsamples..... 42

Figure 2.3: Logarithm of organic content normalized distribution coefficient (log *Koc*) versus Freundlich exponent (*N*) at chemical equilibrium concentrations (*Ce*) equal to 1 µg/L and 1 mg/L..... 45

Figure 2.4: The apparent sorption coefficient normalized by the equilibrium sorption coefficient (*Kda*/*Kd*) versus time d) for three of the subsamples as well as the numerical model results for two of the subsamples..... 48

Figure 2.5: Intraparticle diffusion model lines for one of the subsamples. Apparent sorption distribution coefficient (*Kda*) (L/kg) versus time (d)..... 51

Figure 2.6: Apparent diffusion coefficient (*Da*) (cm^2/s) versus soil organic content *foc* (%) and b) sorption distribution coefficient *Kd* (L/kg)..... 54

Figure 3.1: Palynological kerogen classification scheme for organic mater subgroups present in this study (for more details see Tyson, 1995)..... 70

Figure 3.2: Norman Landfill aquifer properties versus depth. Fraction organic carbon content [*foc* (%)], hydraulic conductivity [K (cm/s)], and classification (USDA) versus depth (ft)..... 78

Figure 3.3: Phenanthrene sorption isotherms for five samples..... 81

Figure 3.4: Logarithm of organic content normalized distribution coefficient (log *Koc*) versus Freundlich exponent (*N*) at chemical equilibrium concentrations (*Ce*) equal to 1 μg/L..... 86

Figure 3.5: The apparent sorption coefficient normalized by the equilibrium sorption coefficient (*Kda*/*Kd*) versus time (d) for all samples as well as the numerical model lines..... 94

Figure 4.1: NMO/S: Sorption kinetic data and model predictions for all three sediment samples..... 115

Figure 4.2: MO/NS: Biological activity..... 117

Figure 4.3: Experimental data of the three systems for all three sediment samples..... 120

Figure 4.4: LMO/S: Experimental data (average of triplicate) and model prediction line with one standard deviation expressed with error bars..... 122

Figure 4.5: A) Example of the model output as was fitted to a set of data in LMO/S for the sediment with the mixture of coaly particles (Slow) and organic coatings (Fast). B) MO/S: Distribution of sorbed chemical in the two grain components of the mixture. C) LMO/S: Distribution of sorbed chemical in the two grain components of the mixture..... 124

Figure 4.6: Concentration degraded with fast biodegradation (k_1= 0.1 1/hr), varied pre-equilibration times (i.e., lag periods for biodegradation) (lag time A=0, B=9.5, and C=35 days), and sorption kinetics..... 127

Figure 4.7: Linear (N = 1) versus nonlinear (N = 0.5). Prediction curves for concentration: A) in solution, B) sorbed, and C) biodegraded..... 131

PREFACE

Natural attenuation is currently one of the most important topics in groundwater management. Sorption and biodegradation are key processes impacting the efficiency of natural attenuation. Although extensive literature has been published on these topics additional research is required. Both processes are represented in ground water models using simplified relationships, which may result in predictions that are orders of magnitude different from actual results.

This dissertation consists of four chapters corresponding to four different refereed journal articles, which have or will be submitted on the above topics. Chapter 1 has appeared in Physics and Chemistry of the Earth (1999, V. 24, No 6, p. 535-541). Chapters 2 and 3 are written according to guidelines established for Environmental Science and Technology; Chapter 2 has been accepted for publication while Chapter 3 has been submitted. Chapter 4 is written for the Journal of Contaminant Hydrology. Below I summarize the focus of each chapter; detailed abstracts appear at the beginning of each chapter.

Chapter 1 presents equilibrium and kinetic sorption results for Canadian River Alluvium (CRA) aquifer material with phenanthrene. CRA was divided into four grain size subgroups and their properties were tested. Sorption properties for grain size subgroups suggested the presence of highly heterogeneous organic matter within each subgroup. This chapter demonstrates the improvement of the kinetic model fit for each subgroup by introducing a fast sorption term in a two-component model. The addition of this fast sorption term greatly improved the modeling for both early time and later time data.

Both the kinetic model and the equilibrium data suggested a highly heterogeneous organic matter in the sediment subsamples. These grain size subsamples were further divided into more homogeneous samples using a magnetic separator. Chapter 2 presents the equilibrium and kinetic properties of these subsamples. Also, Chapter 2 presents data and pictures of the most important organic matter types that affected sorption, including characterization by organic petrology methods. Heterogeneous organic matter was observed to significantly impact equilibrium and kinetic sorption, causing K_{oc} and kinetic sorption properties to vary by one to two orders of magnitude for different organic matter types.

Results in Chapter 2 lead to the obvious question of how does the organic matter vary with aquifer depth. Chapter 3 addresses this question by examining the sorption properties and the organic petrology of four samples taken from different depths of the same aquifer. A significant contribution of this chapter is the use of organic petrology as a quantitative tool for predicting equilibrium sorption properties as a function of organic matter characteristics, which helps quantify the "rubbery and glassy" components previous researchers have alluded to. Organic carbon content values varied by one order of magnitude and sorption capacities varied by two orders of magnitude within a given depth and location for these samples.

Finally, the intraparticle sorption model used in Chapters 1-3 is expanded to include biodegradation in Chapter 4. The model is initially validated with experimental results using the same sediment samples studied in Chapter 2. The validated model is then used to perform sensitivity analyses, which show that sorption nonlinearity is important when studying coupled sorption and biodegradation

processes. The sensitivity analyses also define scenarios where the sorption/ desorption kinetics strongly impact biodegradation kinetics, demonstrating that biodegradation estimates may be off by as much as 49% if nonlinear and nonequilibrium sorption are not accounted for.

In summary, the presence of heterogeneous organic matter in an alluvial sediment has been demonstrated. Each chapter presents different aspects of the impact this heterogeneity has on sorption properties, with the final chapter illustrating the potential impact on biodegradation. This knowledge advances our understanding of natural attenuation, and can help guide us in enhancing this attenuation when so desired.

Here, I would like to acknowledge my co-authors in the four journal articles corresponding to the four dissertation chapters: S. Kleineidam, B. Ligouis, D. Sabatini, and P. Grathwohl of the first two papers, D. Sabatini of the third paper, and C. Gossard, K. Strevett, R. Kolar, and D. Sabatini of the last paper. While these collaborators have helped guide and shape this research, all work presented in these chapters is my original research. The appendices do summarize several supplemental material that are directly attributable to others.

CHAPTER 1

PHENANTHRENE SORPTION WITH HETEROGENEOUS ORGANIC MATTER IN A LANDFILL AQUIFER MATERIAL

ABSTRACT

Phenanthrene was used as a model chemical to study the sorption properties of Canadian River Alluvium aquifer material. Both equilibrium and kinetic sorption processes were evaluated through batch studies. The bulk sample was divided into subsamples with varying properties such as particle size, organic content, equilibration time, etc. to determine the effect of these properties on resulting sorption parameters. The data have been interpreted and the effect of experimental variables was quantified using the Freundlich isotherm model and a numerical solution of Fick's 2nd law in porous media. Microscopic organic matter characterization proved to be a valuable tool for explaining the results. Different organic matter properties and sorption mechanisms were observed for each soil subsample. Samples containing coal particles presented high K_{oc} values. Samples with organic matter dominated by organic coatings on quartz grains presented low K_{oc} values and contained a high percentage of fast sorption sites. The numerical solution of Fick's 2nd law requires the addition of two terms (fast and slow) to properly fit the kinetics of these heterogeneous samples. These results thus demonstrate the need for soil organic matter characterization to predict and explain the sorption properties of a soil sample

containing heterogeneous organic matter and also the difficulty and complexity of modeling sorption in such samples.

INTRODUCTION

Natural attenuation is currently one of the most important topics in groundwater remediation. Sorption equilibria and kinetic properties are very important factors affecting natural attenuation in the subsurface. There is an extensive body of literature that discusses sorption processes; however, very limited information exists on the effects of naturally-occurring heterogeneous soil organic matter on sorption properties.

Karickhoff et al. (1979) published one of the early and important studies on hydrophobic organic compounds. Their research suggested instantaneous equilibrium and linear isotherms demonstrating partition-like sorption. The organic content normalized distribution coefficient (K_{oc}) was found to depend on chemical hydrophobicity as quantified via the chemical's octanol-water partition coefficient (K_{ow}) and solubility. Sorption capacity was observed to be a function of soil organic carbon content and K_{oc}. These observations are true for most aquifer materials (e.g. Estrella et al, 1993; Chiou et al., 1998; and as summarized in Luthy et al., 1997).

More recent work has revealed that in addition to the organic content the nature of the organic matter has a significant impact on sorption capacity and nonlinearity (Grathwohl, 1990; Weber and Huang, 1996; Xing and Pignatello, 1997). A correlation between K_{oc} and O/H ratios illustrated the importance of soil organic

matter quality on sorption capacity (Grathwohl, 1990; Huang and Weber, 1997). Organic matter with different sorption properties has been divided into: (a) soft or rubbery and (b) hard or glassy (Young and Weber, 1995; Xing and Pignatello, 1997). Weber and Huang (1996) introduced the terms of amorphous and condensed organic matter. A critical review paper summarizes all the important soil properties and the sorption processes related to them (Luthy et al., 1997). More than one type of organic matter, as well as the presence of organic particles, can be present in the soil samples. Gustafsson et al. (1997) separated the organic carbon into: (a) organic carbon fraction of the solid matrix (f_{oc}) and (b) soot carbon fraction of the solid matrix, to rationalize previously observed K_{oc} values. Kleineidam et al. (1998) recently used organic petrography methods to characterize organic matter present in sedimentary rocks.

Sorption nonequilibrium can be attributed to intraparticle diffusion (Ball and Roberts, 1991b; Grathwohl, 1998). Recent review papers summarize the slow sorption/desorption of organic compounds in natural particles (Pignatello and Xing, 1996; Luthy et al., 1997). Luthy et al. (1997) presents a correlation between soil properties and sorption kinetics. In the past intraparticle pore diffusion models have been used to describe the long-term sorption kinetics in bulk samples (Ball and Roberts, 1991b; Grathwohl and Reinhard, 1993).

Rügner et al. (1998) used an empirical correlation that predicts long term sorption kinetics of organic pollutants in heterogeneous aquifer materials based on intraparticle porosity and equilibrium sorption capacity of homogeneous constituents of the sample. They also used empirical correlation (i.e., Archie' s law) to determine the mechanisms in sorption experiments.

The objectives of this study were to examine the effects of heterogeneous organic matter on sorption equilibria and kinetic parameters in a sandy aquifer material. Sorption parameters were explained based on organic matter characterization. A numerical solution of Fick's 2nd law was used to model kinetic experiments of the different size fractions. Organic matter characteristics that affected the kinetic properties of sorption are discussed. This study is unique in demonstrating the presence of and petrographically characterizing organic particles in alluvial aquifer materials and in demonstrating the effect of these organic particles on sorption properties.

MATERIALS AND METHODS

Soil was sampled from the closed Norman Landfill which is a United States Geological Survey Toxic Substances Research site in Norman, Oklahoma, USA. The sampling depth was just below the water table at about 3 ft. The initial soil sample was divided into 2 groups with grain size: (a) ≤0.5 mm and (b) >0.5 mm. Sieve analysis was performed on the soil sample with grain size less than 0.5 mm and the sample was separated into 4 subsamples. Code names given to subsamples were based on their grain size. The organic carbon content of these subsamples was analyzed by dry combustion at 850°C (Model 183 Boat Sampling Module, Rosemount) and quantified by an infrared detector for CO_2 (Horiba PIR-2000). Surface area and intraparticle porosity were measured using N_2 and the BET method (ASAP 2010, Micromeritics).

Phenanthrene was used as the model chemical in this study. Phenanthrene ($C_{14}H_{10}$) is a three-ring polycyclic aromatic hydrocarbon with: (a) molecular weight: 178 g mol^{-1}, (b) solubility: 1.29 mg L^{-1} at 25° C, (c) Henry's law constant: $2.6x10^{-5}$ atm m^3 mol^{-1}, and (d) log K_{ow}: 4.6 (Montgomery and Welkom, 1990). The estimated log K_{oc} of phenanthrene is 4.4 (Karickhoff et al., 1979). Phenanthrene was chosen because of its high hydrophobicity (K_{ow}), low volatility (Henry's law constant), and simplicity of analysis. Phenanthrene was diluted to a 100 mg L^{-1} stock solution in methanol. Solutions were prepared with synthetic groundwater that is deionized water with 44 mg L^{-1} $CaCl_2.2H_2O$, 14 mg L^{-1} $CaSO_4$, and 17 mg L^{-1} $NaHCO_3$. Sodium azide was added at a concentration of 200 mg L^{-1} to inhibit biodegradation.

All equilibrium sorption isotherm batch experiments were conducted in triplicate in 10 mL crimp top glass vials. The soil samples were pulverized to assure equilibrium in a reasonable time. The soil samples were mixed with variable phenanthrene concentrations and were shaken for 7 days at constant temperature (20°C) in the dark. Headspace was kept at a minimum. Different solid to water ratios were used due to different sorption capacities of the subsamples.

All sorption kinetic batch experiments were conducted in triplicate in 100 mL crimp top glass vials. The initial phenanthrene concentration used was 0.1 mg L^{-1}. The solid to water ratio was different for each subsample. The vials were stored at 20°C in the dark. Measurements were taken at various time intervals.

For both isotherm and kinetic batch experiments phenanthrene concentrations were measured by a cuvette mode Perkin-Elmer LS-3B Fluorescence Spectrometer. For each batch study blank samples with phenanthrene solutions and

without soil were prepared and monitored. These blank samples did not indicate any significant phenanthrene degradation or sorption on the glassware. At the end of the kinetic experiment phenanthrene was extracted from the solids with hot methanol (60°C) for 4 days (Ball et al., 1997).

To characterize optical properties of organic matter thin sections of the soil subsamples were prepared. Microscopic investigations were carried out on a Leica DMRX photometer microscope. Organic matter was identified and characterized using white light and UV illumination in transmitted and reflected light mode.

DATA MODELING

The sorption distribution coefficient K_d is defined as:

$$K_d = q_e C_e^{-1} \tag{1.1}$$

where q_e is the amount of chemical sorbed per amount of soil and C_e is the equilibrium chemical concentration in solution. Nonlinear isotherms can be described by the Freundlich equation:

$$q_e = K_{fr} C_e^{\ n} \tag{1.2}$$

where K_{fr} is the Freundlich sorption constant and n is the Freundlich exponent. For nonlinear isotherms K_d is concentration dependent and can be described by:

$$K_d = K_{fr} C_e^{n-1} \quad (1.3)$$

The organic content normalized distribution coefficient is described by:

$$K_{oc} = K_d f_{oc}^{-1} \quad (1.4)$$

where f_{oc} is the organic content of the soil. At chemical concentrations equal to 1 μg L^{-1}, K_d equals K_{fr} and $K_{oc} = K_{fr} f_{oc}^{-1}$.

Solute diffusion from an aqueous phase into spherical porous grains can be described by Fick's 2nd law:

$$\partial C \partial t^{-1} = D_a [(\partial^2 C \partial r^{-2}) + (2\partial C (r\partial r)^{-1})] \quad (1.5)$$

where C is the concentration of the chemical, t is time, D_a is the apparent diffusion coefficient, and r is the radial distance from the center of the grain. The apparent diffusion coefficient is described by:

$$D_a = (D_{aq} \varepsilon) [(\varepsilon + K_d \rho) \tau]^{-1} = D_e \alpha^{-1} \quad (1.6)$$

where D_{aq} is the aqueous diffusion coefficient, ε is the intraparticle porosity, ρ is the bulk density, τ is the tortuosity factor, D_e is the effective diffusion coefficient, and α is the capacity factor ($\alpha = \varepsilon + K_d \rho$) (Grathwohl, 1998).

In the present study a numerical solution of Fick's 2nd law was evaluated. This numerical model is described by Jäger (1997) and is based on the finite difference method using the Crank-Nicholson approach. Input data are the grain radius, the solid-to-water ratio, the initial water concentration, the Freundlich parameters, the solid density and the intraparticle porosity. In this study the numerical model was used to fit the sorption kinetic curves and produce values for D_a.

As summarized in Grathwohl (1998) the sorptive uptake curves, expressed as the apparent sorption coefficient (K_{da}) normalized by K_d versus time, are relatively insensitive to different values of β and allow comparison of sorptive uptake at different solid-to-water ratios in a batch experiment. β denotes the ratio of aqueous phenanthrene to sorbed phenanthrene ($M_w M_s^{-1}$) under equilibrium conditions:

$$\beta = M_w M_s^{-1} = (1-F) F^{-1} \qquad (1.7)$$

where F is defined as the fractional uptake at equilibrium:

$$F = M_s (M_{total})^{-1} = 1 (1+\beta)^{-1} \qquad (1.8)$$

where M_w, M_s, and M total are the amount of chemical in the water phase, the solid phase, and the system, respectively.

RESULTS AND DISCUSSION

Soil Analysis

The soil organic content (f_{oc}), surface area (SA), and porosity for each subsample and the composite soil sample are presented in Table 1.1. Fine sand particles (0.125) make up 58% of the composite sample amount but only contribute 29% of the organic content. A large fraction (22%) of the composite sample f_{oc} is associated with the larger grain size (0.5), which makes up only 3% of composite sample amount. While previous studies have generally shown that the finest grain size particles were associated with the highest organic content, as well as the highest K_{oc} values (Kan et al., 1994; Barber, 1994), Ball and Roberts (1991a) did observe higher organic content for the larger size fractions using the Borden sand.

Organic petrography analysis of the different subsamples of the present study showed different types of organic matter for each subsample. The sand size fraction (0.5) includes coal and phytoclast particles as well as amorphous organic matter (AOM) in quartz aggregate matrices. The medium sand size fraction (0.25) mainly includes organic particles in quartz grain coatings. The fine sand size fraction (0.125) mainly includes AOM in quartz grain coatings. The fine grain size fraction (0.063) includes charcoal particles and AOM in quartz grain coatings. All subsamples are highly heterogeneous and contain coal particles. Ongoing research in our laboratory is focusing on quantification of the different organic matter characteristics and

Table 1.1. Soil Analysis

Sample	Effective Diameter	wt	f_{oc}	Fraction foc in subsample	SA	f_{oc} SA^{-1}	PV	Porosity
Code	mm	(%)	(%)	(%)	$m^2 g^{-1}$	µg of C m^{-2}	$cm^3 g^{-1}$	
CRA comp.	≤0.5	100	0.40	100	5.3	830	0.0067	0.017
0.5	0.5-0.25	3	2.90	22	14.0	2100	0.0180	0.044
0.25	0.25-0.125	28	0.51	36	3.9	1300	0.0053	0.014
0.125	0.125-0.063	58	0.20	29	4.3	470	0.0056	0.015
0.063	≤0.063	11	0.52	14	8.5	610	0.0100	0.027

wt: weight fraction of composite; f_{oc}: organic carbon content; SA: surface area; PV: internal pore volume for pore diameter<66.6 nm; CRA comp.: Canadian River Alluvium composite sample

characterization of the organic carbon into different fractions as proposed in Gustafsson et al. (1997); this will be presented in a future publication.

Equilibrium Sorption Isotherms

The 4 subsample sorption isotherms are presented in Fig. 1.1. The isotherms for phenanthrene in the composite sample and all of the subsamples have a Freundlich curvilinear shape suggesting more than just partitioning of phenanthrene into the organic matter. Isotherm constants derived from equilibrium experiments are presented in Table 1.2. The K_{fr} value for the composite soil (1100 ± 95) is consistent with the K_{fr} value calculated based on the sum of the mass-weighed K_{fr} values from the subsamples (1100). In all cases, log K_{oc} values (5.3-5.6) are much higher than K_{ow}-based estimates (Karickhoff et al., 1979; log K_{oc} = 4.4). Barber (1994) and Schüth (1994) also found the same trend with their samples. Barber (1994) attributed this deviation to mineral contribution to sorption or to higher "quality" organic matter than evaluated by Karickhoff et al. (1979). These results demonstrate that organic carbon content alone is not enough to predict K_{fr} values.

Based on the K_{oc} values, there are 2 distinct groups: (a) the sand (0.5) and the finest grain (0.063) size fractions, and (b) the medium (0.25) and fine (0.125) sand fractions. Group (a) presented higher K_{oc} values than group (b). Studying the previous trends, it is obvious that the presence of coal (0.5) and charcoal particles(0.063) in soil samples increases both the amount of organic carbon content present and the K_{oc} value for this fraction. Amorphous organic matter coatings of

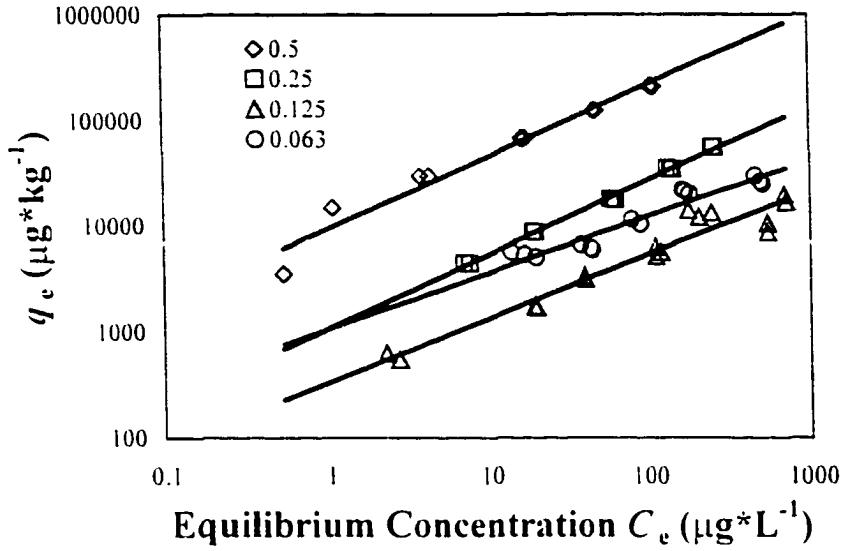


Figure 1.1. Size fraction subsample isotherms. q_e is the amount of phenanthrene sorbed per amount of soil, C_e is the equilibrium phenanthrene concentration. The symbols denote experimental data points and the lines the Freundlich isotherm fit. Subsample code names indicate particle size (as presented in Table 1.1).

Table 1.2. Isotherm Results

Sample	wt	f_{oc}	n	K_{fr}	log K_{oc}	Confidence Interval
	(%)	(%)		($\mu g\ kg^{-1}$) ($L\ \mu g^{-1}$)^n		95%
CRA comp.	100	0.40 ± 0.092	0.65 ± 0.021	1100 ± 95	5.4	5.3 - 5.5
0.5	3	2.90 ± 0.270	0.64 ± 0.043	11000 ± 1300	5.6	5.5 - 5.7
0.25	28	0.51 ± 0.038	0.70 ± 0.013	1100 ± 55	5.3	5.3 - 5.4
0.125	58	0.20 ± 0.011	0.57 ± 0.036	400 ± 61	5.3	5.2 - 5.4
0.063	11	0.52 ± 0.048	0.53 ± 0.044	2100 ± 100	5.6	5.6 - 5.7

For CRA comp., Mass-Weighted K_{fr} = Sum (wt% K_{fr} for each fraction)=1100

wt: weight fraction of composite; f_{oc}: organic carbon content; n: Freundlich exponent; K_{fr}: Freundlich constant; K_{oc}: organic content normalized sorption distribution coefficient; CRA comp.: Canadian River Alluvium composite sample

quartz grains (0.125) produce the lowest K_{oc} value. Even the lowest K_{oc} value of this study (log K_{oc} = 5.2-5.4; 95% confidence interval) is higher than the value estimated by K_{ow} (log K_{oc} = 4.4) due to coal particles present in all subsamples.

The presence of coal particles in soil samples increases the K_{oc} values of these samples. If the coal particles are not considered, the sorption potential of the soil will be underestimated (log K_{oc} = 5.4 versus log K_{oc} = 4.4; Table 1.2 and Karickhoff et al., 1979). This observation is important when predicting subsurface chemical transport. When natural attenuation is considered as a remediation scenario underestimating sorption potential causes an underestimate of the potential risk and lead to unnecessary remediation expenses.

Sorption Kinetics

Figure 1.2 presents the apparent sorption coefficient at a given time (K_{da}) normalized by the equilibrium distribution coefficient (K_d) as a function of time for the 4 subsamples during kinetic experiments. Table 1.3 presents results of experimental and modeling work studying the kinetic sorption properties of the soil samples. The radii used in the model to fit the apparent diffusion coefficient (D_a) were calculated as described by Ball and Roberts (1991b). Bulk soil radius was calculated by the geometric mean and the radius of the fractions weighted by their contribution to the K_{fr} value of the composite sample (Ball and Roberts, 1991b). The apparent diffusion coefficient for phenanthrene and the composite soil sample using the analytical model is very close to the value expected based on the aqueous

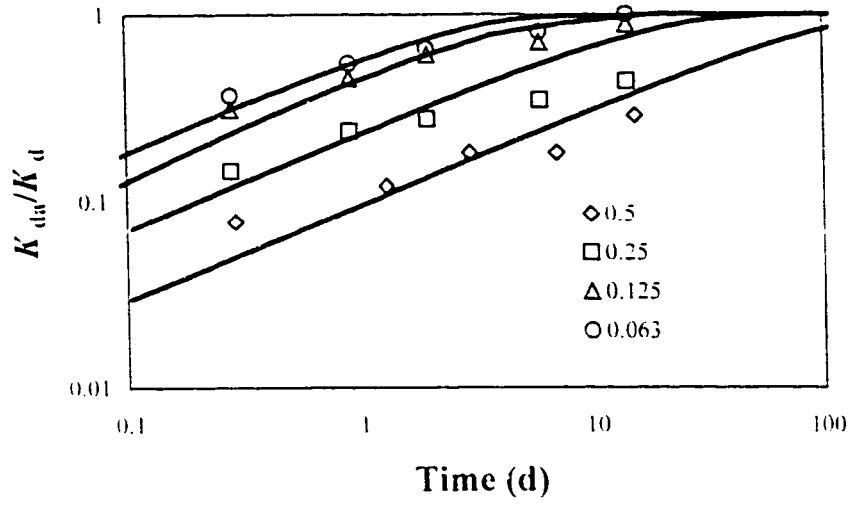


Figure 1.2. Size fraction subsample kinetic experiments. Apparent distribution coefficient, K_{da}, normalized to the equilibrium distribution coefficient, K_d, versus time (d). The symbols denote experimental data points and the line the numerical solution fit. Subsample code names indicate particle size (as presented in Table 1.1).

Table 1.3. Kinetic Sorption Properties based on Numerical Solution

Sample	F	a	$D_a a^{-2}$	D_a	T_1 75% Eq
		(cm)	($1\ s^{-1}$)	($cm^2\ s^{-1}$)	(d)
CRA comp. (a =0.0077 cm)	0.56	0.0077	7.7E-08	7.7E-12	12
CRA comp. (a =0.0100 cm)	0.56	0.0100	8.2E-08	8.2E-12	12
0.5	0.58	0.0180	1.2E-08	3.9E-12	73
0.25	0.54	0.0089	6.4E-08	5.1E-12	16
0.125	0.57	0.0044	3.4E-07	6.6E-12	3
0.063	0.44	0.0027	4.5E-07	3.3E-12	2

F: fractional uptake at equilibrium; a: grain radius; $D_a a^{-2}$: apparent diffusion rate coefficient; D_a: apparent diffusion coefficient; T 75% Eq: time to reach 75% equilibrium; CRA comp.: Canadian River Alluvium composite sample

diffusion coefficient (D_{aq} = 5.8 E-6 cm^2 s^{-1}; Schüth, 1994) of phenanthrene (D_a = 3.4 E-12 cm^2 s^{-1}) (Table 1.3).

In Fig. 1.2 it is obvious that the model does not fit all the data properly; especially longer term (slower) sorption. This is expected because the numerical model used assumes homogeneous samples. To fit all the data properly the introduction of a fast sorption term (X_1) that represents a percent of fast sorption sites in the sample was required (see Fig. 1.3 and Table 1.4). A comparison between the numerical model without and with X_1 for the composite sample is presented in Figure 1.4; illustrating the improved fit when using the two-site model. Table 1.4 presents X_1 and the time needed to reach 75% of equilibrium ($T_2$75% Eq) based on the model adjusted for fast sorption sites. The highest X_1 term was estimated for the subsample that contains AOM coatings (0.125) suggesting a faster sorption mechanism that is not limited by intraparticle diffusion kinetics. The time needed to reach 75% of equilibrium ($T_2$75% Eq) in Table 1.4 is higher than ($T_1$75% Eq) in Table 1.3. The model curves in Fig. 1.2 try to fit both fast and slow data as if they behaved the same and thus does not fit either of them properly. These model curves both overestimate and underestimate the time required to reach equilibrium for the fast sorption sites and the slow sorption sites, respectively. Once a fast sorption term is added (Fig. 1.4) the fast sorption points are fitted well and is better incorporated into the results resulting in longer estimated equilibration times ($T_2$75% Eq > $T_1$75% Eq; Tables 1.4 and 1.3, respectively).

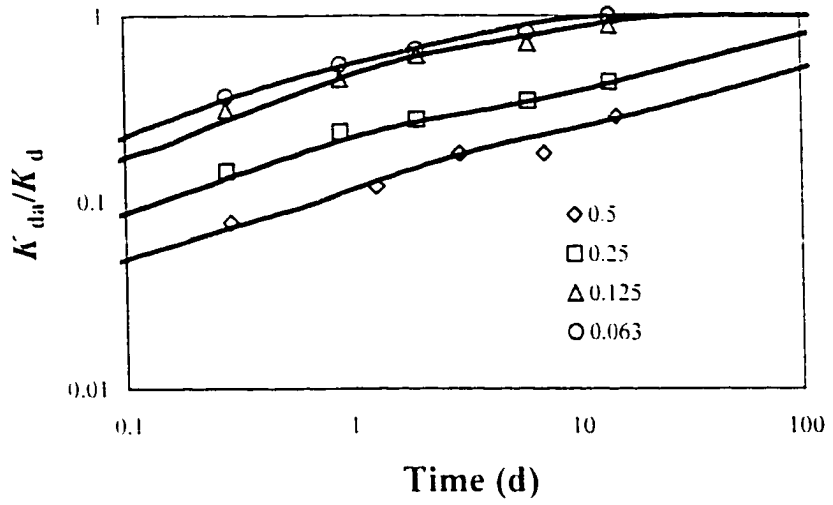


Figure 1.3. Size fraction subsample kinetic experiments. Apparent distribution coefficient, K_{da}, normalized to the equilibrium distribution coefficient, K_d, versus time (d). The symbols denote experimental data points and the line the numerical solution fit adding a fast sorption term (X_1) in the model. Subsample code names indicate particle size (as presented in Table 1.1).

Table 1.4. Percent of Fast Sorption Sites and Time to Reach Equilibrium

Sample	a	X_1	T_2 75% Eq
	(cm)	(%)	(d)
CRA comp.(a =0.0077 cm)	0.0077	20	22
CRA comp.(a =0.0100 cm)	0.0100	20	24
0.5	0.0180	15	290
0.25	0.0089	20	84
0.125	0.0044	40	5
0.063	0.0027	25	3

a: grain radius; X_1: Percent of fast sorption sites; T 75% Eq: time to reach 75% equilibrium; CRA comp.: Canadian River Alluvium composite sample

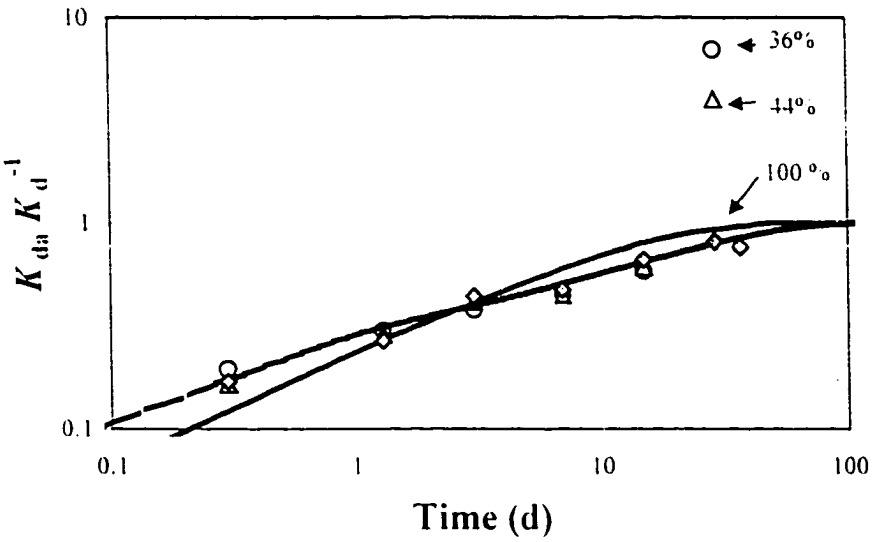


Figure 1.4. CRA composite sample kinetic experiment. Apparent distribution coefficient, K_{da}, normalized to the equilibrium distribution coefficient, K_d, versus time (d). The symbols denote experimental data points, the solid line and the dashed line the numerical solution fit without and with the fast sorption term (Y_1), respectively. Numbers in the legend represent percent of amount recovery at the end of the experiment (last step only) using hot methanol extraction.

Figure 1.4 presents the apparent sorption distribution coefficient (K_{da}) values following the diffusion model prediction line (solid and dashed lines representing the model without and with the adjustment for fast sorption sites, respectively) for the composite sample (CRA comp.). Some of the 30-day measurements deviated from the diffusion model. Although there was NaN_3 present in the reactors this behavior was attributed to biodegradation which, due to the presence of NaN_3, had a lag period of about 15-30 days. To prove this assumption all samples were solvent extracted with hot methanol. For the samples that followed the diffusion model the mass balance was within 90-100% recovery – the remaining samples presented only a 26-76% recovery.

The presence of coal particles and organic coatings in the soil samples thus affected the kinetics of sorption. Kinetic models should cautiously be applied to fit the kinetic properties of soil samples containing heterogeneous organic matter. The model that assumes a homogeneous organic matter behavior by trying to fit the fast sorbing sites will overestimate the time required for sorption to reach equilibrium ($T_1$75% Eq = 12 versus $T_2$75% Eq = 22; Tables 1.3 and 1.4). When incorporating sorption into natural attenuation it is thus important to consider the impacts of heterogeneous organic matter on sorption equilibria and kinetics so as to properly estimate the risk of exposure.

SUMMARY

Batch experiments were conducted to examine sorption equilibria and kinetic sorption characteristics of phenanthrene with the Canadian River Alluvium aquifer material. Sorption isotherms were nonlinear and subsample K_{oc} values were higher than estimated based on the K_{ow} predictions. Two groups of subsamples were found: (a) subsamples with high organic content including organic particles and (b) subsamples with organic matter on quartz grain coatings. Group (a) presented a K_{oc} value higher than group (b).

Modeling of sorption kinetics was best performed by the numerical solution of Fick's 2nd law when was adjusted for the fast sorbing sites. The use of a fast sorption term was necessary for better fit especially for samples with organic coatings. These results demonstrate the importance of organic matter type and heterogeneity on the resulting sorption equilibria and kinetics. Soil samples containing heterogeneous organic matter could present equilibrium and kinetic sorption properties that would be difficult to predict using models developed based on the assumption that organic matter is homogeneous.

Acknowledgment. This study was partially funded by the U.S. National Science Foundation through the Oklahoma EPSCoR program. The authors would like to thank Renate Riehle for TOC measurements and Hermann Rügner of the Universität Tübingen for BET measurements. This research was conducted at the Universität Tübingen while David Sabatini was on sabbatical there as a Senior Fulbright Scholar

and while Hrissi Karapanagioti, his PhD student from the University of Oklahoma, was conducting research with him at the Universität Tübingen.

References

Ball W.P. and Roberts P.V., 1991a. "Long-Term Sorption of Halogenated Organic Chemicals by Aquifer Material. 1. Equilibrium", *Environ. Sci. Technol., V. 25*, No 7, p. 1223-1237.

Ball W.P. and Roberts P.V., 1991b. "Long-Term Sorption of Halogenated Organic Chemicals by Aquifer Material. 2. Intraparticle Diffusion", *Environ. Sci. Technol., V. 25*, No 7, p. 1237-1249.

Ball W.P., Xia G., Durfee D.P., Wilson R.D., Brown M.J., and Mackay D.M., 1997. "Hot Methanol Extraction for the Analysis of Volatile Organic Chemicals in Subsurface Core Samples from Dover Air Force Base, Delaware", *GWMR, V. 17*, No 1, p. 104-121.

Barber L.B., 1994. "Sorption of Chlorobenzenes to Cape Cod Aquifer Sediments", *Environ. Sci. Technol., V. 28*, No 5, p. 890-897.

Chiou C.T., McGroddy S.E., and Kile D.E., 1998. "Partition Characteristics of Polycyclic Aromatic Hydrocarbons on Soils and Sediments", *Environ. Sci. Technol., V. 32*, No 2, p. 264-269.

Estrella M.R., Brusseau M.L., Maier R.S., Pepper I.L. Wierenga P.J., and Miller R.M., 1993. "Biodegradation, Sorption, and Transport of 2,4- Dichlorophenoxyacetic Acid in Saturated and Unsaturated Soils", *Appl. Environ. Microbiol., V.59*, No 12, p.4266-4273.

Grathwohl P., 1990. "Influence of organic matter from Soils and Sediments from Various Origins on the Sorption of Some Chlorinated Aliphatic Hydrocarbons: Implications on Koc Correlations", *Environ. Sci. Technol., V. 24*, No 11, p.1687-1693.

Grathwohl P. and Reinhard M., 1993. "Desorption of Trichloroethylene in Aquifer Material: Rate Limitation at the Grain Scale", *Environ. Sci. Technol., V. 27*, No 12, p.2360-2366.

Grathwohl P., 1998. *Diffusion in Natural Porous Media: Contaminant Transport, Sorption/Desorption and Dissolution Kinetics*, Kluwer Academic Publishers, Boston, Massachusetts.

Gustafsson Ö., Haghseta F., Chan C., Macfarlane J., and Gschwend P.M., 1997. "Quantification of the Dilute Sedimentary Soot Phase: Implications for PAH Speciation and Bioavailability", *Environ. Sci. Tech., V. 31*, No 1, p. 203-209.

Huang W. and Weber W.J.Jr., 1997. "A Distributed Reactivity Model for Sorption by Soils and Sediments 10. Relationships Between Desorption, Hysteresis, and the Chemical Characteristics", *Environ. Sci. Tech., V. 31*, No 9, p. 2562-2569.

Jäger R., 1997. *Modellierung Nichtlinearer Intrapartikel-Diffusion in Heterogenem Aquifermaterial*, Diploma Thesis, University of Tübingen, FRG.

Karickhoff S.W., Brown D.S., and Scott T.A., 1979. "Sorption of Hydrophobic Pollutants on Natural Sediments", *Water Research, V. 13*, p. 241-248.

Kleineidam S., Rügner H., Ligouis B., and Grathwohl P., 1998. "Organic Matter Facies and Equilibrium Sorption of Phenanthrene", *Environ. Sci. Technol.*, submitted.

Kan A. T., Fu G., and Tomson M.B., 1994. "Adsorption/Desorption Hysteresis in Organic Pollutant and Soil/Sediment Interaction", *Environ. Sci. Technol., V. 28*, No 5, p.859-867.

Luthy R.G., Aiken G.R., Brusseau M.L., Cunningham S.D., Gschwend P.M., Pignatello J.J., Reinhard M., Traina S.J., Weber W.J.Jr., and Westall J.C., 1997. "Sequestration of Hydrophobic Organic Contaminants by Geosorbents", *Environ. Sci. Technol., V. 31*, No 12, p.3341-3347.

Montgomery J.H. and Welkom L.M., 1990. *Ground Water Chemicals Desk Reference*, Lewis Publishers, Inc., Chelsea, Michigan.

Pignatello J.J. and Xing B., 1996. "Mechanisms of Slow Sorption of Organic Chemicals to Natural Particles", *Environ. Sci. Technol., V. 30*, No 1, p. 1-11.

Rügner H., Kleineidam S., and Grathwohl P., 1998. "Long Term Sorption Kinetics of Phenanthrene in Aquifer Materials", *Environ. Sci. Technol.*, submitted.

Schüth C., 1994. *Sorptionskinetik und Transportverhalten von Polyzyklischen Aromatischen Kohlenwasserstoffen (PAK) im Grundwasser*, Dissertation, University of Tübingen, FRG.

Weber W.J.Jr. and Huang W., 1996. "A Distributed Reactivity Model for Sorption by Soils and Sediments. 4. Intraparticle Heterogeneity and Phase-Distribution Relations under Nonequilibrium Conditions", *Environ. Sci. Technol., V. 30*, No 3, p. 881-888.

Xing B. and Pignatello J.J., 1997. "Dual-Mode Sorption of Low-Polarity Compounds in Glassy Poly(Vinyl Chloride) and Soil Organic Matter", *Environ. Sci. Technol., V. 31*, No 3, p. 792-799.

Young T.M. and Weber W.J.Jr., 1995. "A Distributed Reactivity Model for Sorption by Soils and Sediments. 3. Effects of Diagenetic Processes on Sorption Energetics", *Environ. Sci. Technol., V. 29*, No 1, p. 92-97.

CHAPTER 2

IMPACTS OF HETEROGENEOUS ORGANIC MATTER ON PHENANTHRENE SORPTION: EQUILIBRIUM AND KINETIC STUDIES WITH AQUIFER MATERIAL

ABSTRACT

Sediment organic matter heterogeneity in sediments is shown to impact the sorption behavior of contaminants. We investigated the sorptive properties as well as the composition of organic matter in different subsamples (mainly grain size fractions) of the Canadian River Alluvium (CRA). Organic petrography was used as a new tool to describe and characterize the organic matter in the subsamples. The samples studied contained many different types of organic matter including bituminous coal particles. Differences in sorption behavior were explained based on these various types of organic matter. Subsamples containing predominately coaly, particulate organic matter showed the highest K_{oc}, the highest nonlinearity of sorption isotherms and the slowest sorption kinetics. Soil subsamples with organic matter present as organic coatings around the quartz grains evidenced the lowest K_{oc}, the most linear sorption isotherms and the fastest sorption kinetics, which was not limited by slow intraparticle diffusion. Due to the high sorption capacity of the coaly particles even when it is present as only a small fraction of the composite organic content (<3%) causes K_{oc} values which are much higher than expected for soil organic

matter (e.g. K_{oc}–K_{ow} relationships). The results show that the identification and quantification of the coaly particles within a sediment or soil sample is a prerequisite to understand or predict sorption behavior of organic pollutants.

INTRODUCTION

Natural attenuation is currently one of the most important topics in groundwater remediation. Sorption equilibrium and sorption/desorption kinetic properties are very important factors affecting natural attenuation of contaminants in the subsurface. While an extensive body of literature discusses sorption processes, little information considers the impact of heterogeneous organic matter on sorption properties.

Karickhoff et al. (*1*) published one of the earlier and more important studies on sorption of hydrophobic organic compounds. Instantaneous equilibrium and linear sorption isotherms were observed and attributed to partition-like sorption. The organic-content-normalized distribution coefficient (K_{oc}) was dependent on chemical hydrophobicity and solubility, as quantified by the chemical's octanol-water partition coefficient (K_{ow}). These observations have been corroborated for numerous media and organic contaminants (*2*, *3*, and as summarized in ref *4*). Organic matter was assumed to be homogeneous and uniformly distributed, with the fraction organic carbon content (f_{oc}) viewed as adequate for characterization processes. However, select studies have shown that a minor fraction of a sample can govern sorption behavior of the bulk sample (*5*, *6*). Other studies have demonstrated that the nature of the organic

matter also has a significant impact on sorption capacity and nonlinearity (*7-12*). A correlation between K_{oc} and O/H ratios illustrated the importance of soil organic matter quality on sorption capacity (*8, 13*).

A conceptual model of organic matter domains (soft or rubbery or amorphous and hard or glassy or condensed) has been presented, with each type of sorbent assigned qualitative sorption characteristics (*9, 10, 14*, summarized in ref *4*). A transition between the two organic matter domains was found (*15*), although their sorption characteristics are still not well established (*16*). Recently, the presence of other organic matter phases (e.g. high-surface-area carbonaceous material, soot, etc.) has been proposed as cause of nonlinear sorption and increased K_{oc} values (*11, 17, 18*). Kleineidam et al. (*19*) characterized organic matter heterogeneity in sedimentary rocks and related organic matter facies to equilibrium sorption properties. Recently, Xia and Ball (*12*) proposed a model that accounts for adsorption and partitioning sorption sites to treat different sorption characteristics. In this specific model adsorption/pore filling is important at low contaminant concentrations while partitioning dominates sorption behavior at higher concentrations. The Polanyi-Manes approach was successful to model such a concept.

Sorption nonequilibrium can be attributed to intraparticle diffusion (*20-22*). Recent review papers summarize the slow sorption/desorption of organic compounds in natural particles (*4, 23*). Intraparticle pore diffusion models have been used to describe the long-term sorption kinetics in bulk samples (*20, 24, 25*). Rügner et al. (*22*) used an empirical correlation that predicts long term sorption kinetics of organic

pollutants based on intraparticle porosity and equilibrium sorption capacity of homogeneous constituents of a heterogeneous aquifer material.

The objectives of this study were as follows: (1) to examine the effects of heterogeneous organic matter on sorption equilibria and kinetic parameters in a sandy aquifer material, (2) to relate variations in sorption properties with characteristics of the organic matter type, and (3) to model the kinetic results using an intraparticle diffusion model (numerical solution of Fick's 2nd law). Variations in equilibrium sorption parameters and sorption kinetics for soil subsamples were explained based on the organic matter characteristic present. This study is unique in demonstrating the presence of heterogeneous organic matter in alluvial aquifer materials (e.g. coal, charcoal, amorphous organic matter, etc.), characterizing these different components and quantifying their impact on sorption properties.

MATERIALS AND METHODS

The Canadian River Alluvial (CRA) aquifer material was sampled from the closed Norman Landfill, which is a U.S.G.S. Toxic Substances Research site. The sampling depth was just below the water table at about 3 ft. The initial sample was divided into two groups with grain diameter size: a) ≤0.5 mm and b) >0.5 mm.

The smaller grain size sample was sieved into four subsamples (0.5 mm-0.25 mm, 0.25 mm-0.125 mm, 0.125 mm-0.063 mm, ≤0.063 mm; nominally decreasing the radius by half for each size fraction) to assess the impact of grain radius on sorption kinetics. Each of these four grain size samples was then separated into two

subsamples using a FRANTZ Magnetic Barrier Laboratory Separator Model LB-1 operated at 1.0 A, 10^{o} longitudinal slope, and 0^{o} lateral slope, resulting in a total of eight subsamples. Generally, the magnetic subsamples were dominated by quartz aggregates containing iron minerals in the clay matrices in the magnetic side, while individual quartz grains dominated the nonmagnetic samples. Magnetic separation of organic matter itself was not expected, unless the organic matter existed as isolated particles, single coal particles or wood residue. This procedure separated soil grains and organic matter associated in various forms to these grains (adsorbed, matrices etc.) due to magnetic properties of the grains and not due to organic matter properties. Coal is normally diamagnetic (*26*). Coal particles associated with pyrite were found in the two larger size fractions in the magnetic side. The presence of pyrite explains the paramagnetic properties of these coal particles. In the absence of pyrite it was not clear how and why magnetic separation would differentiate forms of organic matter. To characterize organic matter, polished thin sections of the soil subsamples were prepared. Microscopic investigations were carried out on a Leica DMRX photometer microscope. Organic matter was identified and characterized using white light and UV illumination in transmitted and reflected light mode. The soil organic matter characterization is done using a palynological classification (*27*). The observations were qualitative in nature; type and frequency (area covered in the thin section) of the organic matter present are summarized in Table 2.1.

Code names given to subsamples in Table 2.1 were based on their grain size and the dominant organic matter found in the thin sections. The subsamples were pretreated with HCl to remove inorganic carbon. The organic carbon content was

TABLE 2.1 Soil Subsamples and Organic Matter Characteristics

Sample Code	Grain Size	Magnetic Separation	Particulate Organic Matter (POM)			Clay Matrix (M)		Organic Coating (C)
	(mm)		Coal (CL)	Charcoal (CH)	Phytoclast (PH)	POM	Amorphous Organic Matter (AOM)	AOM
Code			POM_{CL}	POM_{CH}	POM_{PH}	M_{POM}	M_{AOM}	C_{AOM}
CRA comp.	≤ 0.5	None		x	x		x	x
$0.5M_{AOM}POM_{PH}$	0.5-0.25	Magnetic	x		x		x	
$0.5POM_{CL}$	0.5-0.25	Nonmagnetic	x		x		x	
$0.25POM_{PH}M_{POM}$	0.25-0.125	Magnetic			x	1μm[1]		
$0.25M_{POM}$	0.25-0.125	Nonmagnetic				1-3μm[1]		
$0.125C_{AOM}POM_{PH}$	0.125-0.063	Magnetic			x	5μm[1]	x	x
$0.125C_{AOM}$	0.125-0.063	Nonmagnetic						x
$0.063POM_{CH}C_{AOM}$	≤ 0.063	Magnetic		x				x
$0.063C_{AOM}POM_{CL}$	≤ 0.063	Nonmagnetic	x					x
Presented in Figure 2.1, part:			a, c	b, c	d	c, e, f	c, e, f	g, h

Sample Code: XA_AB_B where: X: size fraction; A_A: most dominant organic matter characteristic; B_B: second dominant organic matter characteristic; POM: particulate organic matter with same particle size as the subsample grain size; M: clay matrix; C: organic coating; CL: coal; CH: charcoal; PH: phytoclast; AOM: amorphous organic matter; CRA comp.: Canadian River Alluvium composite sample

[1] Instead of x that indicates presence numbers indicate POM diameter in the clay matrix.

then analyzed by dry combustion at 850 °C (Model 183 Boat Sampling Module, Rosemount) and quantified by an infrared detector for CO_2 (Horiba PIR-2000). Surface area and intraparticle meso-porosity were measured using N_2 and the BET method (ASAP 2010, Micromeritics) (more details on method are presented in ref 22). The external surface area calculated based on the grain size, was less than 0.1% of the specific surface area measured for all fractions.

Phenanthrene was used as the model chemical in this study. Phenanthrene ($C_{14}H_{10}$) is a three-ring polycyclic aromatic hydrocarbon with: (a) molecular weight: 178 g/mol, (b) solubility: 1.29 mg/L at 25 °C, (c) Henry's law constant: 2.6×10^{-5} atm m^3/mol, and (d) log K_{ow}: 4.6 (28). The estimated log K_{oc} of phenanthrene is 4.4 (1). Phenanthrene was chosen because of its high hydrophobicity (K_{ow}), low volatility (Henry's law constant), and simplicity of analysis. Phenanthrene was diluted to a 100 mg/L stock solution in methanol. Solutions were prepared in synthetic groundwater (deionized water with 44 mg/L $CaCl_2.2H_2O$, 14 mg/L $CaSO_4$, and 17 mg/L $NaHCO_3$). Sodium azide (NaN_3) was added at a concentration of 200 mg/L to minimize bacterial growth and thus biodegradation during batch studies.

All equilibrium sorption experiments were conducted in triplicate in 10 mL crimp-top glass vials. Soil samples for equilibrium studies were pulverized to ensure equilibrium in a reasonable time (7 days). Variable phenanthrene concentrations were added to the soil samples and shaken for 7 days in the dark at constant temperature (20 °C). Headspace in the vials was kept to a minimum. Varying solid to water ratios were used based on different sorption capacities of the subsamples (i.e. to achieve sufficient sorption so that it could be easily quantified while keeping aqueous

concentration above the detection limit). Samples were centrifuged at constant temperature of 20 °C before analysis.

All sorption kinetic experiments were conducted in triplicate in 100 mL crimp-top glass vials. The initial phenanthrene concentration was 0.1 mg/L and the solid to water ratio was different for each subsample depending on the sorption capacity. The vials were stored at 20 °C in the dark and mixed periodically. Before analysis the samples were centrifuged at constant temperature of 20 °C. Measurements were taken at various time intervals. For both isotherm and kinetic batch experiments, aqueous phenanthrene concentrations were measured by a cuvette mode Perkin-Elmer LS-3B fluorescence spectrometer. To assess for fluorescent interferences some samples were analyzed in both UV and fluorescence detectors connected parallel to a HPLC system as well as the cuvette mode fluorescence detector. The results were comparable for all 3 detectors.

For each batch experiment blank samples were prepared and monitored (i.e., phenanthrene without soil). These blank samples did not indicate any significant phenanthrene degradation or sorptive losses on the glassware for the first 37 days. Some of the 30-day measurements showed large concentration differences between the triplicates and these data were not used for discussing the results. Although NaN_3 was present in all the reactors it did not prevent degradation completely; the NaN_3 did result in a lag period of about 15-30 days. To corroborate the onset of biodegradation all samples were solvent extracted with hot methanol at 60 °C for 4 days (*29*). For the triplicates that follow the diffusion model line the mass balance was within 90-100% recovery. Samples with a significantly lower recovery (26-76%)

evidenced large deviations from the intraparticle diffusion model due to degradation losses (*30*).

DATA MODELING

The sorption distribution coefficient K_d can be described by:

$$K_d = q_e / C_e \quad (2.1)$$

where q_e is the mass of chemical sorbed per unit mass of soil and C_e is the equilibrium concentration. Nonlinear isotherms can be described by the Freundlich equation:

$$q_e = K_{fr} C_e^{N} \quad (2.2)$$

where K_{fr} is the Freundlich sorption constant and N is the Freundlich exponent. For nonlinear isotherms K_d can be considered concentration-dependent as follows:

$$K_d = K_{fr} C_e^{N-1} \quad (2.3)$$

The organic carbon content normalized distribution coefficient is described by:

$$K_{oc} = K_d / f_{oc} \quad (2.4)$$

where f_{oc} is the fraction organic carbon content of the sample. For nonlinear isotherms, K_{oc} is also concentration dependent. At a chemical concentration of unity, K_d equals K_{fr} and $K_{oc} = K_{fr} / f_{oc}$.

Solute diffusion from an aqueous phase into spherical porous grains can be described by Fick's 2nd law:

$$\partial C / \partial t = D_a [(\partial^2 C / \partial r^2) + (2\partial C / r\partial r)] \qquad (2.5)$$

where C is the concentration of the chemical, t is time, D_a is the apparent diffusion coefficient, and r is the radial distance from the center of the grain. In the intraparticle diffusion model D_a is defined as:

$$D_a = D_{aq} \varepsilon / (\varepsilon + K_d \rho) \tau_f \qquad (2.6)$$

Where D_{aq} is the aqueous diffusion coefficient, ε is the intraparticle porosity, ρ is the bulk density of the grain, and τ_f is the tortuosity factor (*21*). In the present study, a numerical solution of Fick's 2nd law was utilized. The numerical model is based on the finite difference method using the Crank-Nicholson approach, as described by Jäger (*31*). Model input includes the grain radius, the solid to water ratio, the initial water concentration, the Freundlich parameters, the solid density and the intraparticle porosity. In this study the numerical model was used to fit the sorption kinetic curves and produce values for D_a/a^2. Model calculations are based on minimizing the mean

weighted squared errors between predicted and measured K_d values. The sorptive uptake curves, expressed as normalized K_d versus time, are relatively insensitive to different values of fractional uptake at equilibrium (F) - the chemical mass on solid per total chemical mass - and allow comparison of sorptive uptake at different solid to water ratios in batch experiments (*20*, summarized in ref *21*).

RESULTS AND DISCUSSION

Soil Analysis

Table 2.1 presents the code name and properties of each subsample (i.e., grain size, magnetic separation, and soil organic matter characterization). Other researchers have observed that K_{oc} values differed for the magnetic separated fractions but have not characterized the organic matter to explain these findings (*32, 33*). There are five basic types of organic matter present in our media: (a) coaly particulate organic matter (POM) (i.e. coal, charcoal) (Figure 2.1 a-c), (b) young POM showing fluorescence in UV/blue light (i.e. phytoclast) (Figure 2.1 a, d), (c) quartz aggregates with clay matrices containing coaly POM (Figure 2.1 a, e, f), (d) quartz aggregates with clay matrices containing amorphous (in the palynological classification amorphous describes organic matter that lacks structure under the microscope) organic matter (AOM) in clay matrices (Figure 2.1a, e, f), and (e) grains with AOM coatings (Figure 2.1g, h). Each sample has on or two dominant organic matter characteristics. Coaly

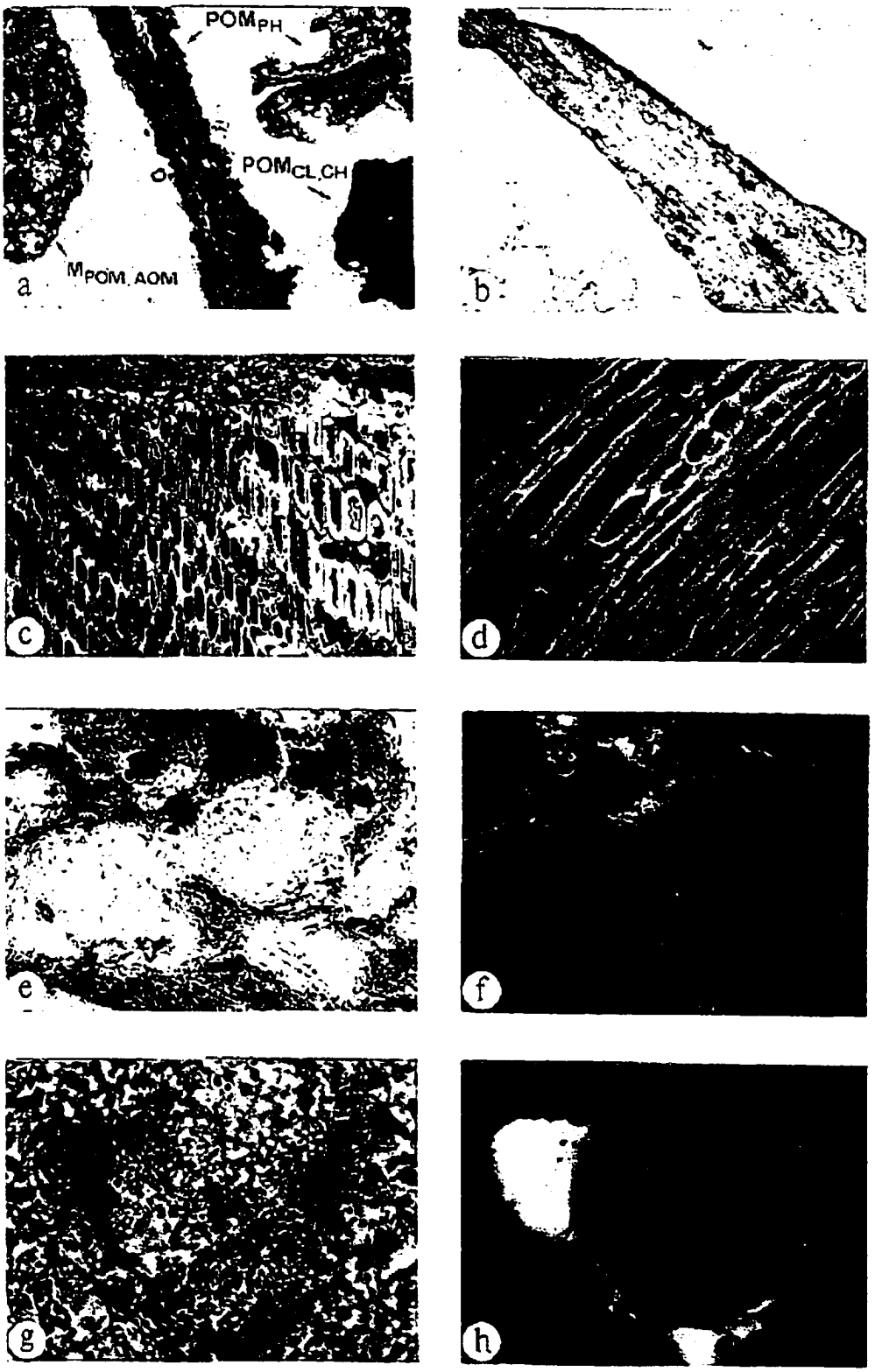

POMPH
POMCL,CH
MPOM, AOM
a
b
c
d
e
f
g
h

FIGURE 2.1 Photomicrographs illustrating the different organic matter present in the samples: (a) overview of different particulate organic matter (POM). Brown phytoclasts (POM_{PH}), opaque particle - coal (POM_{CL}) or charcoal (POM_{CH}), - and quartz aggregate with clay matrix containing amorphous organic matter (M_{AOM}) and POM (M_{POM}); transmitted white light (field 1.58 mm wide), (b) coal particle (POM_{CL}); polished surface, reflected white light, oil immersion, (field 406 µm wide), (c) charcoal particle (POM_{CH}), note the well preserved cellular structure, some of the wood cells are filled with sulfide; polished surface, reflected white light, oil immersion (field 406 µm wide), (d) phytoclast particle (POM_{PH}), the cell wall showing strong yellow-green fluorescence; incident light, fluorescence mode, oil immersion (field 158 µm wide), (e, f) e: quartz aggregates cemented with clay matrix (brown color); transmitted white light, oil immersion (field 158 µm wide), f: strong yellowish fluorescing AOM within the clay matrix (M_{AOM}), non-fluorescing small particles (black) are POM either coal or charcoal particles (M_{POM}); incident light fluorescence mode, oil immersion (field 158 µm wide), (g, h) g: isolated quartz mineral; transmitted white light, oil immersion (field 124 µm wide), h: strong yellow fluorescing organic coating (C_{AOM}); incident light fluorescence mode, oil immersion (field 124 µm wide).

All pictures were taken with a Leitz DMRX microscope, equipped with a WILD MPS48 photoautomat. Filters for the incident light fluorescence mode (UV+V excitation): excitation 355 - 425 nm, beam splitter 455 nm and barrier 470 nm.

POM is contrasted to young POM by absence of fluorescence in blue reflected light under microscopy. Generally, fluorescence decreases with maturity and only AOM and young POM fluoresce (see Figure 2.1) (27).

Coal particles, present in all the samples, are believed to originate from coal seams in New Mexico, where the South Canadian River originates (Energy Resources Map of New Mexico, Map I-1327; U.S.G.S. and New Mexico Bureau of Mines and Mineral Resources, 1981). In one of the subsamples ($0.5M_{AOM}POM_{PH}$) the POM particles were counted visually and found to comprise 15% of the total grains in the subsample. However this percentage does not reflect weight percentages (wt %) because the organic particles are generally less dense than the soil particles. The f_{oc}, surface area, and porosity for each subsample and the bulk soil sample are presented in Table 2.2. Fine sand particles ($0.125C_{AOM}$) with AOM grain coatings make up 40 wt % of the composite sample but only contribute 9% of the organic carbon content for the composite sample. A large fraction (31%) of the composite sample f_{oc} comes from a fraction that accounts for only 2.3 wt % of the composite sample ($0.5M_{AOM}POM_{PH}$). Subsamples with coaly POM are characterized by high organic content while those dominated by AOM coatings of quartz grains are characterized by low organic content (Table 2.2). Samples dominated by coal particles have a small internal meso-pore range porosity ($0.5POM_{CL}$, $0.063M_{AOM}$ POM_{CL}). Coal particles (CL) have a more uniform solid surface whereas phytoclast and charcoal are structured and highly porous particles (Figure 2.1). The presence of clay matrices explains the high porosity for samples where the organic matter is dominated by AOM in clay matrices.

TABLE 2.2 Soil Analysis

Sample Code	Diameter	Dominant Organic matter	wt	f_{oc}	Fraction of composite f_{oc} in subsample	SA	PV	Intraparticle Porosity (ε)
	mm		(%)	(%)	(%)	m^2/g	cm^3/g	
CRA comp.	≤0.5	mixture	100	0.44	100	5.3	0.0067	0.017
$0.5M_{AOM}POM_{PH}$	0.5-0.25	AOM in clay matrix	2.3	5.90	31	17.0	0.0220	0.055
$0.5POM_{CL}$	0.5-0.25	POM - Coal	0.75	1.60	3	1.7	0.0032	0.008
$0.25POM_{PH}M_{POM}$	0.25-0.125	POM – Phytoclast	5.3	1.30	16	12.0	0.0170	0.043
$0.25M_{POM}$	0.25-0.125	POM in clay matrix	23	0.16	8	2.2	0.0031	0.008
$0.125C_{AOM}POM_{PH}$	0.125-0.063	AOM Coating	18	0.51	21	2.5	0.0089	0.023
$0.125C_{AOM}$	0.125-0.063	AOM Coating	40	0.10	9	3.1	0.0041	0.011
$0.063POM_{CH}C_{AOM}$	≤0.063	POM – Charcoal	6.6	0.76	11	12.0	0.0160	0.041
$0.063C_{AOM}POM_{CL}$	≤0.063	AOM Coating	4.4	0.18	2	3.3	0.0010	0.003

Sample Code: XA_AB_B where: X: size fraction; A_A: most dominant organic matter characteristic; B_B: second dominant organic matter characteristic; POM: particulate organic matter; CL: coal; CH: charcoal; PH: phytoclast; AOM: amorphous organic matter; M: clay matrix; C: coating; CRA comp.: Canadian River Alluvium composite sample

wt %: weight fraction of subsample relative to composite; f_{oc}: organic carbon content; SA: surface area; PV: pore volume for pore diameter <66.6 nm; Intraparticle porosity (ε) = PV/(PV+1/ρ) (*32*) assuming that the bulk density of the grain (ρ) equals 2.65g/cm^3 .

Equilibrium Sorption Isotherms

Phenanthrene sorption isotherms demonstrated a Freundlich curvilinear shape, suggesting more than just partitioning of the chemical into the organic matter (some examples are given in Figure 2.2; note log-log plot with slope less than one indicating nonlinearity); this is true both for the composite sample and the subsamples. Freundlich parameters are presented in Table 2.3 for all samples. Sample (0.125 C_{AOM}) shows some deviations from the Freundlich type isotherm in the upper concentration range, which is attributed to experimental error due to dilutions above the instrument linear range. The K_{fr} value for the composite soil sample is not statistically different from the K_{fr} value calculated based on integrating results for subsamples at the 95% confidence level {(1100±170) versus (1500±260), respectively}. A correlation of sorption behavior to organic matter characteristics can only be carried out based on the organic carbon normalized distribution coefficients (K_{oc} values). Between all samples, K_{oc} values (based on K_d at C_e=1 μg/L) varied by two orders of magnitude (log K_{oc} of 4.7-6.3) and were always higher than K_{ow}-based estimates {log K_{oc} = 4.4; (*1*)}. By estimating sorption parameters based on K_{ow} it is automatically assumed that the organic matter is comparable with octanol and exhibits linear sorption isotherms, which is not true for any of the samples. Several researchers have presented results that disagree with K_{ow} based predictions (*8, 11, 19, 33, 34*). The differences observed within the samples can be attributed to the nature of the organic matter present as discussed further below. The fact that K_{oc}

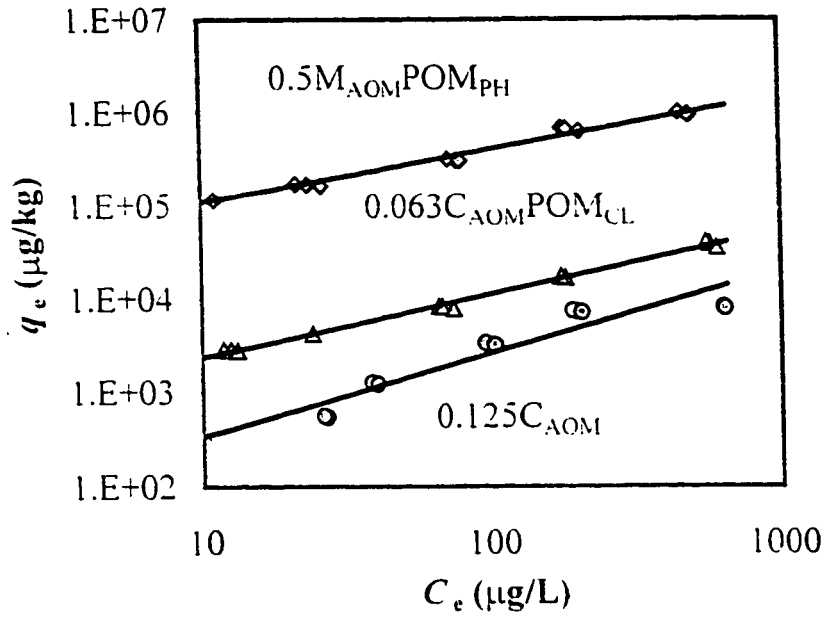


FIGURE 2.2 Phenanthrene sorption isotherms for three subsamples. The chemical in the sorbed phase [q_e (μg of chemical/kg of soil)] versus the chemical equilibrium concentration [C_e (μg/L)] in solution. Sample Code: XA_AB_B where: X: size fraction; A_A: most dominant organic matter characteristic; B_B: second dominant organic matter characteristic; M: clay matrix; AOM: amorphous organic matter; POM: particulate organic matter; PH: phytoclast; C: coating; CL: coal.

TABLE 2.3 Isotherm Results

Sample Code	wt	f_{oc}	N	K_{fr}	Obs.:	R^2	log K_{oc} at C_e = 1 µg/L	log K_{oc} at C_e = 1 mg/L
	(%)	(%)		$(\mu g/kg)(L/\mu g)^N$			95% CI	95% CI
CRA comp.	100	0.44 ± 0.027	0.65 ± 0.021	1100 ± 85	13	0.99	5.3 - 5.5	4.3 - 4.4
$0.5M_{AOM}POM_{PH}$	2.3	5.90 ± 0.640	0.57 ± 0.020	30000 ± 2500	15	0.98	5.6 - 5.8	4.4 - 4.5
$0.5POM_{CL}$	0.75	1.60 ± 0.076	0.55 ± 0.024	33000 ± 2100	15	0.98	6.3 - 6.4	4.9 – 5.1
$0.25POM_{PH}M_{POM}$	5.3	1.30 ± 0.061	0.69 ± 0.033	2700 ± 350	15	0.97	5.3 - 5.4	4.3 – 4.5
$0.25M_{POM}$	23	0.16 ± 0.014	0.74 ± 0.036	230 ± 37	15	0.97	5.1 - 5.2	4.3 – 4.5
$0.125C_{AOM}POM_{PH}$	18	0.51 ± 0.007	0.73 ± 0.032	700 ± 92	15	0.98	5.1 - 5.1	4.2 – 4.4
$0.125C_{AOM}$	40	0.10 ± 0.004	0.89 ± 0.091	43 ± 15	14	0.89	4.6 - 4.7	4.1 - 4.5
$0.063POM_{CH}C_{AOM}$	6.6	0.76 ± 0.038	0.57 ± 0.019	2900 ± 230	15	0.99	5.5 - 5.6	4.2 – 4.3
$0.063C_{AOM}POM_{CL}$	4.4	0.18 ± 0.004	0.68 ± 0.013	490 ± 27	15	1.00	5.4 - 5.5	4.4 – 4.5

Note: ± corresponds to ± 1 standard deviation

Mass Weighted K_{fr} = Sum (wt % * K_{fr} for each fraction)=1500 ± 130

wt %: weight fraction of subsample relative to composite; f_{oc}: organic carbon content; N: Freundlich exponent; K_{fr}: Freundlich constant; Obs.: number of observations for each isotherm; K_{oc}: organic carbon normalized sorption coefficient calculated at chemical equilibrium concentration (C_e) equal to 1 µg/L and 1 mg/L; 95% CI: 95% Confidence Interval.

values are as much as two orders of magnitude greater than K_{ow}-based estimates demonstrate that partitioning into organic carbon content alone is not enough to predict K_{fr} values. Log K_{oc} values were also calculated for a phenanthrene concentration of 1 mg/L; as concentrations approach solubility limits the K_{oc} values approach K_{ow}-based estimates.

Figure 2.3 presents a plot of log K_{oc} values versus Freundlich exponents (N) for low and high equilibrium phenanthrene concentration (1 μg/L and 1 mg/L, respectively). The plot demonstrates an apparent inverse relation between log K_{oc} and N for low equilibrium concentrations (i.e. as N increases, log K_{oc} values decrease). For higher chemical concentrations (close to phenanthrene's solubility limit of 1.29 mg/L), log K_{oc} values are almost the same for all subsamples and very close to the K_{ow}-based estimates (4.4). This observation is in agreement with Xia and Ball (*12*), who state that while at high concentrations linear partitioning dominates the sorption process and K_{ow}-based estimates are valid, at low concentrations a pore-filling process takes place resulting in overall nonlinear sorption isotherms. K_{oc} and N values depend on the processes involved and thus on the type of organic matter present, as further discussed below (see Table 2.3).

The lowest N and highest K_{oc} (log K_{oc} = 6.3) values were found for the subsample dominated by coaly POM particles ($0.5POM_{CL}$) while the highest N and lowest K_{oc} (log K_{oc} = 4.6) values were found for the subsample dominated by AOM coatings of quartz grains (see $0.125C_{AOM}$ in Table 2.3). It is obvious from the observed K_{oc} values that coaly POM particles, even when present as only 3% of the

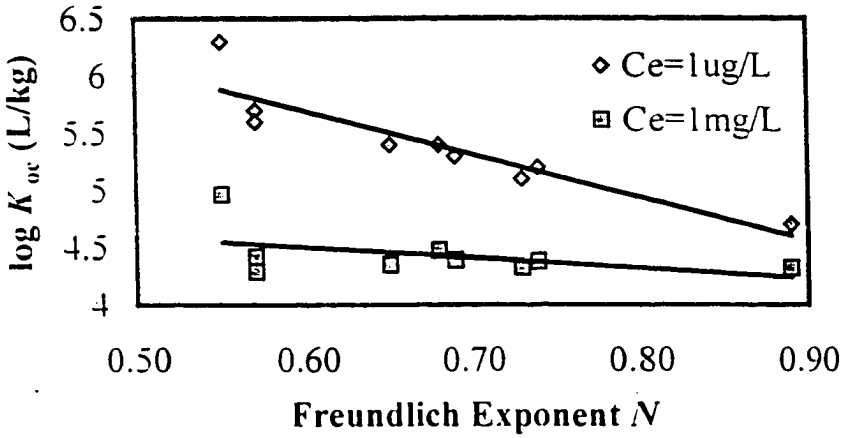


FIGURE 2.3 Logarithm of organic content normalized distribution coefficient (log K_{oc}) versus Freundlich exponent (N) at chemical equilibrium concentrations (C_e) equal to 1 μg/L and 1 mg/L.

composite organic matter, can contribute significantly to the overall sorption. The remaining subsamples show log K_{oc} and N values between these extremes (see Figure 2.3 and Table 2.3). For subsamples with organic matter consisting of both POM and AOM coatings, the highest K_{oc} value corresponds to samples with the highest charcoal present ($0.063POM_{CH}C_{AOM}$), followed by the sample with coal ($0.063C_{AOM}POM_{CL}$), with phytoclasts present in the third sample ($0.125C_{AOM}POM_{PH}$). In the sample with coal particles present in clay matrices ($0.25M_{POM}$), the log K_{oc} value is lower compared to the log K_{oc} value for a sample with isolated coal particles ($0.5POM_{CL}$). While sample ($0.5M_{AOM}POM_{PH}$) is dominated by AOM and phytoclasts, it contains some coaly particles as well (Table 2.1). Its high log K_{oc} (5.7) reflects the presence of coaly POM; while coaly POM does not dominate the sample f_{oc} it does dominate the sample reactivity. Mixed samples tend to have K_{oc} and N values more similar to the coaly particles even though they are present in low percentages. For a prediction of K_{oc} values the quantification of the strongly sorbing coaly POM is essential. Our ongoing work is focusing on this topic. Gustafsson et al. (*18*) found up to 2 orders of magnitude difference between phenanthrene K_{oc} with or without a K_{oc} percentage for what they called a soot phase.

The low N values associated with coal particles suggest that adsorption is dominant due to site limited-surface accumulation (*9*) and/or pore filling mechanism (*12*). Amorphous organic matter coatings of quartz grains produce the lowest K_{oc} value and the most linear isotherm in this study, likely due to the partitioning-type process occurring into these coatings. While the presence of phytoclast particles (i.e. $0.5M_{AOM}POM_{PH}$, $0.25POM_{PH}M_{POM}$) also increases the organic content, phytoclast K_{oc}

values are not as high as the one observed for coal particles. Phytoclast particles present more linear isotherms than coal, suggesting a partition-like mechanism. It has to be pointed out that even the lowest K_{oc} value of this study (log K_{oc} = 4.6-4.7; 95% confidence interval) is still significantly higher than K_{ow}-based estimates, likely due to the coaly POM present in all subsamples. The exact contribution of each organic matter component cannot be easily distinguished in these heterogeneous samples and only overall trends are discussed.

Sorption Kinetics

Figure 2.4 presents the apparent sorption coefficient as a function of time (K_{da}) normalized by the equilibrium distribution coefficient (K_d) for three of the subsamples, and also shows the numerical model results for these data. K_d is the value extrapolated from the Freundlich equation based on the expected aqueous equilibrium concentration $\{K_{fr} C_e^{(N-1)}=[(C_o - C_e)V] /(C_e M)$ where C_o is the initial concentration in solution, V is the solution volume, and M the mass of sediment$\}$. Table 2.4 presents results of experimental data and modeling work studying the kinetic sorption properties of the soil samples. The radii used in the model to fit the diffusion rate constant (D_a/a^2) were calculated based on the grain radii as described by Ball and Roberts (*20*). The diffusion rate constants represent transport both within the organic matter particles and the intraparticle pore space. For this reason grain radius might not always best describe the representative diffusion length.

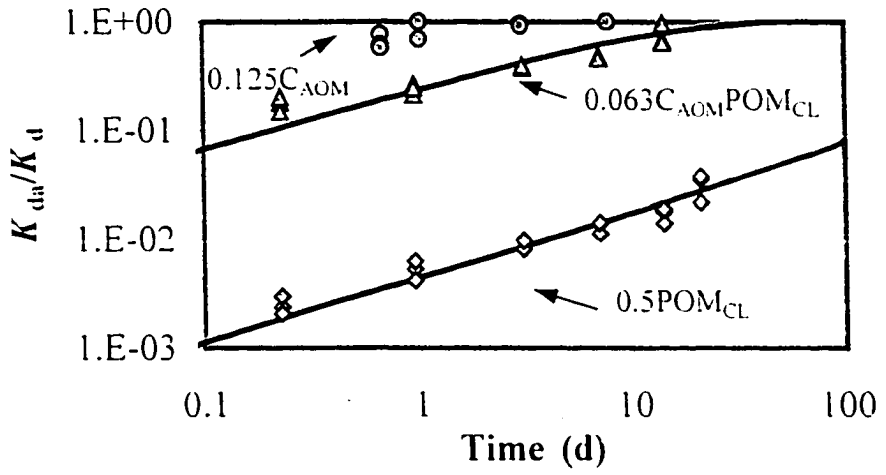


FIGURE 2.4 The apparent sorption coefficient normalized by the equilibrium sorption coefficient (K_{da}/K_d) versus time (d) for three of the subsamples as well as the numerical model results for two of the subsamples. K_d is the value extrapolated from the Freundlich equation based on the expected aqueous equilibrium concentration (given experimental parameters). The intraparticle model does not apply for sample ($0.125C_{AOM}$) because the process is not intraparticle diffusion and internal pore sorption but partitioning into the organic coatings on the exterior of the grains. Sample Code: XA_AB_B where: X: size fraction; A_A: most dominant organic matter characteristic; B_B: second dominant organic matter characteristic; C: coating; AOM: amorphous organic matter; POM: particulate organic matter; CL: coal.

TABLE 2.4 Kinetic Sorption Properties based on Numerical Modeling						
Sample Code	F	a	D_a/a^2	D_a	T 75%	Error
		(cm)	(1/s)	(cm^2/s)	(d)	
CRA comp. (actual sample)	0.56	0.0077	7.7 E-08	4.6 E-12	12	0.046
CRA comp. (pulverized)	0.27	0.0027	4.0 E-07	2.9 E-12	2	0.0023
$0.5M_{AOM}POM_{PH}$	0.79	0.0180	1.4 E-09	4.5 E-13	490	0.079
$0.5POM_{CL}$	0.98	0.0180	1.1 E-10	3.6 E-14	5700	0.040
$0.25POM_{PH}M_{POM}$	0.80	0.0089	1.1 E-08	8.7 E-13	70	0.035
$0.25M_{POM}$	0.55	0.0089	8.7 E-08	6.9 E-12	12	0.190
$0.125C_{AOM}POM_{PH}$	0.73	0.0044	7.6 E-08	1.5 E-12	12	0.040
$0.125C_{AOM}$	0.53	0.0044	N/A	N/A	<1	N/A
$0.063POM_{CH}C_{AOM}$	0.78	0.0027	3.7 E-08	2.8 E-13	20	0.042
$0.063C_{AOM}POM_{CL}$	0.79	0.0027	7.2 E-08	5.4 E-13	12	0.120 (0.027)*

F: fractional uptake at equilibrium (chemical mass on solid per total chemical mass); *a*: grain radius used in the numerical model and is not the effective radius in all cases; D_a/a^2: apparent diffusion rate; D_a: apparent diffusion coefficient (based on the radius of the grain size fraction, in some samples the effective diffusion radius maybe different, data are only presented for comparison purposes); T 75%: time to reach 75% equilibrium; Error: Mean weighted squared error (*22*).

*: For Sample ($0.063C_{AOM}POM_{CL}$) error in parenthesis is the error calculated for the one-component model when the first observation is ignored.; N/A: not analyzed intraparticle diffusion does not apply due to the partition nature of sorption in organic coatings.

The kinetic behavior of the two extreme but more homogeneous subsamples and a third heterogeneous sample (mixture of the two extremes) is presented in Figure 2.4. The fastest sorption kinetics was found in the subsample with AOM coatings ($0.125C_{AOM}$). The intraparticle diffusion model is not applied for this sample because the process is not intraparticle diffusion but partitioning into the organic coatings on the exterior of the grains. Sorption to this kind of organic matter is fast, as noted by other authors (*20*). The subsample dominated by POM (i.e. coal) ($0.5POM_{CL}$) is the slowest sample to reach sorption equilibrium and the intraparticle diffusion model fits the data well (Figure 2.4). The POM radius in this sample is equal to the grain radius. The organic matter of the third subsample ($0.063C_{AOM}POM_{CL}$) is a mixture of two organic matter types (AOM coatings and coal) and its kinetic behavior is in between that expected for subsamples dominated by each individual component. The intraparticle diffusion model does not fit the data as well for this third sample, fitting later data better than the earlier data. The earlier data fall above the model line suggesting the presence of a fast sorbing component in the sample (compare mean weighted squared error for this sample when including the first observation (0.120) versus ignoring this first data (0.027); Table 2.4).

Figure 2.5 presents various attempts to use the intraparticle diffusion model to fit the data for a mixed component subsample ($0.063C_{AOM}POM_{CL}$). Two different models were studied: (a) a one-component model (solid line in Figure 2.5), which assumes that the sample is homogeneous and all the components behave similarly, and (b) a two-component composite model (dashed line in Figure 2.5) which is

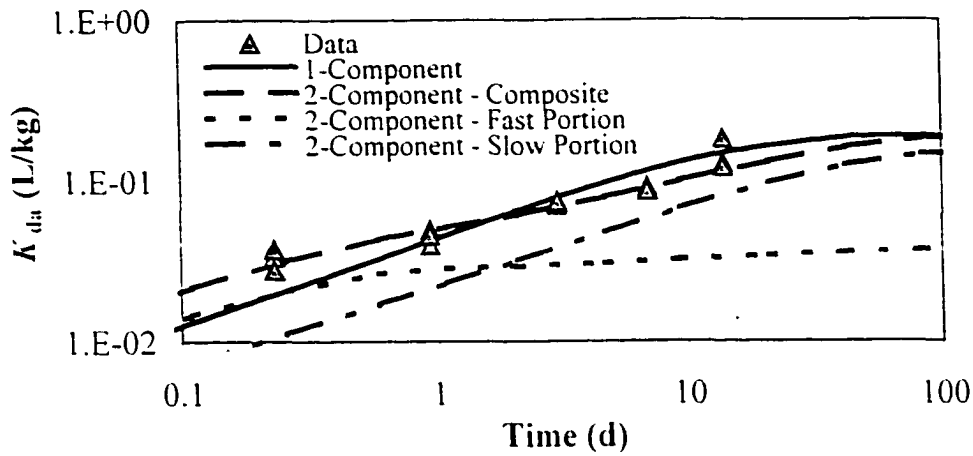


FIGURE 2.5 Intraparticle diffusion model lines for one of the subsamples. Apparent sorption distribution coefficient (K_{da}) (L/kg) versus time (d). Two different models were studied: (a) a one-component model (solid line), which assumes that the sample is homogeneous and all the components behave similarly, and (b) a two-component composite model (dashed line) which is actually a composite (superimpose) of 2 individual components (I) a fast component (dotted line) and (II) a slow component (dashed-dotted line) portion.

actually a composite (superposition) of 2 individual components (I) a fast component (dotted line in Figure 2.5) and (II) a slow component (dashed-dotted line in Figure 2.5) portion. The relative weight percent of the fast and slow components was adjusted until the two-component model best agreed with the experimental data. When the fast and slow components were incorporated into the model, the two-component model line agreed with the data better than the one-component line. The two-component model fits the earlier data and at the same time captures the behavior of the slow component better than the one-component model. Figure 2.5 also presents the kinetic behavior for both the fast and the slow component, corroborating the previously mentioned hypothesis that the fast component affects the earlier time data – reaches equilibrium within one day – while the slow component dominates the later data. We thus recommend the use of the intraparticle diffusion model as a one-component model for homogeneous samples, while the use of a multi-component model is required for heterogeneous samples (as suggested by Kleineidam et al. in ref *35*). Identifying the presence of organic coatings in the sample suggests the use of the two-component model.

The data in Table 2.4 also demonstrate the impact of having POM on sorption kinetics (see small apparent diffusion coefficient (D_a) values in Table 2.4). However, physical properties such as radius and intraparticle porosity are also important in interpreting the results. It is important to compare samples within the same grain size to draw conclusions on the effect of the organic matter type on sorption kinetics. For samples with phytoclast (e.g. $0.5M_{AOM}POM_{PH}$, $0.25POM_{PH}M_{POM}$), the diffusion radius could be smaller than the actual radius since the phytoclast particles usually

have cylindrical shape. The D_a value calculated with the smaller radius could also be smaller than the actual one. For samples with POM in matrices (e.g. $0.25M_{POM}$), D_a could be lower since the effective radius for POM is different from the grain size used. When comparing the three samples with AOM coatings and POM (i.e. $0.25POM_{PH}M_{POM}$, $0.063POM_{CH}C_{AOM}$, and $0.063C_{AOM}POM_{CL}$) the sample with the phytoclast is faster than the other two (see D_a values in Table 2.4).

Figure 2.6a demonstrates that D_a values decreased with increasing f_{oc} in this research. However the data are highly scattered around the line that describes this inverse trend. This data scattering is decreased when D_a is plotted against K_d in Figure 2.6b. The data presented in Figures 2.6a and 2.6b illustrate that with increasing sorption more time is required to reach equilibrium (i.e., sorption reduces the effective diffusion rates and thus increases the time necessary to reach equilibrium). In this case, f_{oc} alone is not enough to explain how sorption affects the effective diffusion coefficient; the K_d value is more representative of the sorption behavior since more than one mechanism is affecting sorption in the subsamples. D_a values are not true for all samples since the grain radius used in the numerical model is different for some samples than the effective radius. However, D_a/a^2 also follows the same trend, supporting the conclusion of diffusion-limited sorption.

Table 2.5 presents a qualitative comparison of the sorption characteristics for each organic matter group evaluated in the CRA. While we divide the samples into two main groups: (a) coaly POM and (b) young soil organic matter, some subsamples possess a mixture of these two groups. Coaly POM presents more nonlinear

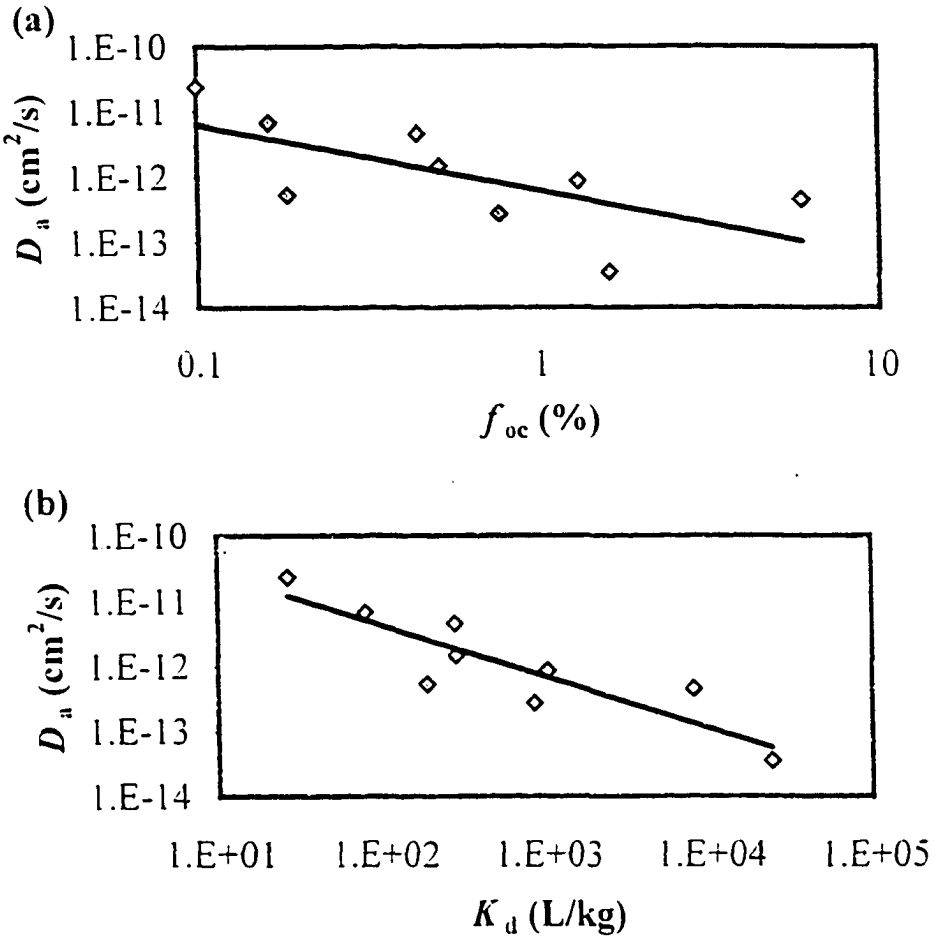


FIGURE 2.6 Apparent diffusion coefficient (D_a) (cm^2/s) versus (a) soil organic content f_{oc} (%) and (b) sorption distribution coefficient K_d (L/kg).

TABLE 2.5 Qualitative Comparison of Organic Matter Sorption Characteristics

Organic Matter Groups	Petrography	Isotherm	K_{oc}	Mechanism	Kinetics
Coaly Particulate Organic Matter	Particulate Organic Matter Isolated and in Clay Matrices (Coal, Charcoal)	More nonlinear	High	Adsorption (site limited)	Slower
Young Soil Organic Matter	Particulate Organic Matter (Phytoclast), Amorphous Organic Matter in Clay Matrices, and Amorphous Organic Matter Coatings	Less nonlinear	Low	Partitioning	Faster
Mixture of two groups	Mixed	Nonlinear	Intermediate	Mixed	Intermediate

isotherms, higher K_{oc} values, slower kinetics (Tables 2.3 and 2.4), and the sorption mechanism is site limited - site limited adsorption and/or pore filling, as discussed in Chiou and Kile (*11*) and Xia and Ball (*12*). Young soil organic matter results in more linear sorption isotherms (or more linear than the coaly organic matter), lower K_{oc} values that are close to K_{ow}-based estimates (4.4 for phenanthrene), faster sorption kinetics (Tables 2.3 and 2.4), and a partitioning sorption mechanism (*1*, *12*). The mixture of these two groups tends to have the characteristics of the coaly POM. Even if the fraction percentage of the coaly POM is low, its impact on sorption behavior can be significant at low chemical concentrations (this study; ref *18*).

In summary, our observations demonstrate that even a fairly simple river alluvium sample can contain heterogeneous organic matter and that this heterogeneous organic matter can significantly impact sorption equilibrium and kinetics. In addition, we have shown that petrographic characteristics of the heterogeneous organic matter can help explain the variations in sorption properties. For example, the presence of coaly particles in a sample increases its sorption capacity, results in nonlinear sorption isotherms, and increases the equilibration time. Even small fractions of coaly materials can dominate the sorption capacity. Conversely, organic matter coatings have lower sorption capacities and equilibrate rapidly, requiring the addition of a fast sorption term in an intraparticle diffusion model. Recognizing the presence and importance of organic matter heterogeneities will facilitate interpretation of sorption data and could lead to prediction of sorption behavior for samples with heterogeneous organic matter.

Acknowledgment. This study was partially funded by the U.S. National Science Foundation through the EPSCoR program. The authors would like to thank Renate Riehle for TOC measurements and Hermann Rügner for BET measurements, both from the Universität Tübingen. This research was conducted at the Universität Tübingen while D. A. Sabatini was on sabbatical there as a Senior Fulbright Scholar and while the first author, his PhD student from the University of Oklahoma, was conducting research with him at the Universität Tübingen. Samples studied in this research were taken from the Norman Landfill Research Site, which is a USGS Toxic Substances Research Site (http://wwwok.cr.usgs.gov/norlan/site.html). We acknowledge the assistance of Mr. Scott Christenson in obtaining samples from the site.

Nomenclature

a	grain radius (cm)
AOM	amorphous organic matter
C	coatings
C	chemical aqueous concentration
C_e	equilibrium aqueous concentration of chemical (μg/L)
CH	charcoal
CL	coal
D_a	apparent diffusion coefficient (cm^2/s)
D_{aq}	aqueous diffusion coefficient (cm^2/s)

D_a/a^2 diffusion rate constant (1/s)

ε intraparticle porosity

F fractional uptake at equilibrium (chemical mass on solid per total chemical mass)

f_{oc} fraction organic carbon content (%)

K_d sorption distribution coefficient (L/kg)

K_{da} apparent sorption distribution coefficient (L/kg)

K_{fr} Freundlich sorption constant $[(\mu g/kg)(L/\mu g)^N]$

K_{oc} organic content normalized distribution coefficient (L/kg)

K_{ow} octanol-water partition coefficient

N Freundlich exponent

PH phytoclast

POM particulate organic matter

PV pore volume for pore diameter <66.6 nm (cm^3/g)

q_e mass of chemical sorbed per mass of soil ($\mu g/kg$)

ρ bulk density

r radial distance from the center of the grain

SA surface area (m^2/g)

τ_f tortuosity factor

t time (d)

T 75% time to reach 75% equilibrium (d)

wt % weight fraction of composite (%)

References

1. Karickhoff, S.W.; Brown, D.S.; Scott, T.A. *Water Research* **1979**, 13, 241-248.

2. Estrella, M.R.; Brusseau, M.L.; Maier, R.S.; Pepper, I.L.; Wierenga, P.J.; Miller, R.M. *Appl. Environ. Microbiol.* **1993**, 59, 4266-4273.

3. Chiou, C.T.; McGroddy, S.E.; Kile, D.E. *Environ. Sci. Technol.* **1998**, 32, 264-269.

4. Luthy, R.G.; Aiken, G.R.; Brusseau, M.L.; Cunningham, S.D.; Gschwend, P.M.; Pignatello, J.J.; Reinhard, M.; Traina, S.J.; Weber, W.J.Jr.; Westall, J.C. *Environ. Sci. Technol.* **1997**, 31, 3341-3347.

5. Barber, L.B.; Thurman, M.E.; Runnells, D.D. *J. Cont. Hydrol.* **1992**, 9, 35-54.

6. Weber, W.J.Jr.; McGinley, P.M.; Katz, L.E. *Environ. Sci. Technol.* **1992**, 26, 1955-1962.

7. Garbarini, D.R.; Lion, L.W. *Environ. Sci. Technol.* **1986**, 20, 1263-1269.

8. Grathwohl, P. *Environ. Sci. Technol.* **1990**, 24, 1687-1693.

9. Weber, W.J.Jr.; Huang, W. *Environ. Sci. Technol.* **1996**, 30, 881-888.

10. Xing, B.; Pignatello, J.J. *Environ. Sci. Technol.* **1997**, 31, 792-799.

11. Chiou, C.T.; Kile, D.E. *Environ. Sci. Technol.* **1998**, 32, 338-343.

12. Xia G.; Ball W.P. *Environ. Sci. Technol.* **1999**, 33, 262-269.

13. Huang, W.; Weber, W.J.Jr. *Environ. Sci. Technol.* **1997**, 31, 2562-2569.

14. Young, T.M.; Weber, W. J.Jr. *Environ. Sci. Technol.* **1995**, 29, 92-97.

15. Leboeuf, E.J.; Weber, W.J.Jr. *Environ. Sci. Technol.* **1997**, 31, 1697-1702.

16. Graber, E.R.; Borisover, M.D. *Environ. Sci. Technol.* **1998**, 32, 3286-3292.

17. Chiou, C.T. *Environ. Sci. Technol.* **1995**, 29, 1421-1422.

18. Gustafsson, Ö.; Haghseta, F.; Chan, C.; MacFarlane, J.; Gschwend, P.M. *Environ. Sci. Technol.* **1997**, 31, 203-209.

19. Kleineidam, S.; Rügner, H.; Ligouis, B.; Grathwohl, P. *Environ. Sci. Technol.* **1999**, 33, 1637-1644.

20. Ball, W.P.; Roberts, P.V. *Environ. Sci. Technol.* **1991a**, 25, 1237-1249.

21. Grathwohl, P. *Diffusion in Natural Porous Media: Contaminant Transport, Sorption/Desorption and Dissolution Kinetics*. Kluwer Academic Publishers, Boston, Massachusetts, 1998.

22. Rügner, H.; Kleineidam, S.; Grathwohl, P. *Environ. Sci. Technol.* **1999**, 33, 1645-1651.

23. Pignatello, J.J.; Xing, B. *Environ. Sci. Technol.* **1996**, 30, 1-11.

24. Grathwohl, P.; Reinhard, M. *Environ. Sci. Technol.* **1993**, 27, 2360-2366.

25. Harmon, T.C.; Roberts, P.V. *Environ. Sci. Technol.* **1994**, 28, 1650-1660.

26. Van Krevelen, D.W. *Coal Typology, Physics, Chemistry, and Constitution*, 3rd Edition, Elsevier, 1993.

27. Tyson, R.V. *Sedimentary Organic Matter: Organic Facies and Palynofacies*. Chapman & Hall, London, 1995.

28. Montgomery, J.H.; Welkom, L.M. *Ground Water Chemicals Desk Reference*. Lewis Publishers, Inc., Chelsea, Michigan, 1990.

29. Ball, W.P.; Xia, G.; Durfee, D.P.; Wilson, R.D.; Brown, M..J.; Mackay, D..M. *GWMR* **1997**, 17, 104-121.

30. Karapanagioti, H.K.; Sabatini, D.A.; Kleineidam, S.; Grathwohl, P.; Ligouis, B. *Physics and Chemistry of the Earth* **1999, 24, 535-541**.

31. Jäger, R. *Modellierung Nichtlinearer Intrapartikel-Diffusion in Heterogenem Aquifermaterial*, Diploma Thesis, University of Tübingen, FRG, 1997.

32. Ball, W.P.; Roberts, P.V. *Environ. Sci. Technol.* **1991b**, 25, 1223-1237.

33. Barber, L.B. *Environ. Sci. Technol.* **1994**, 28, 890-897.

34. Schüth, C. *Sorptionskinetik und Transportverhalten von Polyzyklischen Aromatischen Kohlenwasserstoffen (PAK) im Grundwasser*. Dissertation. University of Tübingen, FRG. 1994.

35. Kleineidam, S.; Rügner, H.; Grathwohl, P. *Environ. Toxic. Chem.* **1999**, accepted.

CHAPTER 3

IMPACTS OF HETEROGENEOUS ORGANIC MATTER ON PHENANTHRENE SORPTION: DIFFERENT AQUIFER DEPTHS

ABSTRACT

Alluvial aquifer samples from the same depth but different locations and from different depths at the same location were characterized and evaluated both for the nature of their organic matter and their sorption properties. Both equilibrium and kinetic sorption were evaluated using batch studies with phenanthrene. Organic petrology was used both qualitatively and quantitatively to explain and predict the patterns of sorption for each sample. Organic carbon content values varied by one order of magnitude and sorption capacities varied by two orders of magnitude within a given depth and location for these samples. The sorption isotherms ranged from nonlinear to virtually linear. The organic content normalized distribution coefficients (K_{oc}) varied significantly between organic matter subgroups as did the time to reach equilibrium. We were able to correlate these variations in sorption behavior with the organic matter type in subgroups. K_{oc} values were assigned to each organic matter subgroup and were used along with the fraction of each organic matter subgroup to predict the composite K_{oc} values. Close agreement between predicted and measured K_{oc} values validated this approach. Using the subgroup K_{oc} values and literature fraction organic carbon (f_{oc}) values the sorption distribution coefficients were also

predicted within the 95% confidence intervals for the measured values. Our results also demonstrate that opaque organic matter fractions dominate the sorption process, and that quantifying this fraction alone can virtually predict the sample K_{oc} value.

INTRODUCTION

Sorption of hydrophobic organic compounds is directly related to the organic matter naturally present in the sediments. Recognizing the effects of the organic matter nature on the sorption properties was a significant step in studying this important process (Garbarini and Lion, 1986; Grathwohl, 1990; Weber and Huang, 1996; Xing and Pignatello, 1997; Gustafsson et al., 1997; Chiou and Kile, 1998; Kimani Njoroge et al., 1998; Xia and Ball, 1999; Kleineidam et al., 1999; Rügner et al., 1999; Karapanagioti et al., 1999a). While many researchers have proposed conceptual models of the organic mater in sediments according to their sorption behavior (Young and Weber, 1995; Weber and Huang, 1996; Xing and Pignatello, 1997; summarized in Luthy et al., 1997), the organic matter domains and their sorption properties are not yet well established (Graber and Borisover, 1998).

Recently it has been recognized that high surface area carbonaceous material (e.g. charcoal-like material) may be present in the sediment organic matter. Sorption capacity and nonlinearity have been attributed to small amounts of this material (Chiou, 1995; Chiou and Kile, 1998). Kimani Njoroge et al. (1998) assumed a dual behavior of organic matter based on its occurrence in the surface soil profile. They used a regression analysis to determine the sorption behavior for the shallow-like and

deep-like (less hydrophobic) organic matter, and observed one order of magnitude variability in organic carbon content-normalized distribution coefficient (K_{oc}) values. They were able to relate the organic carbon fraction values for each organic matter type (i.e., shallow or deep–like) to the organic carbon fractions measured for the extractable humic and fulvic acids of each soil depth.

Gustafsson et al. (1997) used a thermal oxidation method to measure the organic carbon fraction that would be attributed to two different organic phases: (a) soil organic matter and (b) a soot phase. The K_{oc} value for the soil organic matter was estimated based on octanol-water partition coefficient (K_{ow}) (Karickhoff et al., 1979) and the K_{oc} for the soot phase was taken from literature reports on activated carbon. Using this analysis they were able to predict the sorption capacity of their samples.

Kleineidam et al. (1999) used organic petrology methods to characterize organic matter in sedimentary rocks. They were able to assign a range of K_{oc} values for the different organic matter facies, and demonstrated the heterogeneity of soil organic matter both in terms of nature and sorption behavior. Karapanagioti et al. (1999a) used a similar approach and demonstrated the heterogeneity of the organic matter within an aquifer sediment sample. In this study it was also evident that the presence of more mature organic matter facies impacted sorption more than the presence of recent organic matter in higher quantities. While both of these studies used organic petrology as a qualitative tool to explain the variabilities between observed sorption results and literature values, neither study quantitatively predicted sorption based on organic petrology characterization.

Karapanagioti et al. (1999a) demonstrated the heterogeneity of organic matter within an aquifer sediment sample. Obvious questions raised by this work are: (a) how representative is this sample of the entire aquifer and (b) what organic matter heterogeneities can be found with different aquifer depths that would affect the sorption properties. West et al. (1994) found the organic carbon distribution to be highly complex within an aquifer. They reported the occurrence of organic matter both in particulate form and in organic coatings, with the majority being organic coatings. Kimani Njoroge et al. (1998) found a decrease in organic matter hydrophobicity with depth, but they limited their research to surface soils (up to 2.3 m depth). Allen-King et al. (1998) tried to correlate sorption and hydraulic conductivity using a facies-based approach. However, since they did not include the organic carbon content of each facies into their analysis, some of their sorption results are difficult to interpret based on the nature of the facies alone.

The objectives of this study were: (1) to characterize organic matter heterogeneity both spatially and with depth in an alluvial aquifer and (2) to quantitatively predict K_{oc} and sorption distribution coefficient (K_d) values for each sediment based on organic petrology characterization. This study is unique in not only characterizing the sediment organic matter of different aquifer depth samples, but also quantitatively relating organic petrological properties with the sediment sorption behavior. We propose a method for utilizing easily obtainable organic petrology properties to predict K_{oc} values for a given sample.

MATERIALS AND METHODS

The Canadian River Alluvial (CRA) aquifer material was sampled from the closed Norman Landfill, which is a U.S.G.S. Toxic Substances Research site. The shallow sample (~3 ft) was taken just below the water table near well 47 (http://wwwok.cr.usgs.gov/norlan/site.html). The remaining samples were from different depths of a common core taken south of well 80, which was obtained with a geo-probe rig.

All samples were air-dried before they were used for analysis. Sieve and hydrometer tests were used to determine the grain size distribution for the sand and the sandy loam layers, respectively (Lambe, 1951; Page et al. 1982). The organic carbon content for all samples studied in sorption experiments was analyzed by dry combustion at 850 °C (Model 183 Boat Sampling Module, Rosemount) and quantified by an infrared detector for CO_2 (Horiba PIR-2000). Remaining samples were analyzed for organic carbon content by the EPA laboratory in Ada, OK, using RSKSOP-102 and RSKSOP-120. Hydraulic conductivities were measured with constant head and falling head column tests for the sand and the sandy loam layers, respectively (Bouwer, 1978). Surface area and intraparticle meso-porosity were measured using N_2 and the BET method (ASAP 2010, Micromeritics). The external surface area, calculated based on the grain size, accounted for less than 0.1% of the surface area measured for all samples.

Phenanthrene was used as the model chemical in this study. Phenanthrene ($C_{14}H_{10}$) is a three ring polycyclic aromatic hydrocarbon with: (a) molecular weight:

178 g/mol, (b) solubility: 1.29 mg/L at 25 °C, (c) Henry's law constant: 2.6×10^{-5} atm m^3/mol, and (d) log K_{ow}: 4.6 (Montgomery and Welkom, 1990). The estimated log K_{oc} of phenanthrene is 4.4 (Karickhoff et al., 1979). Phenanthrene was chosen because of its high hydrophobicity (K_{ow}), low volatility (Henry's law constant), and simplicity of analysis. Phenanthrene was prepared as a 100 mg/L stock solution in methanol, so that the percentage of methanol introduced in each sample was always below 1%. Test solutions were prepared in synthetic groundwater (deionized water with 44 mg/L $CaCl_2.2H_2O$, 14 mg/L $CaSO_4$, and 17 mg/L $NaHCO_3$). Sodium azide (NaN_3) was added at 200 mg/L to inhibit bacterial growth and thus biodegradation during batch studies.

All equilibrium sorption experiments were conducted in triplicate in 10 mL crimp-top glass vials. Sediment samples for equilibrium studies were pulverized to assure equilibrium in a reasonable time (7 days). Variable phenanthrene concentrations were added to the sediment samples and shaken for 7 days in the dark at room temperature (around 23 °C). Headspace in the vials was kept to a minimum. Solid-to-water ratios were varied to account for differing sorption capacities of the subsamples (i.e., to achieve sufficient sorption so that it could be easily quantified while keeping aqueous concentration above the detection limit).

All sorption kinetic experiments were conducted in triplicate in 20-100 mL crimp-top glass vials. The initial phenanthrene concentration was 100 μg/L and the solid-to-water ratio was different for each subsample depending on the sorption capacity (as above). The vials were stored at room temperature (around 23 °C), in the dark and shaken periodically. Measurements were taken at various time intervals.

For both isotherm and kinetic batch experiments, aqueous phenanthrene concentrations were measured by an RF-551 Shimadzu variable wavelength fluorescence detector in cuvette mode. For each batch experiment blank samples were prepared and monitored (i.e., phenanthrene without sediment). These blank samples did not indicate any significant phenanthrene degradation or sorptive losses on the glassware for the duration of the experiment. Sediments without phenanthrene blanks verified that the sediment did not generate peaks in the same wavelength as phenanthrene. Some samples were analyzed both in the HPLC and cuvette mode with both a UV and a fluorescence detector; these readings showed no significant differences.

ORGANIC PETROLOGY METHODS

The sediment sample organic matter was characterized by preparing dispersed organic pellets with Buehler Epoxide epoxy. The pellets were polished with a Buehler Ecomet III Grinding and Polishing Apparatus. Initially, organic matter identification was attempted with reflected light. However, due to the low fraction organic carbon content (f_{oc}), only a couple of recent organic particles were located. To optimize the identification, the organic matter required concentration prior to analysis.

The organic matter of 4 depth samples was isolated and strew slides of the concentrated organic matter were prepared by Core Laboratories, Inc. Carrollton, TX. Microscopic investigations were conducted at the University of Oklahoma using a Vickers M17 Research Microscope. Organic matter was identified and characterized

using white and fluorescent light in transmitted and reflected light mode. The percentages of each organic matter subgroup were determined using a point counter and the sizes of the organic particles were determined using a grid of 38 by 38 μm.

Based on the color and appearance of the amorphous organic matter, Core Laboratories estimated the thermal appearance index (TAI) of the organic matter. The organic matter present in all 4 samples had a TAI equal to 1, suggesting recent organic matter.

The classification of organic matter that is used in this chapter is based on the palynological schematic key for organic matter in thermally immature to marginally mature sediments, as proposed by Tyson (1995). Figure 3.1 summarizes the palynological classification scheme used (i.e., since there were no zooclast particles present this group is omitted from Figure 3.1). The organic matter found in the samples is divided into two main groups that are then divided into additional subgroups: (a) structureless formations, both fluorescent and non-fluorescent, called the "amorphous group" and (b) structured particles, both opaque up to edge, non-fluorescent and translucent (at least at edge of particle) fluorescent and non-fluorescent particles called the "phytoclast group".

The fluorescent subgroup of the amorphous group is typically heterogeneous, consisting of a truly amorphous matrix ultimately derived from phytoplankton or bacteria and is called amorphous organic matter (AOM). The non-fluorescent subgroup of the amorphous group is primarily intra- and extra-cellular amorphous material produced by biodegradation of land plants and is called humic gel. The

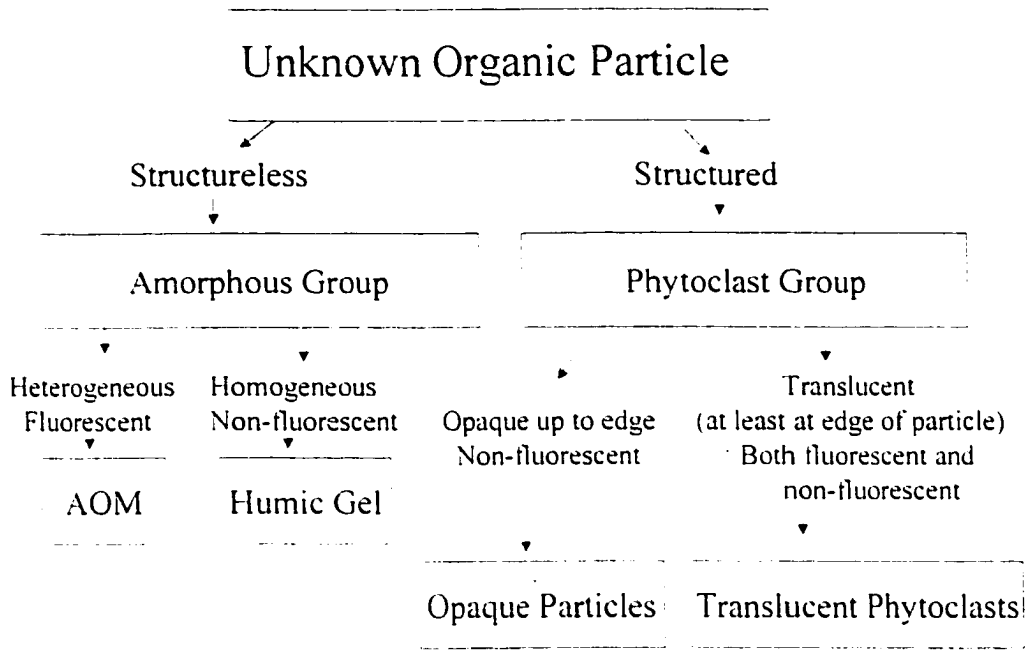


FIGURE 3.1 Palynological kerogen classification scheme for organic mater subgroups present in this study (for more details see Tyson, 1995).

opaque non-fluorescent particles of the phytoclast group are oxidized or carbonized woody tissues including charcoal and are called opaque particles. The translucent particles of the phytoclast group include recent woody fragments that might fluoresce or not as well as spores, pollen, and cuticles that would fluoresce and are called translucent phytoclast particles. These are the 4 organic matter subgroups that were found in our samples and are used to explain the sorption behavior of the sediment samples.

DATA MODELING

For linear isotherms, the sorption distribution coefficient K_d can be described by:

$$K_d = q_e / C_e \tag{3.1}$$

where q_e is the mass of chemical sorbed per unit mass of sediment and C_e is the equilibrium concentration. Nonlinear isotherms can be described by the Freundlich equation:

$$q_e = K_{fr} C_e^{\ N} \tag{3.2}$$

where K_{fr} is the Freundlich sorption constant and N is the Freundlich exponent. For nonlinear isotherms K_d can be considered concentration-dependent as follows:

$$K_d = K_{fr} C_e^{N-1} \quad (3.3)$$

The organic carbon content-normalized distribution coefficient (K_{oc}) is described by:

$$K_{oc} = K_d / f_{oc} \quad (3.4)$$

where f_{oc} is the fraction organic carbon content of the sample. For nonlinear isotherms K_{oc} is also concentration dependent. At a chemical concentration of unity, K_d equals K_{fr} and $K_{oc} = K_{fr} / f_{oc}$.

Gustafsson et al. (1997) suggested the presence of a soot-carbon fraction in soil organic carbon that affects the soil sorption behavior. They predicted K_d values according to the following relationship:

$$K_d = f_{oc} K_{oc} + f_{sc} K_{sc} \quad (3.5)$$

where f_{sc} is the soot-carbon fraction and K_{sc} is the soot-carbon-normalized partition coefficient.

Kimani Njoroge et al. (1998) assumed there are two different types of organic matter, referred to as the shallow-like and the deep-like. The shallow soils presented the shallow-like behavior, the deep soils the deep-like behavior and the soils in between had a mixed behavior. The deep-like organic matter is less sorbing than the shallow-like. They predicted K_d values according to the following relationship:

$$K_d = f_{oc\text{-}shallow} K_{oc\text{-}shallow} + f_{oc\text{-}deep} K_{oc\text{-}deep} \quad (3.6)$$

where $f_{oc\text{-}shallow}$ and $f_{oc\text{-}deep}$ are mass fractions of shallow-like f_{oc} and deep-like f_{oc}, and $K_{oc\text{-}shallow}$ and $K_{oc\text{-}deep}$ are K_{oc} values assigned to these two different organic matter types. Their observations and model are based on samples of a soil profile extending only 2.3 m below surface.

We will assume that each organic matter subgroup contributes to the sediment sorption behavior in a different manner and will attempt to determine the cumulative K_{oc} value for each sample. By summing the products of the subgroup K_{oc} values (K_{ocOM}) and particle fractions, estimated based on the relative number of particles ($\%OM_i = OM_i / OM_b$), the cumulative K_{oc} value for each sample can be estimated using:

$$K_{oc} = \sum \% OM_i K_{ocOMi} \quad (3.7)$$

where the indices i and b are used to distinguish values referring to an individual subgroup and to the bulk sample, respectively.

An alternative method for estimating sorption is to assign a fraction organic carbon ($\%OC_{OMi}$) to each organic matter subgroup. The total sample $\% OC_b$ would be:

$$\% OC_b = \sum \% OM_i \% OC_{OMi} \quad (3.8)$$

In this case the K_d will be predicted based on:

$$K_d = \sum K_{ocOM_i} (\% OM_i \ \% OC_{OM_i} / \% OC_b) f_{oc} \quad (2$$

where $[(\% OM_i \ \% OC_{OM_i} / \% OC_b) f_{oc}]$ is the estimated fraction of f_{oc} found in e organic matter subgroup.

Solute diffusion from an aqueous phase into spherical porous grains can described by Fick's 2nd law:

$$\partial C / \partial t = D_a [(\partial^2 C / \partial r^2) + (2\partial C / r\partial r)] \quad (3$$

where C is the concentration of the chemical, t is time, D_a is the apparent diffu coefficient, which accounts for sorption-retarded diffusion and intraparticle tortuo and r is the radial distance from the center of the grain. In the present study, to m nonlinear sorption a numerical solution of Fick's 2nd law was utilized. The nume model is based on the finite difference method using the Crank-Nicholson appro as described by Jäger (1997). Model input includes the grain radius, the soli water ratio, the initial water concentration, the Freundlich parameters, the density and the intraparticle porosity. In this study the numerical model was use fit the sorption kinetic curves by minimizing the mean weighted squared between predicted and measured K_d values. The model produces values for apparent diffusion rate constant D_a/a^2. The sorptive uptake curves, expresse

normalized K_d versus time, are relatively insensitive to different values of fracti uptake at equilibrium (F) - the chemical mass on solid per total chemical mass - allow comparison of sorptive uptake at different solid-to-water ratios in b experiments (Ball and Roberts, 1991; see Grathwohl, 1998 for an excellent summa

RESULTS AND DISCUSSION

Site Description / Fluvial History and Aquifer Profile

The closed Norman Landfill, a U.S.G.S. Toxic Substances Research Sit located in Cleveland County, OK (http://wwwok.cr.usgs.gov/norlan/site.html). site is part of the South Canadian River alluvium in Central Oklahoma. The aq of interest is within the Canadian River Alluvium (CRA), a quaternary formation thickness ranging from 0 to 13 meters (Breit et al., 1996). The quaternary all formation overlies the Hennessey Group that is the youngest of the Per formations in the county. The Hennessey consists of reddish brown shale with s interbeds of siltstone and fine-grained sandstone (Soil Survey of Cleveland Co 1987). The Hennessey group has a low transmissivity and is considered the aqui lower confining layer.

The Quaternary alluvium consists mainly of sand, silt, clay, and some g (detailed results provided below). The sediments eroded from Permian strata w and to the west of the county, and from rock units lying west and northwest withi South Canadian River drainage basin. Quaternary sediments, generally depo

within the past million years, were laid down mainly as flood plain or alluvial ter deposits. Some of the sand and silts have been windblown into dunes (Soil Surve Cleveland County, 1987).

The first 6.5 ft of the CRA formation have been characterized as Gracemore Series. Gracemore sediments were formed in sand deposits by moving water near the South Canadian River. The first foot is characterized as lo fine sand whereas sediments from 1 to 6.5 ft are characterized as fine sand with 35 weight % fines and less than 1% organic carbon content (Soil Survey of Cleve County, 1987). Depths to the water table range from 0.5 to 5 ft (Soil Surve Cleveland County, 1987; Dunlap et al., 1976).

Coring results suggest that the aquifer can be divided into five general d zones (see Table 3.1 and Figure 3.2). Starting from the surface there are two zones (Zones 1 and 2) with the upper sand zone being finer and containing hi organic carbon. These 2 zones constitute the shallow aquifer. The next zon consists of two sandy loam layers with a sand layer intermixed. This zone (3) has hydraulic conductivity and an order of magnitude higher organic carbon co compared to the aquifer sand zones (1, 2, and 4) (see Figure 3.2). The 4th zone (another sand layer with coarser grain size than the first and second zone, whi consistent with the sedimentation theory – coarser particles settle first. This extends from 20 to 32 ft below land surface and comprises the lower alluvial aq The distinction between the upper and lower aquifer is not always apparent (Fi

TABLE 3.1 Aquifer Profile – Core Samples Taken South of Well 80

Zone	Depth	Median grain size	passed 200 sieve (< 75μm)	f_{oc}	K	Classification
	(ft)	(μm)	(%)	(%)	(cm/s)	U.S.D.A.
1 (1)[a] (1')[b]	0-6.5 (6-6.5) (~3)	89 (89) (89)	7.0 (4) (11)	0.0480±0.0056 (0.041) (0.4000±0.0920)	1.6E-03 ± 2.6E-04 (N/A) (N/A)	very fine sand (very fine sand) (very fine sand)
2 (2)	6.5-12 (6.5-8)	200 (180)	1.2 (0.7)	0.0140±0.0100 (0.021)	7.2E-03 ± 2.2E-04 (N/A)	fine sand (fine sand)
3 (3)	12-16 (14-16)	210 (210)	33 (27)	0.3400±0.2000 (0.200)	8.2E-05 ± 1.3E-05 (N/A)	sandy loam (sandy loam)
3a	16-18	210	2.3	0.0140	3.0E-03 ± 1.5E-04	fine sand
3b	18-20	210	37	0.2200	4.1E-04 ± 4.0 E-05	sandy loam
4 (4)	20-32 (28-30)	330 (350)	2.8 (1.8)	0.0081±0.0092 (0.0260)	2.1E-02 ± 4.3E-04 (N/A)	medium sand (medium sand)
4a	32	330&gravel	2.2	0.0570	N/A	medium sand with gravel
4b	33	330&gravel	41	0.0570	N/A	sandy loam
4c	34	330&gravel	2.2	0.0570	N/A	medium sand with gravel
5	35	10	72	0.0270	8.5E-05 ± 5.2E-05	silt loam

f_{oc}: fraction organic carbon content; K: hydraulic conductivity measured in the laboratory; N/A: not analyzed; U.S.D.A.: United States Department of Agriculture

[a] Sample data in parentheses are for the samples that were used in the sorption studies.

[b] Sample taken near well 47.

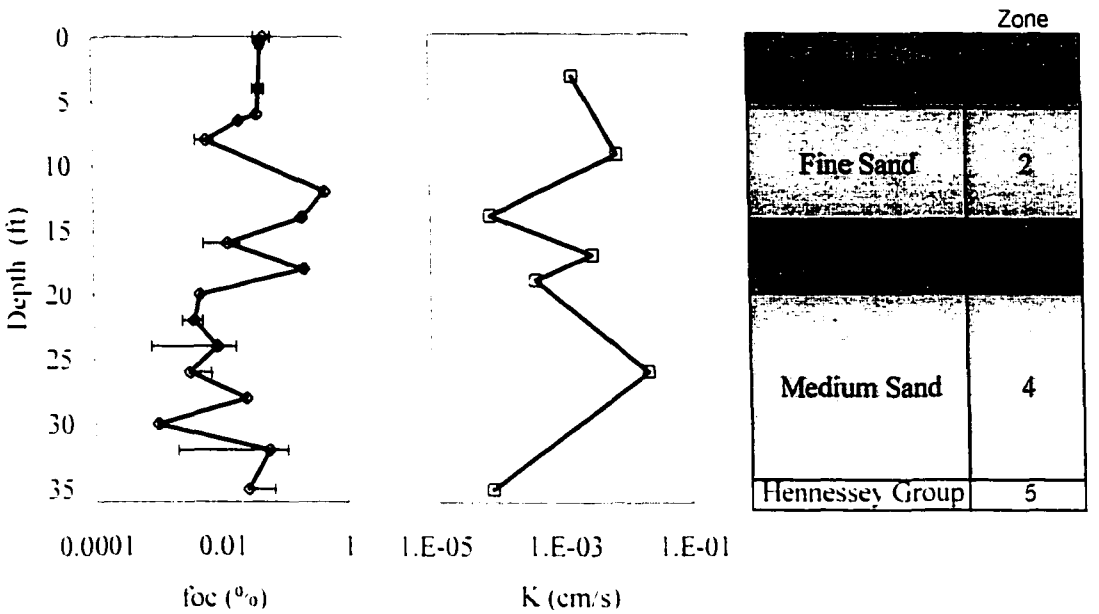


FIGURE 3.2 Norman Landfill aquifer properties versus depth. Fraction organic carbon content [f_{oc} (%)], hydraulic conductivity [K (cm/s)], and classification (USDA) versus depth (ft).

1997). As was concluded from a tracer test conducted at the site, the sandy lc layer is not continuous and the two aquifers meet at some points (Knox, 19' Finally, there are intermixed gravel and mud-ball layers just above the Henne: Group which is the confining layer of the Norman Landfill aquifer (this is zone Table 3.1).

Sediment Analysis

Four samples were chosen from the core for further characterization. Tl samples were selected from the aquifer sand zones - one from each zone 1, 2, ar [(a) 6-6.5, (b) 6.5-8, and (c) 28-30 ft] and one sample from the sandy loam zor (14-16 ft). Previous research characterized a 3 ft sample from a nearby well (Table 3.1 presents the sediment analysis of these samples, as discussed below.

From Table 3.1 both the (~3 ft) sample and the (6-6.5 ft) sample belong tc first zone and have similar physical characteristics; however, the (~3 ft) sar organic matter content, as well as its organic petrology characteristics, are c different from the (6-6.5 ft) sample. The organic carbon fraction is an orde magnitude higher for the (~3 ft) sample and the organic matter is very div including both recent and mature organic matter with amorphous organic m (AOM) coatings dominating the fraction and mature opaque particles dominatin sorption behavior. More detailed information on this sample is presented elsew (Karapanagioti et al., 1999a; Karapanagioti et al., 1999b); results are summarized to compare with new samples. The organic matter of the (6-6.5 ft) sample is r

recent and less heterogeneous than the (~3 ft) sample (more detailed discus follows). Results for these two samples thus demonstrate that the organic m amount and nature are spatially heterogeneous in the surface zone of the aquifer. is expected because the surface zone is most affected by human activity and variat in vegetation. Thus, a single sediment sample should not be considered represent of an aquifer material.

Comparing the f_{oc} values for the 4 different depth samples, a slight decrea observed from the (6-6.5 ft) sample (zone 1) to (6.5-8 ft) sample (zone 2) (see Fi 3.2). However, overall the three sand (6-6.5, 6.5-8, and 28-30 ft) samples (i.e. two aquifers or zones 1, 2, and 4) have similar foc values (0.041, 0.021, and 0.0 respectively) which is an order of magnitude lower than the sandy loam zone 3 (1 ft) sample f_{oc} value (0.20%). Organic petrology analysis demonstrated that the sc of organic matter in all zones is translucent phytoclast particles except in the se zone where humic gel is dominant. The reason for this deviation in the second is not apparent. However, both translucent phytoclast particles and humic gel ar rank materials (Tyson, 1995). Microscopic observations also showed that the av organic particle diameter decreased with increasing depth.

Equilibrium Sorption Isotherms

Phenanthrene sorption isotherms were observed to be nonlinear (note lo plot in Figure 3.3 with slope less than one indicating nonlinearity; see Table 3.2 values). The Freundlich curvilinear isotherm shape suggests that phenanthrene d

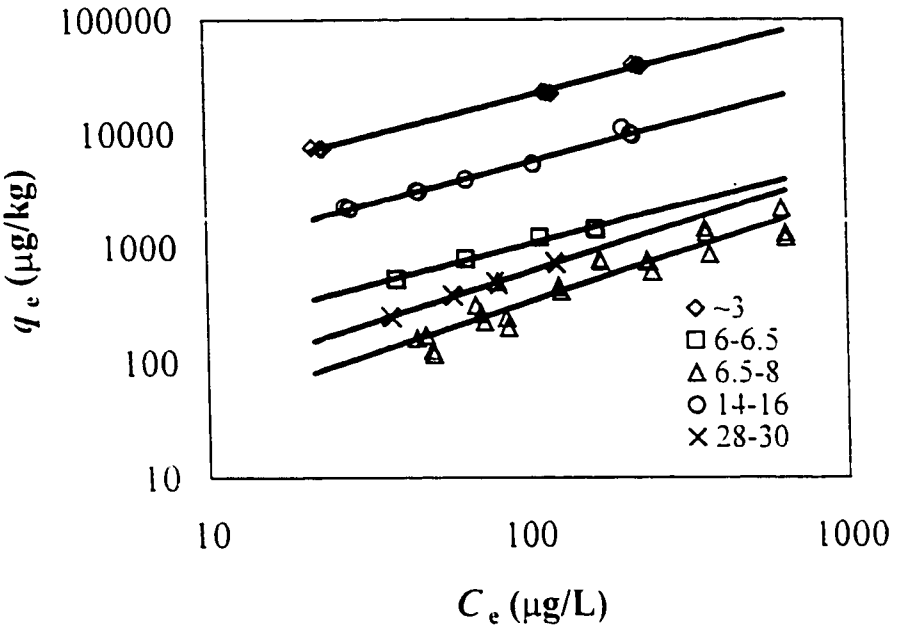


FIGURE 3.3 Phenanthrene sorption isotherms for five samples. Phenanthrene in sorbed phase [q_e (µg of phenanthrene/kg of sediment)] versus phenanthrene equilibrium aqueous concentration [C_e (µg/L)]. Sample numbers appearing in legend correspond to sampling depth in ft (see Tables 3.1 and 3.2).

TABLE 3.2 Isotherm Results

Zone	Depth	f_{oc}	N	K_f	Obs.	R^2	log K_{oc} at C_e=1 mg/L	log K_{oc} at C_e=1 µg/L	Predominant Organic Matter
	(ft)	(%)		(µg/kg)(L/µg)^N			95% CI	95% CI	
1	6-6.5	0.041	0.71 ± 0.031	40 ± 5.5	12	0.98	4.0 – 4.2	4.9 - 5.1	Translucent phytoclasts (AOM coatings and mature opaque particles)
(1')	(~3)	(0.400)	(0.65 ± 0.021)	(1100 ± 95)	13	(0.99)	(4.3 – 4.4)	(5.3 - 5.5)	
2	6.5-8	0.021	0.91 ± 0.064	5.0 ± 1.7	25	0.90	4.0 – 4.2	4.1 - 4.7	Humic gel
3	14-16	0.200	0.74 ± 0.023	180 ± 18	15	0.99	4.1 – 4.2	4.9 - 5.1	Translucent phytoclasts
4	28-30	0.026	0.89 ± 0.028	10 ± 1.2	12	0.99	4.2 – 4.3	4.5 - 4.7	Translucent phytoclasts

f_{oc}: fraction organic carbon content; N: Freundlich exponent; K_f: Freundlich constant; Obs.: number of observations for each isotherm; K_{oc}: organic carbon normalized sorption coefficient calculated at chemical equilibrium concentration (C_e) equal to 1 mg/L and 1 µg/L; CI: Confidence Interval; AOM: amorphous organic matter

Note: ± corresponds to ± standard deviation

Sample data in parentheses are for (~3 ft) sample taken near well 47; all other samples taken from core south of well 80

more than simply partition into the organic matter. Isotherm constants derived fi equilibrium experiments are presented in Table 3.2. The sorption capacity (K_{fr}) of two surface samples (~3 and 6-6.5 ft) vary by almost two orders of magnitude. f_{oc} of these samples varies by an order of magnitude, thus causing the K_{oc} values t relatively close between the two samples (Table 3.2). In addition the N values similar for the two samples. The sorption capacity (K_{fr}) also varies by almost orders of magnitude for the 4 different depth samples. N values (Table 3.2) indi the presence of highly nonlinear isotherms in certain samples (e.g. 0.65 for the (~ sample) while the isotherms approach linearity for other samples (e.g. 0.91 for (6.5-8 ft) sample). These results again illustrate the spatially heterogeneous natur sorption in this alluvial aquifer.

When sorption is nonlinear K_{oc} values are concentration dependent. concentrations close to phenanthrene's solubility (e.g. 1 mg/L) the dominant sorp mechanism is partitioning (Xia and Ball, 1999) and K_{oc} values are close to the . based estimates (log K_{oc} = 4.4; Karickhoff et al., 1979) (see Table 3.2). For lo concentrations (e.g. 1 μg/L), the phenanthrene K_{oc} value for the (6.5-8 ft) samp similar to K_{ow}-based estimate, whereas the rest of the samples evidenced slightl much higher K_{oc} values (as much as one order of magnitude). Table 3.3 presents quantitative organic petrology results of the 4 different depth samples. All 4 sam contain predominantly recent organic matter (i.e., translucent phytoclasts, humic Recent organic matter is expected to have K_{oc} values equal to or lower than the based estimates (Karapanagioti et al., 1999a). Because of the low organic conte these samples we could not determine the presence of organic coatings using

TABLE 3.3 Organic Petrology of the Four Different Depth Samples

Organic matter subgroup (log K_{ocOMi}; % OC_{OMi})	% OM_i			
	Depth (ft)			
	6-6.5	6.5-8	14-16	28-30
Translucent phytoclasts (4.1; 0.59)	81	34	78	87
Humic gel (4.1; 0.59)	5.7	60	2.2	4.4
AOM (5.1; 0.75)	3.6	4.8	5.4	3.1
Opaque particles (5.8; 0.63)	10	1.2	14	5.0
log K_{oc} (K_{oc} predicted based on Equation 3.7)	4.9	4.4	5.0	4.7
95% Confidence Interval for Measured log K_{oc}	4.9 - 5.1	4.1 - 4.7	4.9 - 5.1	4.5 - 4.7
log K_{oc} (K_{oc} predicted based on opaque particles only) (% of sample K_{oc})	4.8 (79)	3.9 (40)	4.9 (79)	4.5 (63)
log K_{oc} (K_{oc} predicted based on Equation 3.11)	4.9	4.3	5.0	4.6
% OC_b (% OC_b predicted based on Equation 3.8)	0.60	0.60	0.60	0.59
K_d (L/kg) (K_d predicted based on Equation 3.9)	34	5.7	220	13
95% Confidence Interval for Measured K_{fr} (μg/kg)(L/μg)^N = K_d at C_e = 1μg/L	30 - 95	2.6 - 9.8	150 - 230	7.7 - 13

K_{oc}: organic carbon normalized sorption coefficient; % OM_i: fraction of each organic matter subgroup in the sample; K_{ocOMi}: K_{oc} assigned to each organic matter subgroup; AOM: amorphous organic matter; %OC_b: total organic carbon fraction for the whole sample; K_d: sorption distribution coefficient; K_{fr}: Freundlich sorption constant; C_e: equilibrium aqueous concentration of chemical Data on the organic petrology of (~3 ft) sample are presented in Karapanagioti et al. (1999b)

dispersed organic pellets. The presence of organic particles was determined thro both the dispersed organic pellets and the strew slides with organic matter isolates the (~3 ft) sample the predominant organic matter is AOM coatings, but high num of mature opaque particles (identified as vitrinitic coal and charcoal particles) v present that produced a high K_{oc} value (as high as 5.4). More details on the org petrology of the (~3 ft) sample is discussed in Karapanagioti et al. (1999a).

While K_{oc} gives an indication of the organic matter sorption affinity and the sample sorption capacity, N values suggest possible sorption mechanisms. Fi 3.4 summarizes results for the 4 depth samples from this study and the (~3 ft) sar and subsamples studied in Karapanagioti et al. (1999a). At low concentrations inverse trend between log K_{oc} and N is observed for all samples, suggesting that increasing sorption affinity the sorption mechanism changes from partitioning to limited-surface accumulation (Weber and Huang, 1996), solid precipit (Gustafsson and Gschwend, 1997) and/or pore filling (Xia and Ball, 1999). trend is consistent with results of Karapanagioti et al. (1999a) and Kleineidam (1999).

The organic matter in the (6.5-8 ft) sample, which had the lowest K_{oc} v (Table 3.2) is primarily humic gel. Small amounts of structured organic matter found in this sample. The elevated percentages of opaque particles in the (6-6. and (14-16 ft) samples explain the higher K_{oc} values for these samples (Table For the (28-30 ft) sample, the presence of opaque particles is lower than in the (ft) and (14-16 ft) samples, but higher than in the (6.5-8 ft) sample and its K_{oc} val

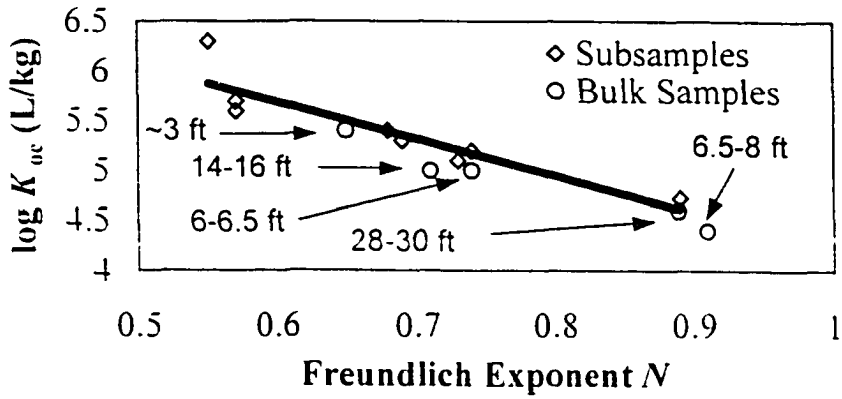


FIGURE 3.4 Logarithm of organic content normalized distribution coefficient (K_{oc}) versus Freundlich exponent (N) at chemical equilibrium concentrations equal to 1 μg/L. Diamonds correspond to subsamples of (~3 ft) sample used Karapanagioti et al. (1999a), whereas circles correspond to bulk (~3 ft) and o samples used in this study. Sample numbers that appear in the graph correspon sampling depth in ft (see Table 3.2).

in between these two groups. Although these two samples (i.e. 6.5-8 ft, 28-3(have different organic petrology, both combinations of organic matter types c: similar sorption behavior. Careful interpretation of sample organic petrology can help explain their sorption behavior.

Sorption potential decreased from the shallow zone 1 to the next sand zor as was observed by Kimani Njoroge et al. (1998), but then sorption increased a due to the sandy loam zone 3. Thus the sorption capacity in our case is depender both depth and depositional formation. We do not suggest that the litholo composition is responsible for the sorption behavior, as was presented by Allen-I et al. (1998), but that the organic matter must be characterized in each sampl predict the sorption behavior with that material.

K_{oc} predictions

By combining the fraction of organic matter subgroups (OM_i) measured ir samples with the K_{oc} for each organic matter subgroup (K_{ocOMi}) we attempte predict the overall K_{oc} value for each sample (see Equation 3.7). Since it wa: possible to isolate each organic matter subgroup and determine their (K_{ocOMi}) va different (K_{ocOMi}) values were tried to fit the K_{oc} values for two samples (6-6.5 6.5-8 ft); these values were then used to predict the sorption for the other samples.

The K_{oc} values assigned to each organic matter subgroup were selected b on the trends presented by Kleineidam et al. (1999), who also used phenanth.

Opaque particles are expected to demonstrate the highest sorption whereas the hu substances and phytoclasts are expected to have lower sorption than AOM. intercept of the regression line in Figure 3.4 for N equal to 1 is log K_{oc} = 4.1. This K_{oc} value was assigned to the organic matter subgroups (i.e., humic gel, translu phytoclasts) where the partitioning mechanism is expected to dominate and isotherms are expected to be linear. This value (log K_{oc} = 4.1) is also similar to the K_{oc} values for C_e = 1 mg/L (Table 3.2). For equilibrium concentrations close to solubility of a chemical (Solubility of phenanthrene is 1.29 mg/L) a partition sorption is expected (Xia and Ball, 1999) and thus K_{oc} values at these concentrat are representative of the partition type media. AOM and opaque particle subgr were assigned higher K_{oc} values with consideration of Kleineidam et al. (1' results.

It is important to note that while the assigned log K_{oc} values for each org matter subgroup follow the same trend as Kleineidam et al. (1999), our values f to the (6-6.5 ft) and (6.5-8 ft) samples are slightly lower than their lower end. Th expected since our sediment is more recent (Quaternary) compared to the sedin used by Kleineidam et al. (1999) (Triassic to Quaternary) and thus our organic m is more recent. Also, in our previous studies we have observed K_{oc} differe between recent and mature organic matter, with the recent organic matter havin lower value (Karapanagioti et al., 1999a).

The fitted K_{ocOMi} values for the (6-6.5 and 6.5-8 ft) samples, were use predict the composite K_{oc} values for the (14-16 ft) and (28-30 ft) samples. predicted values were within the 95% confidence interval of the experimer

determined log K_{oc} values (see Table 3.3). This quantitative analysis corroborates premise that characterizing and quantifying the organic matter heterogeneity allow prediction of contaminant sorption characteristics.

By examining more carefully Table 3.3 one can note that the opaque parti account for the majority of the sorption. For example, in (14-16 ft) sample the opa particles account for only 14% of the organic matter but they are responsible for of the sample K_{oc} value. To simplify the petrological analysis required one c determine only the percent opaque particles in each sample and predict sample values through a simplified form of equation (3.7):

$$K_{oc} = \%\ OM_{op}\ K_{oc\ op} + (1 - \%\ OM_{op})\ K_{oc\ partitioning} \qquad (3$$

where $\%\ OM_{op}$ is the fraction of opaque particles in the sample, $K_{oc\ op}$ is the K_{oc} v assigned to opaque particles of the sample, and $K_{oc\ partitioning}$ is the K_{oc} value assi to the remaining partitioning media of the sample. Using this approach K_{oc} v were calculated for the samples and are presented in Table 3.3. The values pred were again within the 95% confidence interval for the experimentally determine K_{oc} values. Equation 3.11 simplifies the use of petrological data and demonstrates the importance of the opaque particles on the sorption behavior sample.

K_d predictions

K_d is concentration dependent for nonlinear isotherms and is equal to K_f C_e = 1 μg/L. To predict these K_d values the following steps were necessary:

a) % OC_{OMi} values, the amount of organic content present in organic mat were assigned to each organic matter subgroup (see Table 3.3). Accord to Tyson (1995) the average % OC_b for recent sediments is 59%. Us values based on % OC_{OMi} value ranges summarized by Tyson (1995), % OC_b of the (6-6.5 ft) sample was fitted to be equal to 0.60. The % (values for the rest of the samples were within ± 0.01 of this value. Th OC_{OMi} values assigned for each organic matter subgroup were taken fi a summary table given by Tyson (1995). In this table the proposed m of % OC_{OMi} for recent sediment organic matter is 59%, for the typ kerogen that AOM belongs to is 75% when immature and for imma coal is 63%. The range of % OC_{OMi} for peat is 47-60%, for wood is 65%, for soil humic compounds around 65%, for lipids is around 69% for wood charcoal 63-86%. The translucent phytoclasts and the humic were compared to peat, wood, and soil humic compounds, AOM immature type II kerogen and lipids, and the opaque particles to the w charcoal and immature coal.

b) By multiplying the K_{ocOMi} and the f_{oc} fraction (% OC_{OMi} f_{oc}/% (assigned to each organic matter subgroup with the % OM_i it is possib predict the K_d value of each sample.

According to Table 3.3 the K_d values predicted using equation (3.9) are within 95% confidence interval for measured K_{fr} values (where K_{fr} equals K_d values at C 1μg/L). To perform this analysis, consideration of all aspects of organic ma characterization and classification was necessary. Both the maturity of the org. matter and the organic matter subgroups present were considered when sorp properties were assigned. For a quantitative prediction of the sample sorp properties, a good understanding of both the nature and the sorption behavior of c organic subgroup along with quantitative organic petrology data is necessary.

In summary, we have proposed and evaluated two methods for u petrological data for the samples and other literature data to predict sample sorp properties (K_{oc}, K_d). Both methods resulted in predictions that were within the ' confidence interval of observed data. To make these methods more robust propose focusing on sorption with the opaque particles which could minimize effort in obtaining petrological data as well as literature data. The predict utilizing this simplified method are also within the 95% confidence intervals. simplified method also demonstrates the dominant role opaque particles pla establishing sorption properties.

Sorption Kinetics

Table 3.4 lists the surface area and the intraparticle porosity for the sam Surface area and intraparticle porosity seem to be proportional to the clay co rather than foc values of each sample. The sandy loam (14-16 ft) sample has one

TABLE 3.4 Sample Properties Important for Their Kinetic Sorption Behavior

Zone	Depth	SA	PV	Intraparticle Porosity	≤ 0.063 mm	a	a_{OP}
	(ft)	(m^2/g)	(cm^3/g)		%	(cm)	(cm)
1	6-6.5	3.4	0.0045	0.0120	4.0	0.0077	0.0085
(1')	(~3)	(5.3)	(0.0067)	(0.0170)	11	(0.0077)	(N/A)
2	6.5-8	1.0	0.0015	0.0040	0.7	0.0077	0.0034
3	14-16	15	0.0190	0.0480	27*	0.0100	0.0011
4	28-30	1.4	0.0021	0.0055	1.8	0.0100	0.0006

SA: surface area; PV: pore volume for pore diameter <66.6 nm; Intraparticle porosity = PV/(PV+1/ρ) (Ball and Roberts, 1991a) assuming that the bulk density of the grain (ρ) equals 2.65g/cm^3; a: grain radius used in the numerical model; a_{OP}: average organic particle radius as measured with the microscope; N/A: not analyzed

* less than 0.075 mm

Sample data in parentheses are for (~3 ft) sample taken near well 47; all other samples taken from core south of well 80.

order of magnitude higher surface area and intraparticle porosity than the (6.5-8 28-30 ft) samples. The surface (~3 and 6-6.5 ft) samples have similar surface a and porosity values although their organic content and petrology are different discussed above). The radii used in the model to fit the diffusion rate (D_a/a^2) v calculated as described by Ball and Roberts, (1991).

Figure 3.5 presents the apparent sorption coefficient at a given time (normalized by the equilibrium distribution coefficient (K_d) as a function of time all samples. Table 3.5 presents results of experimental data and modeling w studying the kinetic sorption properties of the sediment samples.

The three sand (6-6.5, 6.5-8, and 28-30 ft) samples reached equilibrium wi 9-14 days, the sandy loam (14-16 ft) sample within 24 days, and by model predict the (~3 ft) sample with the organic particles required 63 days to reach equilibri biodegradation began after 39 days. The (~3 ft) sample presents a different kir behavior due to its slow diffusion within the organic particles. Organic matter c than mature opaque particles in this sample (i.e. organic coatings) reach equilibi faster than the rest of the samples as observed by the deviation between early data points with the intraparticle diffusion model (see Figure 3.5). The addition fast sorption term was necessary to fit the data properly, as discussedelsew (Karapanagioti et al., 1999b). The intraparticle diffusion rate coefficient (D_a/a^2) the time to reach 90% equilibrium (T 90%) for the sandy loam (14-16 ft) samp the lowest and longest, respectively, for the other samples. This sample also ha highest surface area and intraparticle porosity. However, the sorption

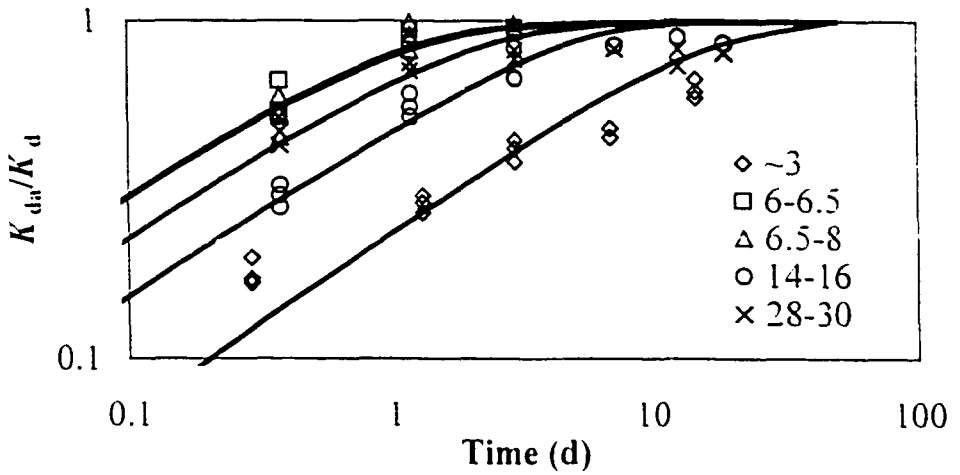


FIGURE 3.5 The apparent sorption coefficient normalized by the equilib sorption coefficient (K_{da}/K_d) versus time (d) for all samples as well as the nume model lines. Sample numbers appearing in legend correspond to sampling depth i.

TABLE 3.5 Kinetic Sorption Properties						
Zone	Depth	F	C_e	D_a/a^2	T 90%	Error
	(ft)		µg/L	(1/s)	(d)	
1	6-6.5	0.30	74	1.3E-06	1.8	0.015
(1')	(~3)	(0.56)	(50)	(7.7E-08)	(24)	0.046
2	6.5-8	0.32	71	1.3E-06	1.5	0.037
3	14-16	0.49	54	2.8E-07	5.3	0.018
4	28-30	0.50	53	6.9E-07	3.0	0.027

F: fractional uptake at equilibrium (chemical mass on solid per total chemical mass); C_e: equilibrium aqueous concentration of chemical for the kinetic experiment; D_a/a^2: apparent diffusion rate coefficient; T 90%: time to reach 90% equilibrium; Error: Mean Weighted Squared Error (Defined as the mean of (K_d measured-K_d predicted/K_d predicted)^2 for the time steps with measurements) (Rügner et al., 1999)

Sample data in parentheses are for (~3 ft) sample taken near well 47; all other samples taken from core south of well 80.

kinetics ($D_a a^-$ and T 90%) for the rest of the samples do not appear to corresp with the variations in the intraparticle porosity for these samples (Tables 3.4 and 3 The organic particles average radius decrease with depth, but this does not seen affect the sorption non-equilibrium (see T 90% in Table 3.4).

Based on the organic matter subgroups these five samples can be divided two categories a) (~3 ft) and (14-16 ft) and b) the rest of the samples. The ma opaque particles present in the (~3 ft) sample affect the diffusion rate and resul longer equilibrium times for this sample. The higher intraparticle porosity of the (16 ft) sample results in intraparticle diffusion limited sorption and lo equilibration times. The nature of the organic matter and intraparticle porositie the other samples result in similar diffusion rates and shorter equilibration tir Thus, these results demonstrate that both the organic matter subgroups and intraparticle porosity affect the diffusion rates and sorption kinetics.

Contaminant Transport and Fate

One of the objectives of the present work was to demonstrate the import of spatial heterogeneities in sediment properties as they impact sorption equilibria kinetics within an alluvial aquifer. Modeling is necessary to predict contami movement in the subsurface. Modeling a heterogeneous aquifer based homogeneous assumptions could lead to significant errors. The sorption capacity observed to vary by almost two orders of magnitude for samples from the s location but different depths and at the same depth but different locations (se

values in Table 3.2). Samples in this study varied in organic carbon content, orga matter type, and thus, sorption capacity. Variations in organic matter properties thus sorption capacities with depth can lead to differential retardation factors contaminant flow velocities with depth.

Among the depth samples, the upper sample (zone 1) has lower hydra conductivity, higher sorption capacity, and similar sorption kinetics compared to s zone 2 (see Tables 3.1, 3.2, and 3.4). Thus, greater sorption will occur in sand zo than 2. Sorption is higher in the sandy loam zone 3 than any of the sand zones (and 4), but the contaminant plume will tend to move parallel to and around the sa loam zone 3 because of its low hydraulic conductivity. Due to its high sorp potential and slow kinetics, zone 3 would act as a sorption sink during breakthro and a desorption source during elution, resulting in leading front and desorp tailing. The deeper sand layer (zone 4) has higher sorption capacity than the s zone 2; however, sorption kinetics are slower and groundwater flow is faster. suggests that although the deeper sand zone has potential to sorb more contami than the second sand zone, it may not have time to achieve its whole sorption cap (i.e., nonequilibrium transport may be more dominant). Thus, variations in sorp equilibria and kinetic properties of the different depths of the aquifer can predi explain variations in contaminant transport and fate behavior. Future research seek to couple this fundamental information with field observations of contami transport at this site.

Acknowledgment. This study was partially funded by the U.S. National Scie Foundation through the EPSCoR program. Samples studied in this research v taken from the closed Norman Landfill, which is a USGS Toxic Substances Rese Site (http://wwwok.cr.usgs.gov/norlan/site.html). We acknowledge the assistanc Mr. Scott Christenson in obtaining samples from the site. The authors would lik thank Renate Riehle for TOC measurements and Dr. Hermann Rügner for I measurements, both working in the Hydrogeochemistry Laboratory of Prof. Dr. F Grathwohl in the Universität Tübingen, Germany. The authors would also lik thank Cynthia Paul from EPA, Ada for TOC measurements, Dr. George Breit f U.S.G.S. for sharing his mineralogy data, Amy Hamilton for the sieve and hydron analysis, Tuan Van Doan for the hydraulic conductivity measurements, Dr. Rc Knox and Becky Ziebro from the University of Oklahoma for obtaining the sedi cores from the Norman Landfill, Prof. Dr. Peter Grathwohl and Dr. Sy Kleineidam from the Universität Tübingen, Germany and Dr. William Lyon f EPA, Ada for their input on the sample organic petrology interpretation. The aut would especially like to thank Mr. Brian Cardott from the Oklahoma Geolo Survey for his help in assessing the organic petrology of the samples and providi access to his Vickers M17 Research Microscope.

Nomenclature

a	grain radius (cm)
a_{OP}	average organic particle radius as measured with the microscope (c

AOM	amorphous organic matter
b	as an index refers to the bulk sample
C	chemical aqueous concentration
C_e	equilibrium aqueous concentration of chemical (μg/L)
D_a	apparent diffusion coefficient (cm^2/s)
D_a/a^2	diffusion rate (1/s)
F	fractional uptake at equilibrium (chemical mass on solid per total chemical mass)
f_{oc}	fraction organic carbon content (%)
f_{sc}	soot-carbon fraction
i	as an index refers to individual organic matter subgroups
K	hydraulic conductivity
K_d	sorption distribution coefficient (L/kg)
K_{da}	apparent sorption distribution coefficient (L/kg)
K_{fr}	Freundlich sorption constant [(μg/kg)(L/μg)^n]
K_{oc}	organic content normalized distribution coefficient (L/kg)
K_{ocOMi}	K_{oc} value assigned to each organic matter subgroup
$K_{oc\ op}$	K_{oc} value assigned to opaque particles
$K_{oc\ partitioning}$	K_{oc} value assigned to the partitioning media of the sample
K_{ow}	octanol-water partition coefficient
K_{sc}	soot-carbon-normalized partition coefficient
% OC_b	fraction organic carbon of the whole sample
OM_i	as an index refers to organic matter subgroups as opposed to the w

	sample
$\%\ OM_i$	fraction of each organic matter subgroup in the sample
$\%OM_{op}$	fraction of opaque particles in the sample
N	Freundlich exponent
PV	pore volume for pore diameter <66.6 nm (cm^3/g)
q_e	mass of chemical sorbed per mass of sediment (μg/kg)
r	radial distance from the center of the grain
SA	surface area (m^2/g)
t	time (d)
T 90%	time to reach 90% equilibrium (d)

References

Soil Survey of Cleveland County, Oklahoma, 1987.

Allen-King R.M.; Halket R.M.; Gaylord D.R.; Robin M.J.L. *Water Resour.* **1998**, 34, 385-396.

Ball W.P.; Roberts P.V. *Environ. Sci. Technol.* **1991**, 25, 1237-1249.

Bouwer, H. *Groundwater Hydrology*, Mc Graw-Hill Book Company, New Y 1978.

Breit G.N.; Cozzarelli I.M.; Johnson R.D.; Norvell J.L.S. *Geological Societ America Abstracts with Programs*, **1996**, 28, A-258.

Chiou, C.T. *Environ. Sci. Technol.* **1995**, 29, 1421-1422.

Chiou, C.T.; Kile, D.E. *Environ. Sci. Technol.* **1998**, 32, 338-343.

Dunlap W.J.; Shew D.C.; Robertson J.M.; Toussaint C.R. *In Proceedings, Resea Symposium on gas and leachate from landfills*, **1976,** Rutgers University Co College, New Brunswick, New Jersey, March 24-26, 1975, p. 96-110, USEPA 60(76-004.

Fisher, K.D. *A comparative analysis of the hydraulic parameters of the Canac River Alluvium near the Norman Landfill site*. Master's Thesis, The University Oklahoma, Norman, OK,1997.

Garbarini, D.R.; Lion, L.W. *Environ. Sci. Technol.* **1986**, 20, 1263-1269.

Graber, E.R.; Borisover, M.D. *Environ. Sci. Technol.* **1998**, 32, 3286-3292.

Grathwohl, P. *Environ. Sci. Technol.* **1990**, 24, 1687-1693.

Grathwohl, P. *Diffusion in Natural Porous Media: Contaminant Transp Sorption/Desorption and Dissolution Kinetics*, Kluwer Academic Publishers, Boston, Massachusetts, 1998.

Gustafsson Ö.; Gschwend P.M. *ACS symposium series* **1997**, 671, 365-381.

Gustafsson, Ö.; Haghseta, F.; Chan, C.; MacFarlane, J.; Gschwend, P.M. *Envi Sci. Technol.* **1997**, 31, 203-209.

Jäger R., *Modellierung Nichtlinear Intrapartikel-Diffusion in Heterogenem Aquifermaterial*, Diploma Thesis, University of Tübingen, FRG, 1997.

Karapanagioti H.K.; Kleineidam S.; Ligouis B.; Sabatini D.A.; Grathwohl P. *Envi Sci. Technol.* **1999a** accepted July 14.

Karapanagioti, H.K.; Sabatini, D.A.; Kleineidam, S.; Grathwohl, P.; Ligouis. *Journal of Physics and Chemistry of the Earth* **1999b**, 24, 535-541.

Karickhoff S.W.; Brown D.S.; Scott T.A. *Water Research* **1979,** 13, 241-248.

Kimani-Njoroge B.N.; Ball W.P.; Cherry R.S. *J. Cont. Hydrol.* **1998**, 29, 347-377

Kleineidam S.; Rügner H.; Ligouis B.; Grathwohl P. *Environ. Sci. Technol.*, **1999** 1637-1644.

Knox, R.C., University of Oklahoma, Norman, OK, 1999, personal communicatic

Lambe T.W. *Soil Testing for Engineers*, J.W., p.29-42, 1951.

Luthy, R.G.; Aiken, G.R.; Brusseau, M.L.; Cunningham, S.D.; Gschwend, P.M.; Pignatello, J.J.; Reinhard, M.; Traina, S.J.; Weber, W.J.Jr.; Westall, J.C. *Environ. Technol.* **1997**, 31, 3341-3347.

Montgomery J.H.; Welkom L.M., *Ground Water Chemicals Desk Reference*, Lewis Publishers, Inc., Chelsea, Michigan,1990.

Page A. L.; Miller R. H.; Keeney D.R.,. *Methods of Soil Analysis, Part 1*, Agronor No. 9, Part 1, 2nd Edition, ASA, SSSA, Madison, Wisconsin,1982.

Rügner, H.; Kleineidam, S.; Grathwohl, P. *Environ. Sci. Technol.* **1999**, 33, 1(1651.

Tyson, R.V. *Sedimentary Organic Matter: Organic Facies and Palynofa* Chapman & Hall, London, 1995.

Weber W.J.Jr.; Huang W., *Environ. Sci. Technol.* **1996**, 30, 881-888.

Xia G.; Ball W.P., *Environ. Sci. Technol.* **1999**, 33, 262-269.

Xing, B.; Pignatello, J.J. *Environ. Sci. Technol.* **1997**, 31, 792-799.

Young, T.M.; Weber, W. J.Jr. *Environ. Sci. Technol.* **1995**, 29, 92-97.

CHAPTER 4

Model Coupling Intraparticle Diffusion/Sorption, Nonlinear Sorption and Biodegradation Processes

Abstract

Diffusion, sorption and biodegradation are key processes impacting efficiency of natural attenuation. While each process has been studied individu limited information exists on the kinetic coupling of these processes. In this cha a model is presented that couples nonlinear and nonequilibrium sorption (intrapar diffusion) with biodegradation kinetics. Initially these processes are stu independently (i.e., intraparticle diffusion, nonlinear sorption and biodegradati with appropriate parameters determined from these independent studies. Then, coupled processes are studied, with an initial data set used to deter biodegradation constants that were subsequently used to successfully predict behavior of a second data set. The validated model is then used to condu sensitivity analysis, which reveals conditions where biodegradation bec desorption rate-limited. If the chemical is not pre-equilibrated with the soil pri the onset of biodegradation, then fast sorption will reduce aqueous concentrations thus biodegradation rates. Another sensitivity analysis demonstrates the import of including nonlinear sorption in a coupled diffusion/sorption and biodegrad model. While predictions based on linear sorption isotherms agree well with solu concentrations, this approach overestimates the percentage of contami

biodegraded by as much as 50%. This research suggests that a nonlinear sorpt term must be coupled with diffusion/sorption and biodegradation models accurately predict bioremediation and natural attenuation processes.

4.1 Introduction

Natural attenuation is currently one of the most important topics groundwater quality management. Diffusion, sorption and biodegradation are processes impacting the efficiency of natural attenuation. While each process been studied individually, limited research has coupled the kinetics of th processes. Research on the interplay of diffusion/sorption and biodegrada processes is necessary to accurately predict the magnitude of natural attenuation.

Naphthalene bioavailability was shown to be sorbent specific (Guerin Boyd, 1993). The same microbial species demonstrated different biodegrada behavior for naphthalene sorbed on different soils (i.e. low organic content vs. h organic content soils). In phenanthrene biodegradation studies with model sc (glass or polystyrene beads), the nature and interrelation of porosity hydrophobicity were found to be very important (Nam and Alexander, 19 Organic content, porosity, and hydrophobicity are known parameters that im diffusion-limited and hydrophobic-motivated sorption. Another example pres aged phenanthrene to have lower biodegradation rates as compared to freshly ac phenanthrene (Hatzinger and Alexander, 1995). Therefore previous research demonstrated that diffusion/sorption processes impact biodegradation proces

However, most studies have focused on an individual process (i.e. biodegrada kinetics) without studying and coupling other processes (i.e. sorption kinetics).

Quantifying and coupling kinetics for all three processes is a challenging t Most of the proposed models assume that sorption is linear and desorption kin follow a first order rate law (Angley et al., 1992; Estrella et al., 1993; Fry and Is 1994; Brusseau et al. 1999). Recently, Cornelissen et al. (1998) proposed a order, two-compartment model to describe desorption. Only limited studies h incorporated intraparticle diffusion in the coupling of linear sorption biodegradation (Scow and Hutson, 1992; Chung et al., 1993).

None of the studies mentioned above have included nonlinear sorption in t coupled models. Recent studies have shown that sorption kinetics can be hi dependent on intraparticle diffusion (Rügner et al., 1999; Karapanagioti et al., 19 Also different samples containing varying types of organic matter can demons linear ($N = 1$) or highly nonlinear (N as low as 0.38) sorption isotherms (Kleine et al., 1999; Karapanagioti et al., 1999). Nonlinearity causes diffusion coefficien be concentration dependent and to increase by a factor of ten or more du desorption (Grathwohl, 1998).

The hypothesis of the present study is that incorporating a nonlinear sorp term in a model coupling intraparticle diffusion, sorption and biodegradation more accurately predict contaminant fate. The objectives of this study are as foll (1) to study the effect of microbe addition to systems in which heterogeneous nonlinear sorption behavior are already well-characterized, (2) to develop a m that couples intraparticle diffusion, nonlinear sorption and biodegradation, (3

validate the model with experimental data, and (4) to determine the effect of sorp nonlinearity on the overall system behavior. To our knowledge this study is uniqu studying nonlinear sorption coupled with intraparticle diffusion and biodegrada kinetics with natural media.

4.2 Methods

4.2.1 Experimental

The Canadian River Alluvial (CRA) aquifer material was sampled from closed Norman Landfill, which is a U.S.G.S. Toxic Substances Research site. sampling depth was just below the water table at about 1 m. Subsan characteristics important to sorption behavior are summarized in Table 4.1 described in further detail elsewhere (Karapanagioti et al., 1999). Subsan nomenclature (Table 4.1) was based on the dominant organic matter found in org petrology thin sections. Table 4.1 also summarizes important sorption properties were found in Karapanagioti et al. (1999).

Phenanthrene was used as the model chemical in this study. Phenanth ($C_{14}H_{10}$) is a three ring polycyclic aromatic hydrocarbon with the follo properties: a) molecular weight of 178 g/mol, b) solubility of 1.29 mg/L at 25 °C Henry's law constant of 2.6×10^{-5} atm m^3/mol, and d) log K_{ow} of 4.6 (Montgomery

TABLE 4.1 Important Sediment Sample and Sorption Properties (Karapanagioti et al., 1999)

Sample Code	Grain Size	Dominant Organic Matter	f_{oc}	ε	N	K_{fr}	log K_{oc} at C_e = 1 μg/L	D_a/a^2
	(mm)		(%)			(μg/kg) (L/μg)^N	95 % CI	(1/s)
Coaly	0.5 – 0.25	Coaly Particles	1.60	0.008	0.55 ± 0.024	33000 ± 2500	6.3 – 6.4	1.1 E-10
Organic Coatings	0.125 - 0.063	Amorphous Organic Matter Coatings	0.10	0.011	0.89 ± 0.091	43 ± 15	4.6 – 4.7	N/A
Mixture	≤ 0.063	Amorphous Organic Matter Coatings and Coaly Particles	0.18	0.003	0.68 ± 0.013	490 ± 27	5.4 – 5.5	7.2 E-08

f_{oc}: organic carbon content; ε: intraparticle porosity N: Freundlich exponent; K_{fr}: Freundlich constant; K_{oc}: organic carbon normalized sorption coefficient calculated at chemical equilibrium concentration (C_e) equal to 1 μg/L; 95% CI: 95% Confidence Interval; ±: corresponds to ± 1 standard deviation; D_a/a^2: apparent diffusion rate

Welkom, 1990). The K_{ow}-based estimate for log K_{oc} of phenanthrene is (Karickhoff et al., 1979). Phenanthrene was chosen because of its h hydrophobicity (K_{ow}), low volatility (Henry's law constant), and simplicity analysis. Phenanthrene was prepared in a 100 mg/L stock solution in methanol. preparing the experimental vials, the methanol percent was always below Solutions were prepared in synthetic ground water (deionized water with 44 m $CaCl_2.2H_2O$, 14 mg/L $CaSO_4$, and 17 mg/L $NaHCO_3$). Sodium azide (NaN_3) added at a concentration of 200 mg/L to minimize bacterial growth and t biodegradation (for abiotic studies).

1-hydroxy-2-naphthoic acid (1H2N) is commonly identified as one phenanthrene's bacterial biodegradation byproducts (Stringfellow and Aitken, 19 Machate et al., 1997). 1H2N was identified in this study by analyzing fluorescence detector spectra. Calibration solutions of 1H2N were prepared using method described above for phenanthrene solutions. Aqueous phenanthrene and hydroxy-2-naphthoic acid (1H2N) concentrations were measured by an RF-Shimadzu variable wavelength fluorescence detector in cuvette mode. Excitation emission wavelengths used were as follows: (a) 249 and 345 for phenanthrene and 249 and 415 for 1H2N, respectively.

To isolate microorganisms (MO), bulk CRA sediment samples were m with glass beads and deionized water, shaken for 30 min and then filtered throu 10 μm filter paper (Koelbel-Boelke et al., 1988). Part of the filtrate was introduce

synthetic groundwater solutions of phenanthrene. Once the phenanthrene degraded, additional phenanthrene was added to increase MO biomass.

MO isolation was accomplished by inoculating an agar plate contai phenanthrene with 0.1 mL of inoculum (Evenson and Strevett, 1999). The agar p contained the mineral salt media present in synthetic ground water along with 15 agar and 1.0 mL of a 100 mg/L phenanthrene solution. The plates were incubated for 10 days at 30 °C. At the end of the incubation period, two colony t were observed and the description of each was recorded. Each colony type streaked for isolation on fresh mineral salt media agar plates containing phenanthr A wet mount was then performed on both colonies.

One set of batch experiments (system) was prepared with no sediment three different systems were prepared for each of the three sediment samples Table 4.2 for details on experimental variables): (a) MO/NS: phenanthrene solu with MO added but no sediment (NS), (b) NMO/S: sediment and phenanth solutions with NaN_3 added to inhibit biodegradation, sorption alone was monit (c) MO/S: sediment and phenanthrene solutions with MO added, and (d) LM sediment and phenanthrene solutions that equilibrated for 17 days before MO added at a lower density. After phenanthrene was depleted in MO/NS addit phenanthrene was added (up to 0.1 mg/L each time), with aqueous phenanthrene 1H2N concentrations subsequently monitored until the phenanthrene was depl In LMO/S, one tenth of the MO density added in MO/S was introduced.

All kinetic experiments were conducted in triplicate in 20 mL crim Teflon-lined glass vials. The initial phenanthrene concentration was 0.1 mg/L an

TABLE 4.2 Experimental Variables for the Different Systems

System	Addition of NaN_3	Addition of sediments (Number of sediments)	Addition of MO	Day MO added	MO density
MO/NS	No	No	Yes	0	MO
NMO/S	Yes	Yes (3)	No	-	-
MO/S	No	Yes (3)	Yes	0	MO
LMO/S	No	Yes (3)	Yes	17	0.1 MO

MO: microorganisms; NS: no sediment added; NMO: no microorganisms added;
S: sediment added; LMO: less microorganisms added

solid-to-water ratio was different for each subsample depending on the sorp capacity (see Table 4.3). The vials were stored at room temperature (around 23 and in the dark and periodically mixed. Measurements were taken at various intervals.

Blank samples were prepared and monitored for each batch experiment (phenanthrene without soil). These blank samples indicated no signifi phenanthrene degradation or sorptive losses on the glassware for the first 33 d Since some of the 33-day measurements showed large concentration differe between the triplicates, these data were not included when interpreting the res Although NaN_3 was present in all the reactors prepared for NMO/S, degradation eventually occur. However, the NaN_3 did cause a lag period of about 33 c consistent with results of our previous studies (Karapanagioti et al., 1999).

4.2.2 Modeling

Modeling nonlinear sorption was accomplished using a numerical solutic Fick's 2nd law. Fick's 2nd law describes solute diffusion from an aqueous phase spherical porous grains; a one-dimensional form in the radial direction follows:

$$\partial C / \partial t = D_a [(\partial^2 C / \partial r^2) + (2\partial C / r\partial r)]$$

where C is the chemical concentration, t is time, D_a is the apparent diffi coefficient, and r is the radial distance from the center of the grain. In

TABLE 4.3 NMO/S: Parameters of Sorption Kinetic Experiment					
Sample Code	S/W ratio	a	F	C_e	T 75%
	mg/20mL	(cm)		(μg/L)	(d)
Coaly	3.3	0.0180	0.49	53	2100
Organic Coatings	700	0.0044	0.48	55	[illegible]
Mixture	140	0.0027	0.50	53	21

S/W ratio: solid to water ratio expressed as mg of sediment per 20 mL of solution; a: grain radius used in the numerical model; F: fractional uptake at equilibrium (chemical mass on solid per total chemical mass); C_e: estimated phenanthrene concentration at equilibrium; T 75%: time to reach 75% equilibrium

intraparticle diffusion model D_a is defined as:

$$D_a = D_{aq}\,\varepsilon\,/\,\{(\varepsilon + K_d\,\rho)\,\tau_f\} \qquad (1$$

where D_{aq} is the aqueous diffusion coefficient, ε is the intraparticle porosity, K_d is sorption distribution coefficient, ρ is the bulk density of the grain, and τ_f is tortuosity factor (Grathwohl, 1998).

The numerical model is solved using the finite difference method with Cr: Nicholson time stepping, as described by Jäger (1997). Model input includes grain radius, the solid-to-water ratio, the initial water concentration, the Freun isotherm parameters, the solid density and the intraparticle porosity. In this study numerical model was used to predict sorption kinetics based on results obtaine Karapanagioti et al. (1999).

A biodegradation term is added to this model in a manner similar to that u by Scow and Hutson (1992) (whereas their model includes only linear sorption, o solution incorporates nonlinear sorption). The grain-exterior-solution concentrati is adjusted at the end of each time step by the net effect of biodegradation and chemical diffusion into or out of the grain. Biodegradation in the outer solution follows first order kinetics, which is a simplification of Monod kinetics (Scow an Hutson, 1992):

$$-dC/dt = k_1 C$$

where k_1 is the first-order rate constant for biodegradation.

4.3 Results and discussion

4.3.1 Sorption kinetic behavior

Figure 4.1 presents the sorption kinetic data and the model predictions NMO/S. The model input values, as summarized in Table 4.1, were obtained fro previous study (Karapanagioti et al., 1999). Three sediment fractions were sele because of the difference in their equilibrium and kinetic sorption behavior.

In the present study the fractional uptake at equilibrium (F) – the chem mass on solid per total chemical mass – is similar for all three samples, as prese in Table 4.3. This allows direct comparison of the sorption kinetic prope between the three samples. The experimental data in Figure 4.1 agree well model predictions based on diffusion-limited intraparticle sorption. As summa in Table 4.3, the sediment containing coaly particles requires more time to r equilibrium (T 75% = 2100 d), whereas the sample with organic coatings rea equilibrium much more quickly (T 75% < 1 d). The sample with a mixture of c particles and organic coatings has a behavior in between these two extremes (T = 21 d). This three orders of magnitude difference in equilibration times is du different sorption mechanisms for varying organic matter types (Karapanagioti e 1999). When organic matter is dominated by coaly particles diffusion-lir sorption controls the system while phenanthrene partitioning into organic coating

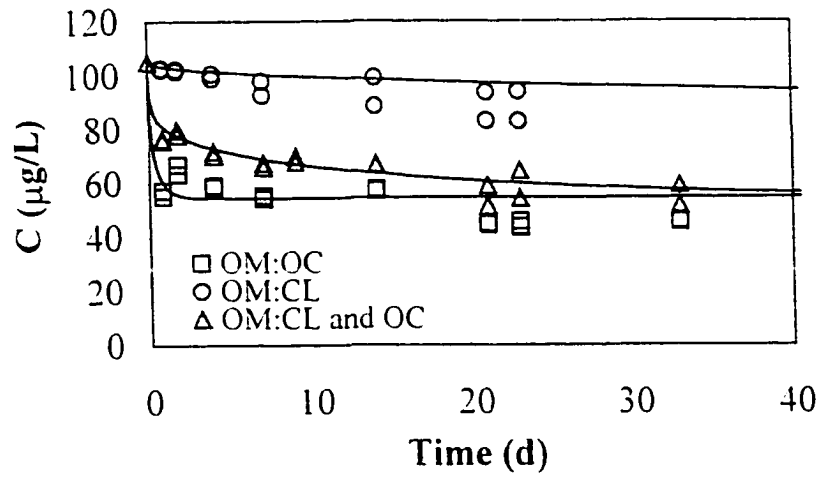


FIGURE 4.1 NMO/S: Sorption kinetic data and model predictions for all three sediment samples. (Organic matter (OM) originates from OC: Organic Coatings, Coaly Particles)

very rapid.

4.3.2 Phenanthrene Biodegradation

Figure 4.2 presents the biological activity in MO/NS. The biodegrada constant k_1 was calculated to be 0.043 1/hr for the first phenanthrene addition · Table 4.4). This value is consistent with literature values for phenanthi biodegradation (Nam and Alexander 1998; Laor et al., 1999; Rouse et al., 1999) chemicals in lab-contaminated sediments (Cornelissen et al., 1998). Phenanthi was added several times to the system; after each phenanthrene depletion biodegradation byproduct 1H2N was observed, supporting the occurrence microbial degradation (Stringfellow and Aitken, 1994; Machate et al., 1997). transient concentrations of 1H2N indicate that it is both being formed and deple thus, we cannot perform a mass balance on 1H2N to account for phenanthrene los:

Aliquots from the initial culture, which were plated on agar contai phenanthrene, yielded two colonies. The first colony was a Gram-negative bact i.e., a mucoid colony that appeared circular, entire, convex, and white. This co did not grow as an isolate with phenanthrene-based agar. This synergistic bac was identified with 87% confidence as a *Pseudomonas putida*. The second co was a filamentous, flat, white colony with a dark inner circle. From microsc observations, this second colony appears to be a fungi. Further investigation u both colonial and microscopic morphology techniques, combined with dichoton keys, revealed that the fungus was *chrysosporium* with 97% confidence (Evenson Strevett, 1999). Mineral salts agar with phenanthrene was used in this experime isolate microorganisms capable of degrading phenanthrene because these were

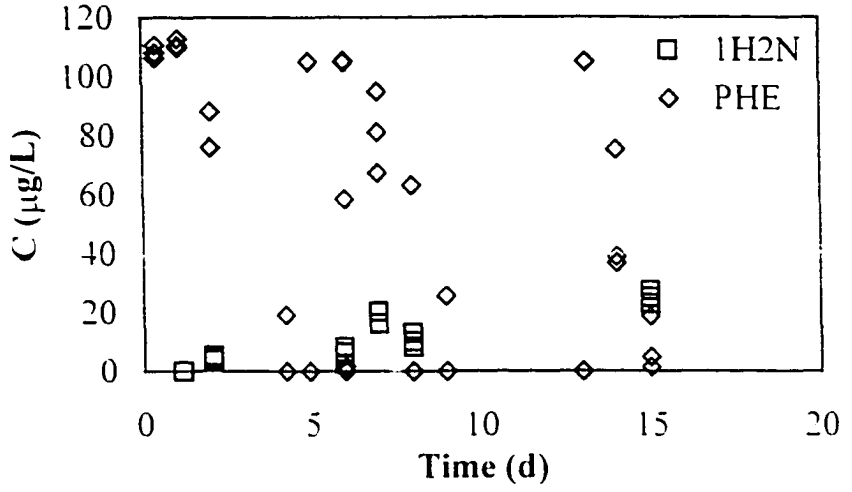


FIGURE 4.2 MO/NS: Biological activity with multiple phenanthrene additions : transient production loss of 1H2N metabolite (1H2N: 1-hydroxy-2-naphthoic acic PHE: phenanthrene).

TABLE 4.4 Lag time and first order biodegradation rate constant

System	Sediment	Lag Time (d)	k_1 (1/hr)	k_1 (1/hr) 95% CI
MO/NS	-	1	0.043 ± 0.019	0.021 - 0.065
MO/S	Coaly	3.3	0.040 ± 0.020	0.017 - 0.063
	Organic Coatings	4	0.080 ± 0.026	0.050 - 0.110
	Mixture	1.8	0.050 ± 0.020	0.027 - 0.073

Lag Time: lag time before biodegradation starts; k_1: biodegradation rate constant;
±: corresponds to ± 1 standard deviation; CI: Confidence interval.

organisms of interest in this study. Since 1H2N was identified, we hypothesize the fungal colony degraded phenanthrene to an intermediate that the bacteria c use and produce 1H2N (Evenson and Strevett, 1999).

Figure 4.3 presents the data of NMO/S, MO/S, and LMO/S for each of three sediments. Relative concentrations (C_s/C_o) less than 1.0 at early ti demonstrate initial fast sorption. From Figure 4.3, it is obvious that MO addi causes the phenanthrene concentration to decrease, ultimately below the detec limit. In MO/S there is a brief lag time and then phenanthrene is depleted. In LM phenanthrene concentration follows the same path as in NMO/S until MO is ad After MO addition in LMO/S the phenanthrene concentration decreases with a fl slope than in MO/S, demonstrating that the lower microbial population reduces rate of biodegradation. These trends are consistent with results of other researc (Sherrill and Sayler, 1980; Scow and Alexander, 1992).

4.3.3 Model Validation

Table 4.4 presents the biodegradation parameters for MO/NS and MO/ fitted by the model. Average values for k_1, along with standard deviations calculated based on triplicate samples. While variations are observed, biodegradation rate constants are statistically the same, with 95% confidence each case and sediment. According to Laor et al. (1999) attached cells might h higher degradation rate (up to 2.2 times higher k_1) than suspended MO. Thu rates for all the MO/NS and MO/S samples were compared. The same study sug

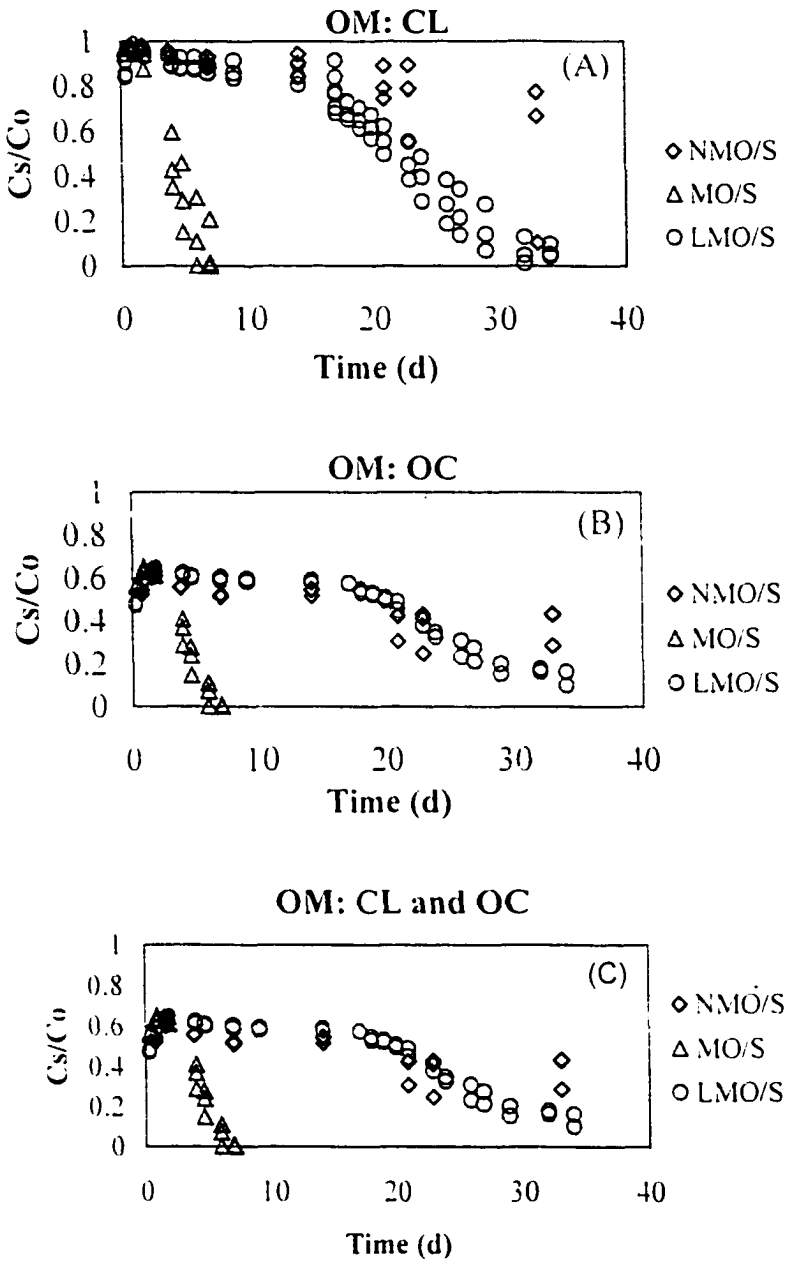


FIGURE 4.3 Experimental data of the three systems for all three sediment sampl

[Organic matter (OM) originates from OC: Organic Coatings (A), CL: Coaly Part. (B) or both (C)]. Note: C_s/C_o <1.0 for short times is due to initial fast sorption.

that the externally sorbed chemicals are more bioavailable, and thus the degrada rates would be higher than for cases where sorption is limited by diffusion. Park e (1999) observed the opposite effect: biodegradation rate coefficients decreased (factor of 27%) for attached cells due to reduced surface area with attachment. results do not statistically corroborate either theory (i.e., Laor et al., 1999 or Pa al., 1999).

In the LMO/S case the microbial population was ten times lower. Thus biodegradation values presented in Table 4.4 were divided by a factor of 10 to pr the biodegradation behavior for LMO/S. To use this method we assume that the density is so low that k_1 is biomass density dependent (Sherrill and Sayler, 1 Equation 4.3 then can be rewritten as follows (Simkins and Alexander, 1 Alexander, 1994):

$$-dC/dt = k_1 C = k_2 B C \qquad (4.3)$$

where k_2 is the second order rate constant and B is the MO cell density. Sinc MO cell number is difficult to obtain for natural mixed cultures, we assume tha LMO/S (with one-tenth the MO addition) equation 4.4 can be written as follows:

$$-dC/dt = k_2 [0.1\ B]\ C = 0.1\ [k_2 B]\ C = 0.1\ k_1\ C = k_1'\ C$$

If k_1' is the biodegradation rate constant for LMO/S, then $k_1' = 0.1\ k_1$. Figur presents the aqueous solution data and the model prediction lines (with one stan

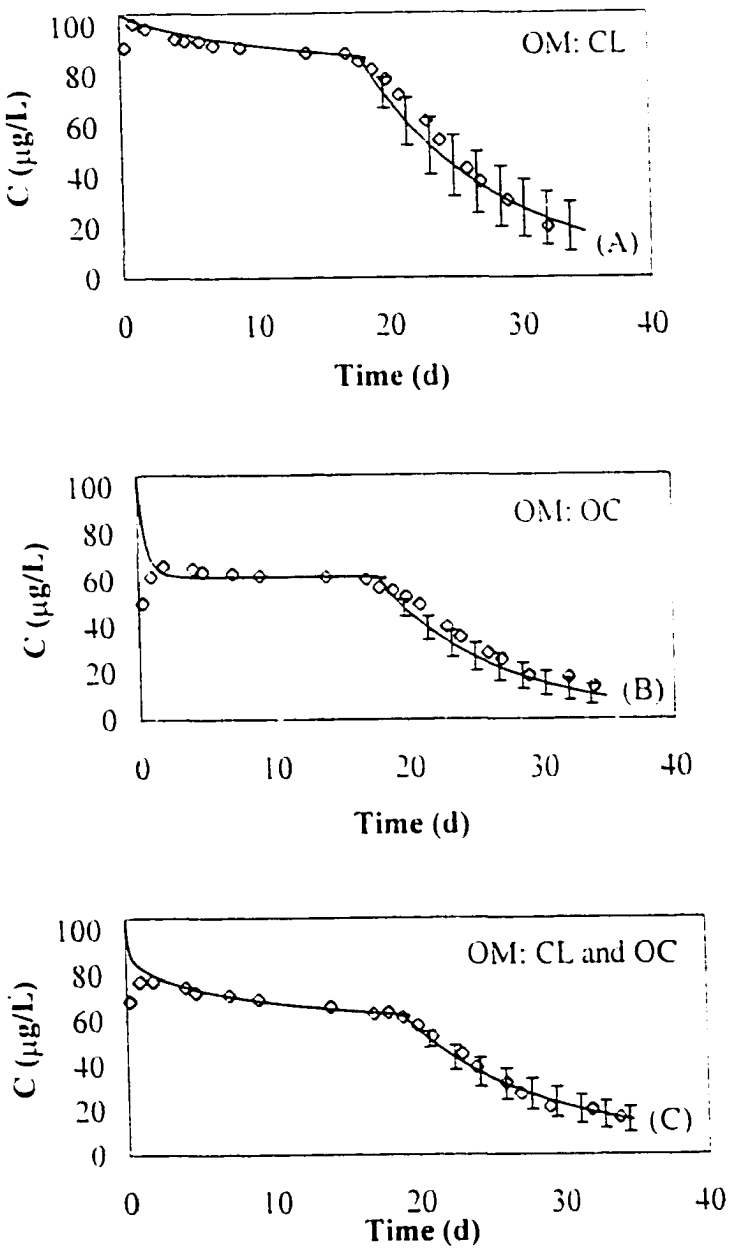


FIGURE 4.4 LMO/S: Experimental data (average of triplicate) and model prediction line with one standard deviation expressed with error bars. [Organic m: (OM) originates from OC: Organic Coatings (A), CL: Coaly Particles (B) or both

deviation) for LMO/S based on this assumption. The excellent agreement betw the data and the model validates both the analysis approach and the m assumptions. Based on these encouraging results, we will further analyze m predictions below.

The model calculates the chemical concentration distributed between t compartments: the solution, the grain, and the amount biodegraded (all expresse an aqueous solution concentration). Figure 4.5A presents an example of the m output for each of these three compartments. Since a lag time exists prior to the o of biodegradation, the initial decrease in aqueous concentration is due to contami sorption. When biodegradation starts, the solution concentration decre dramatically, whereas the sorbed concentration decreases smoothly (i.e., desorp commences because of the decreasing aqueous concentration). However, desorp occurs less slowly than biodegradation, causing aqueous concentrations to decre Since biodegradation is concentration dependent (for the assumed 1st order proc the degradation rate also decreases with time (as the aqueous concentra decreases). The model can also predict the chemical concentration distributior different grain components (i.e. components with different diffusion/sorp properties). For the same sediment, as biodegradation occurs earlier and is f (MO/S), the fast component responds more readily to the onset of biodegradation desorbs faster than the slower component (see Figure 4.5B). In the exa presented in Figure 4.5C, the grain component with fast sorption (i.e. org coatings) reaches a lower plateau much faster than the slower component (i.e. coa

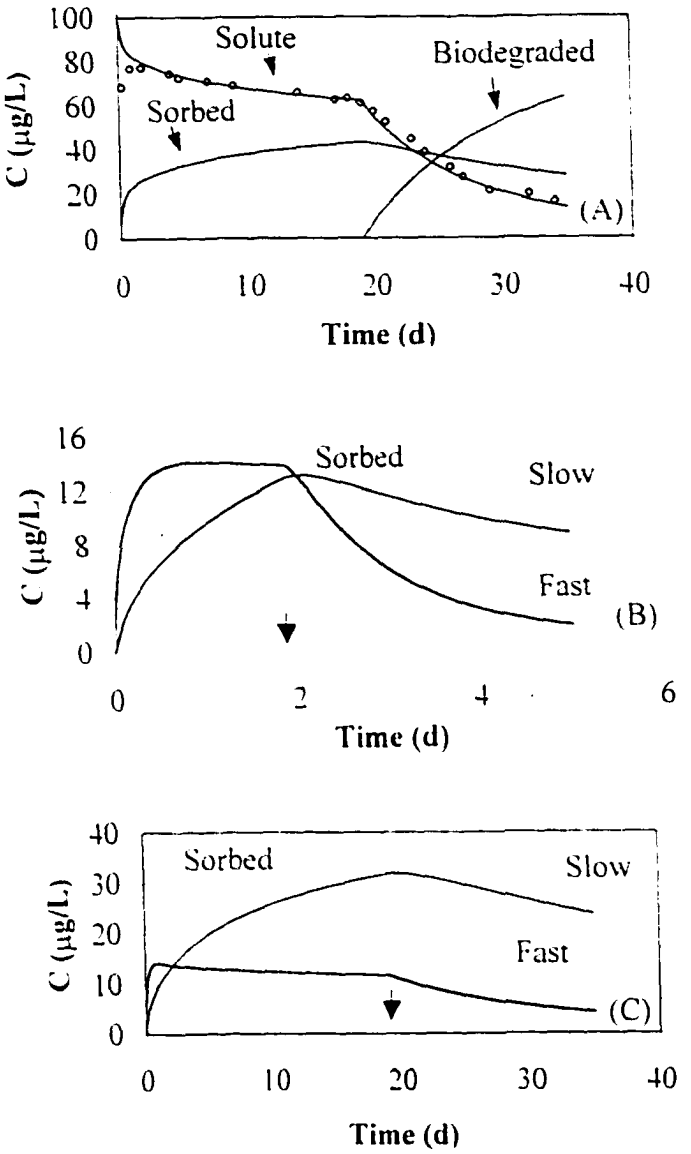


FIGURE 4.5 (A) Example of the model output as fitted to a set of data in LMO/S for the sediment with the mixture of coaly particles (Slow) and organic coatings (Fast). Lines present the concentration in solution, sorbed and biodegraded. (B) MO/S: Distribution of sorbed chemical in the two grain components of the mixture (C) LMO/S: Distribution of sorbed chemical in the two grain components of the mixture. (arrows in (B) and (C) indicate when biodegradation starts)

particles), which has a higher sorption capacity. In this case (LMC biodegradation is slower so both of the components have time to respond to concentration gradient caused by biodegradation and seem to desorb with the s rate (compare slopes after day 19).

4.3.4 Sensitivity Analysis

Based on experimental validation, we will now perform a sensitivity anal on the model. In the sensitivity analysis, we explore factors causing biodegrad to be desorption-rate limited. Table 4.5 summarizes the parameters varied anc combinations that produced desorption-rate limited biodegradation (note that in analysis the sorption distribution coefficient was not varied). Figure 4.6 compare effect of fast and slow (diffusion-limited) sorption on the rate of biodegradatio varying lag times. The lines presented in Figure 4.6 are the outputs for concentration degraded as when biodegradation is fast with varied pre-equilibr times (lag times) and sorption kinetics.

When there was no equilibration time between the solute and the sedi before biodegradation started (i.e., no lag time – Case A in Figure 4.6), fast sor has the greater impact on biodegradation. When sorption is fast the aqu concentration decreases faster and the lower aqueous concentration decrease biodegradation rate. When biodegradation is fast and sorption is slow there competition for the substrate until the substrate concentration is low biodegradation becomes desorption rate limited.

TABLE 4.5 Sensitivity Analysis				
lag (d)	% Eq	k_1 (1/hr)	Fast Sorption	Slow Sorption
0	0 / 0	F (0.1)	DRL	(DRL only for low Cw)
0	0 / 0	I (0.01)	DRL	-
0	0 / 0	S (0.001)	DRL	-
0.12	50 / N/A	F (0.1)	Same as 93%	N/A
9.5	93 / 50	F (0.1)	-	DRL
35	98 / 84	F (0.1)	-	DRL
35	98 / 84	I (0.01)	-	DRL
35	98 / 84	S (0.001)	-	-

lag: lag time before biodegradation starts; % Eq: percent of equilibrium reached before biodegradation started given for both Fast Sorption / Slow Sorption; N/A: not analyzed;
k_1: biodegradation rate constant expressed as F: fast, I: intermediate, and S: slow.
k_1 values chosen to cover a range of values given in the literature (Nam and Alexander 1998; Laor et al., 1999; Rouse, 1999); DRL: desorption rate limited;
Cw: phenanthrene aqueous concentration

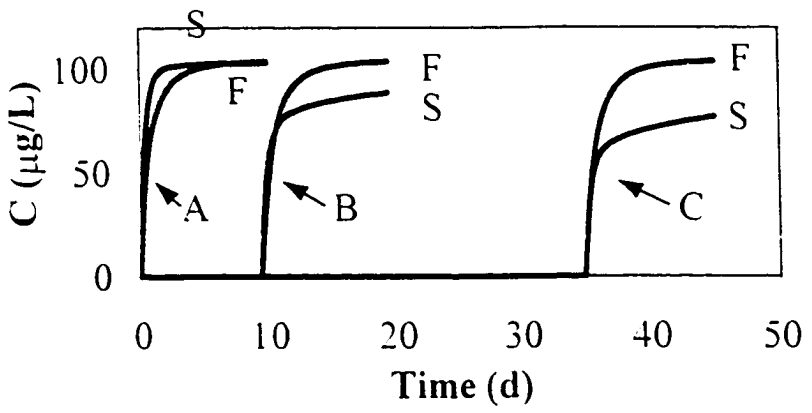


FIGURE 4.6 Concentration degraded with fast biodegradation (k_1= 0.1 1/hr), va pre-equilibration times (i.e., lag periods for biodegradation) (lag time A=0, B=9.5 and C=35 days), and sorption kinetics (S: slow sorption; F: Fast sorption).

When some of the solute is already sorbed before biodegradation commer (i.e., Cases B and C in Figure 4.6), biodegradation is desorption rate limited w sorption is slow (diffusion-limited). When sorption is fast, desorption does not l biodegradation compared to when the sorption is slow (compare fast line shapes slow ones in Case B and C of Figure 4.6) because as the aqueous concentratic degraded, more solute desorbs. However, when sorption is slow, biodegradatic desorption rate limited for fast biodegradation rates. For slow biodegradation r (see Table 4.5) there is enough time for both slow and fast sorption to occur, and biodegradation is not desorption-rate limited.

Previous researchers using other models and parameters (i.e., higher diffu coefficients, higher biodegradation rates, and lower sorption coefficients) (Scow Hutson, 1992; Chung et al., 1993; Scow et al., 1995) have seen similar trend: most of the observations presented here. According to calculations propose Chung et al. (1993), diffusion-limited sorption for variables used in the present s cannot be ignored (especially for the sample with organic matter dominated by (particles). The use of a coupled model is recommended to capture the effe sorption kinetics on biodegradation rates. Even without varying the sor coefficient there is a pronounced effect on the biodegradation curve shape by vai the sorption kinetic properties (see Figure 4.6). When there are sorbing/desorbing fractions in the sediment, the use of a two compartment, first-(desorption model seems adequate to describe the initial step of fast desor (Cornelissen et al., 1998). Whereas the same model is not capable of prec describing these processes when biodegradation becomes desorption-rate limited

model describes accurately the diffusion-limited desorption kinetics and therefore biodegradation kinetics.

4.3.5 Linear versus Nonlinear

Table 4.6 presents another sensitivity analysis that was performed demonstrate the effect of adding nonlinear sorption to the coupled diffusion-lin sorption and biodegradation model. The following parameters were varied du this analysis: the lag time before biodegradation, the biodegradation rate constant aqueous concentration in equilibrium and thus the sorption distribution coeffic and the diffusion rate. The sorption linearity comparison is between N = 1 and 0.5. One of the sediment samples evaluated in this study demonstrated an N valu 0.55 (see Table 4.1), and Kleineidam et al. (1999) presented samples with N valu low as 0.38. Thus, while an N value of 0.5 is highly nonlinear, it is not an extr value. In all cases of the sensitivity analysis, the general trend was the same example is presented in Figure 4.7.

Figure 4.7A presents the behavior of the aqueous solution when sorpti linear compared to nonlinear (N = 1 vs. 0.5, respectively). These results re careful interpretation to avoid making wrong conclusions. Looking only a aqueous concentration, the response appears to be similar for linear and nonl sorption, suggesting that it is not necessary to account for nonlinear sorp However, Figure 4.7B shows that nonlinear desorption kinetics will be much sl than would be predicted by the linear model. Concurrently, biodegradation will

TABLE 4.6 Sensitivity Analysis: Linear versus Nonlinear Sorption

lag	Eq	k_1	C_e	K_{deq}	Sorption	Linear (N=1.0) versus Nonlinear (N=0.50)			L_1 *10^{-6} (100 L_1/C_e)	L_2 *10^{-6} (100 L_2/C_e)
(d)		(1/hr)	(μg/L)	(L/kg)		Solution	Desorption	Biodegradation		
0	N	I (0.01)	53	140	Slow	S	F	F	2.7 (5.1)	1.4 (2.6)
0	N	S (0.001)	53	140	Slow	S	F	F	3.2 (6.0)	1.6 (3.0)
0	N	F (0.1)	53	140	Fast	S	F	F	13 (25)	9.6 (18)
0	N	I (0.01)	53	140	Fast	S	F	F	9.5 (18)	5.5 (10)
9.5	N	F (0.1)	53	140	Slow	S	F	F	5.3 (10)	2.7 (5.1)
9.5	Y	F (0.1)	53	140	Fast	S	F	F	13 (25)	6.9 (13)
0	N	I (0.01)	5.3	290	Slow	S	F	F	0.35 (6.6)	0.19 (3.6)
0	N	I (0.01)	530	66	Slow	S	F	F	18 (3.4)	9.2 (1.7)
0	N	I (0.01)	5.3	290	Fast	S	F	F	1.6 (30)	1.0 (19)
0	N	I (0.01)	530	66	Fast	F/S	FF	F	34 (6.4)	16 (3.0)
9.5	N	F (0.1)	5.3	290	Slow	S	F	F	0.76 (14)	0.41 (7.7)
9.5	Y	F (0.1)	5.3	290	Fast	S	F	F	2.6 (49)	1.6 (30)
9.5	Y	F (0.1)	530	66	Fast	S	F	F	47 (8.9)	19 (3.6)

lag: lag time before biodegradation starts; Eq: Y: yes or N: no, indicate if sorption equilibrium is reached before biodegradation starts; k_1: biodegradation rate constant expressed as F: fast, I: intermediate, and S: slow. k_1 values chosen to cover a range of values given in the literature (Nam and Alexander 1998; Laor et al., 1999; Rouse, 1999); C_e: estimated phenanthrene concentration at equilibrium; K_{deq}: estimated sorption distribution coefficient at equilibrium; N: Freundlich exponent; S: slower or F: faster, indicate the solute depletion, desorption, and biodegradation rate assuming linear sorption compared to nonlinear; F/S: suggest that depletion was first faster and then slower for linear sorption; FF: suggest that both sorption and desorption were faster for linear sorption; L_1: is the absolute maximum difference between the two model prediction lines (linear versus nonlinear); L_2: is the square root of the

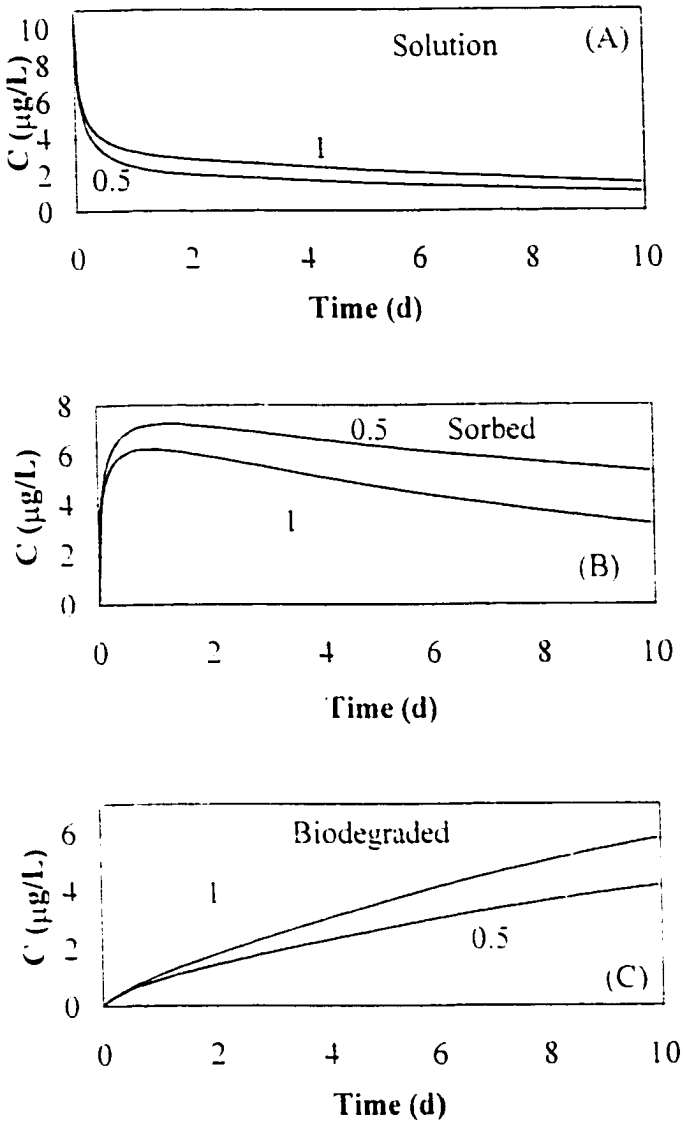


FIGURE 4.7 Linear (N = 1) versus nonlinear (N = 0.5) sorption coupled diffu: limited sorption and biodegradation kinetics. Prediction curves for concentration in solution, (B) sorbed, and (C) biodegraded.

be slower than the linear model would predict (see Figure 4.7C). Although the li model captures the overall aqueous behavior, it overestimates both the rat desorption and biodegradation, and thus the actual fate of the chemical. The li model suggests that much more of the chemical is removed (degraded) from system, whereas a portion of the chemical is actually still inside the grain due t nonlinear desorption behavior. In the case of Figure 4.7, the difference is 30% w is significant enough to require use of a nonlinear-based model.

How critical is it to include nonlinear sorption in the model? Table presents two columns with typical error norms used to compare two model out the first column presents the maximum absolute difference and the second the sq root of the mean of the difference squared for the degradation curves. These differences have also been normalized by the estimated equilibrium concentrati be able to compare cases where the concentrations were different. The factors cause the highest differences are fast sorption and fast biodegradation. Also hi sorption capacity (or lower equilibrium concentration) increases the diffe between the predictions. The greatest concentration normalized maximum abs difference in results was 49% and the concentration normalized square root o mean of the difference squared was 30% between the linear and the nonl predictions. It should be noted that much higher sorption coefficients have observed elsewhere (Karapanagioti et al., 1999), suggesting that this analys accurate and reasonable. Differences of that magnitude suggest that it is critic consider nonlinear sorption as a variable in a coupling diffusion/sorption biodegradation model.

4.4 Conclusions

This research documents the development of a model that cou diffusion/sorption and biodegradation, validates with experimental data, and uses model to perform sensitivity analyses. The model includes intraparticle diffus nonlinear sorption, and biodegradation kinetics. When biodegradation commer with chemical introduction, then fast sorption limits the biodegradation. W biodegradation starts after some lag period, the chemical has time to sorb be biodegradation commences and slow sorption causes biodegradation to be desorpt rate limited (if biodegradation is relatively fast).

The uniqueness of our model is the incorporation of nonlinear sorpt While the linear sorption model captured the behavior of aqueous concentrati differences of up to 49% were found between the linear and the nonlinear predic for the concentration that was desorbed, and the linear model overestimated concentration degraded. Consequently, if a linear model is used inappropriatel the field, the degradation potential and risk reduction will be overestimated. It is critical to consider nonlinear sorption in models estimating biodegradation, na attenuation, and bioremediation.

Acknowledgements

This study was partially funded by the U.S. National Science Foundation throug EPSCoR program. I would like to thank Chris Gossard and Dr. Kolar for the m development and Carrie Evenson and Dr. Strevett for phenanthrene-degra

microbe isolation and identification. I would also like to thank Prof. Dr. Grathwohl from the Universität Tübingen, Germany for providing us with intraparticle diffusion code, Dr. K. Scow from U.C. Davis for providing us with code, Tuan Van Doan from O.U. for his assistance in obtaining the experimental d Samples studied in this research were taken from the Norman Landfill Research S which is a USGS Toxic Substances Research (http://wwwok.cr.usgs.gov/norlan/site.html). I acknowledge the assistance of Scott Christenson in obtaining samples from the site.

References

Alexander M., 1994. Biodegradation and Bioremediation, Academic Press, Diego.

Angley J.T., Brusseau M.L., Miller W.L., and Delfino J.J., 1992. "Nonequilibr Sorption and Aerobic Biodegradation of Dissolved Alkylbenzenes du Transport in Aquifer Material: Column Experiments and Evaluation Coupled Process Model", Environ. Sci. Technol., 26, (7), 1404-1410.

Brusseau M.L., Xie L., and Li L., 1999. "Biodegradation During Contami Transport in Porous Media: 1. Mathematical Analysis of Controlling Fact J. of Cont. Hydraul., 37, (3), 269.

Chung G.Y., Mc Coy B.J., and Scow K.M., 1993. "Criteria to Assess W Biodegradation is Kinetically Limited by Intraparticle Diffusion Sorption", Biotechol. Bioeng. 41, (6), 625-632.

Cornelissen G., Rigterink H., Ferdinandy M.M.A., and Van Noort P.C.M., 1 "Rapidly Desorbing Fractions of PAHs in Contaminated Sediments Predictor of the Extend of Bioremediation", Environ. Sci. Technol., 32, 966-970.

Estrella M.R., Brusseau M.L., Maier R.S., Pepper I.L. Wierenga P.J., and M R.M., 1993. "Biodegradation, Sorption, and Transport of Dichlorophenoxyacetic Acid in Saturated and Unsaturated Soils", A Environ. Microbiol., 59, (12), 4266-4273.

Evenson C. and Strevett K., 1999. University of Oklahoma, unpublished data.

Fry V.A. and Istok J.D., 1994. " Effects of Rate-Limited Desorption on the Feasib of In-Situ Bioremediation", Wat. Resour. Res., 30, (8), 2413-2422.

Grathwohl P., 1998. Diffusion in Natural Porous Media: Contaminant Trans Sorption/Desorption and Dissolution Kinetics, Kluwer Academic Publis Boston, Massachusetts.

Guerin W.F. and Boyd S.A., 1993. "Bioavailability of Sorbed Naphthalen Bacteria: Influence of Contaminant Aging and Soil Organic Carbon Cont in Sorption and Degradation of Pesticides and Organic Chemicals in Soil, Science Society of America and American Society of Agronomy, Sp Publication No 32, Madison, Wisconsin.

Hatzinger P.B. and Alexander M., 1995. "Effect of Aging of Chemicals in Soi their Biodegradability and Extractability", Environ. Sci. Technol., 29, 537-545.

Jäger R., 1997. Modellierung Nichtlinearer Intrapartikel-Diffusion in Heteroge Aquifermaterial, Diploma Thesis, University of Tübingen, FRG.

Karapanagioti H.K., Kleineidam S., Ligouis B., Sabatini D.A., and Grathwoh 1999. "Impacts Of Heterogeneous Organic Matter On Phenanthrene Sorp Equilibrium And Kinetic Studies With Aquifer Material", Environ. Technol., accepted.

Karickhoff S.W., Brown D.S., and Scott T.A., 1979. "Sorption of Hydroph Pollutants on Natural Sediments", Wat. Res., 13, 241-248.

Kleineidam S., Rügner H., Ligouis B., and Grathwohl P., 1999. "Organic M Facies and Equilibrium Sorption of Phenanthrene", Environ. Sci. Tech 33, (10),1637-1644.

Koelbel-Boelke J., Tienken B., and Nehrkorn A., 1988. "Microbial Communiti the Saturated Groundwater Environment I: Methods of Isolation Characterization of Heterotrophic Bacteria", Microbial Ecology, 16, 17-2

Laor Y., Strom P.F., and Farmer W.J., 1999. " Bioavailability of Phenanth Sorbed to Mineral-Associated Humic Acid", Wat. Res., 33, (7), 1719-172

Machate T., Noll H., Behrens H., and Kettrup A., 1997. "Degradation Phenanthrene and Hydraulic Characteristics in a Constructed Wetland", \ Res., 31, (3), 554-560.

Montgomery J.H. and Welkom L.M., 1990. Ground Water Chemicals D Reference, Lewis Publishers, Inc., Chelsea, Michigan.

Nam K. and Alexander M., 1998. "Role of Nanoporosity and Hydrophobicit Sequestration and Bioavailability: Test with Model Solids", Environ. Technol., 32, (1), 71-74.

Park J.H., Zhao X., and Voice T.C., 1999. "Comparison of Biodegradation Kir Parameters for Naphthalene in Batch and Column Systems by *Pseudom Putida*", in review.

Rouse J.D., Furukawa K., and Morimura K., 1999. "Bioremediation of Petrol Hydrocarbon Contaminants Using Anionic Surfactants", Report submitte The Japanese Ministry of Education (Monbusho). Project Number 096805

Rügner H., Kleineidam S., and Grathwohl P., 1998. "Long Term Sorption Kinetic Phenanthrene in Aquifer Materials", Environ. Sci. Technol., 33, (10), 1(1651.

Sherrill T.W. and Sayler G.S., 1980. "Phenanthrene Biodegradation in Freshw Environments", Appl. Environ. Microbiol., 39, 172-178.

Simkins S. and Alexander M., 1984. "Models for Mineralization Kinetics with Variables of Substrate Concentration and Population Density", Appl. Env Microbiol., 47, (6), 1299-1306.

Scow K.M. and Alexander M., 1992. "Effect of Diffusion on the Kinetic Biodegradation: Experimental Results with Synthetic Aggregates", Soil Soc. Am. J., 56, 128-134.

Scow K.M. and Hutson J., 1992. "Effect of Diffusion and Sorption on the Kineti Biodegradation: Theoretical Considerations", Soil Sci. Soc. Am. J., 56, 127.

Scow K.M., Fan S., Johnson C., and Ma G.M., 1995. "Biodegradation of Sc Chemicals in Soil", Environmental Health Perspectives, 103, Supplem (Biodegradation), 93-95.

Stringfellow W.T. and Aitken M.D., 1994. "Comparative Physiology of Phenanth Degradation by Two Dissimilar Pseudomonas Isolated from a Creo Contaminated Soil", Can. J. Microbiol., 40, 432-438.

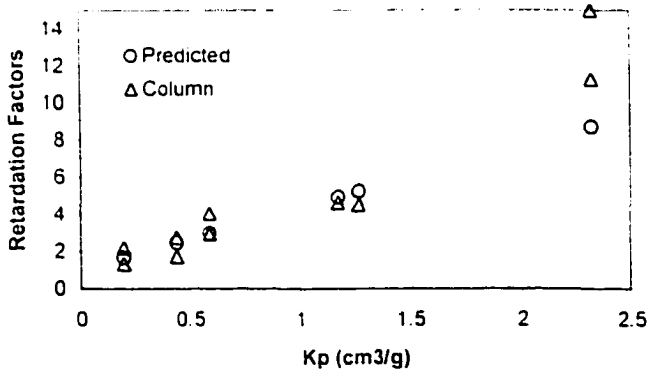
APPENDICES

Appendix A

Preliminary Batch and Column Studies – Chapters 1 and 2.

Chemical	K_{ow}	Log K_{ow}	K_p (cm^3/g)	K_p / K_{ow}	Predicted R_f	Col.1 R_f	Col.2 R_f
Benzene	130	2.1	0.20	0.0015	1.6	1.3	2.2
Toluene	450	2.7	0.44	0.00099	2.5	1.7	2.7
o-Xylene	890	3.0	1.3	0.0014	5.2	4.5	N/A
Ethyl-benzene	1300	3.1	1.2	0.00087	4.9	4.6	N/A
Chloro-benzene	690	2.8	0.59	0.00086	3.0	2.9	4.04
Di-chloro-benzene	2400	3.4	3.3	0.0014	12	N/A	N/A
Naphthalene	2300	3.4	2.3	0.0010	8.7	11	15
Phenanthrene	37,000	4.6	50	0.0013	170	N/A	N/A

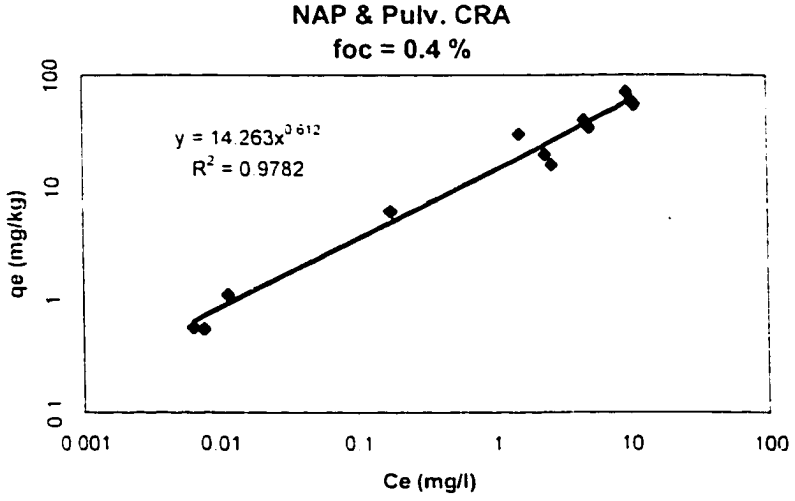
K_{ow}: octanol-water partition coefficient (reference *28* of Chapter 2); K_p: sorption partition coefficient measured after 48 hours of solution-media contact (experimer were performed with unaltered Canadian River Alluvium); R_f: retardation factor; Predicted R_f: predicted R_f based on batch K_p values ($R_f = 1+(\rho_b/n)\ K_p$); Col.1 R_f: actual R_f value measured in a column experiment with pore water velocity 10 cm/l Col.2 R_f: actual R_f value measured in a column experiment with pore water veloci cm/h

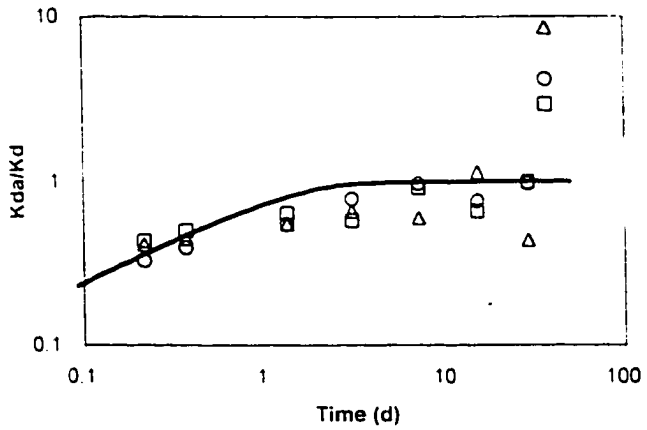


Difference between the predicted and actual column retardation factor for naphthalene (last point in Figure) suggests that 48 hrs of contact time between the media and the chemical solution is not enough time for sorption to reach equilibri

Appendix B

Supplement to Chapter 1 – Tables 1.2 and 1.3: Naphthalene Equilibrium and Kine Sorption Properties





Properties	N	K_{fr}	Log K_{oc}	D_α/α^2	T 75%
Naphthalene	0.61	14	3.5	7.1E-07	1.1

N: Freundlich exponent; *Kfr*: Freundlich constant ((mg/kg)(L/mg)^N); *Koc*: organic carbon normalized sorption coefficient calculated at chemical equilibrium concentration (*Ce*) equal to 1 mg/L (Note: naphthalene solubility: ~30 mg/L); D_α: apparent diffusion rate (1/s); T 75%: time to reach 75% equilibrium (d)

Appendix C

Supplement to Chapter 1 – Bold numbers in last column are presented in Figure 1.- and discussed in page 21: Hot Methanol Extraction

Sample	Initial Mass	Mass Left	Mass in Solution	Mass in Soil	Mass Recovered	Mass Lost	Mass Recoverec
ID*	µg	µg	µg	µg	µg	µg	%
CRA comp. A	11.1	10.1	1.13	1.83	2.96	1.00	**36**
CRA comp. B	11.1	9.3	4.81	4.50	9.31	1.80	**100**
CRA comp. C	11.1	10.1	1.76	2.18	3.93	1.00	**44**
0.5 A	11.9	10.3	2.16	1.33	3.48	1.60	43
0.5 B	11.9	10.3	0.12	1.59	1.71	1.60	28
0.5 C	11.9	10.3	3.01	1.73	4.73	1.60	53
0.25A	11.1	10.1	2.96	1.31	4.26	1.00	47
0.25 B	11.1	10.1	5.05	1.33	6.38	1.00	66
0.25 C	11.1	10.1	6.86	2.13	9.00	1.00	90
0.125 A	11.9	10.1	2.61	0.80	3.41	1.80	44
0.125 B	11.9	10.1	5.27	2.00	7.28	1.80	76
0.125 C	11.9	9.3	4.58	3.51	8.09	2.60	90
0.063 A	11.9	9.3	6.14	2.98	9.13	2.60	99
0.063 B	11.9	10.1	2.72	0.93	3.65	1.80	46
0.063 C	11.9	10.1	0.11	1.22	1.33	1.80	26

*Sample ID: corresponds to Sample Code in Chapter 1 with A, B, and C indicatin triplicate vial ID.

Appendix D

Supplement to Chapter 1 – Tables 1.3 and 1.4: Model Error

Sample	Error		
	Figure 1.2 considering all timestep measurements	Figure 1.2 Without considering first timestep measurement	Figure 1.3
CRA comp.	0.046	0.028	0.0069
0.5	0.096	0.042	0.0160
0.25	0.138	0.138	0.0600
0.125	0.021	0.013	0.0100
0.063	0.056	0.055	0.0390

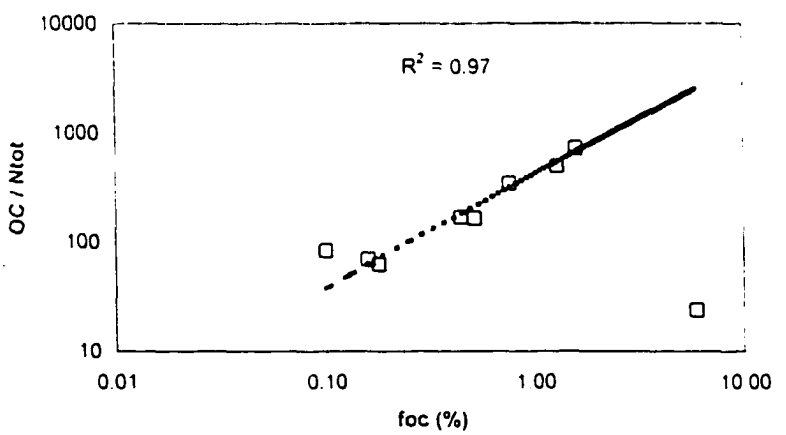
Sample Code is based on grain size in mm except for CRA comp.: Canadian River Alluvium composite sample; Error: Mean weighted squared error (reference *22* of Chapter 2).

Appendix E

Supplement to Chapter 2 – Table 2.2: Elemental Analysis

Sample Code	C	H	N_{tot}	OC/N_{tot}
CRA comp.	0.98	0.026	0.0026	170
$0.5M_{AOM}POM_{PH}$	5.90	0.022	0.2500	24
$0.5POM_{CL}$	1.60	0.019	0.0022	730
$0.25POM_{PH}M_{POM}$	1.90	0.015	0.0026	500
$0.25M_{POM}$	0.43	0.012	0.0023	70
$0.125C_{AOM}POM_{PH}$	1.30	0.017	0.0031	160
$0.125C_{AOM}$	0.36	0.019	0.0012	83
$0.063POM_{CH}C_{AOM}$	1.60	0.015	0.0022	350
$0.063C_{AOM}POM_{CL}$	0.68	0.017	0.0029	62

Sample Code: same as in Chapter 2; C: total carbon; H: total hydrogen; N_{tot}: total nitrogen; (C,H,N_{tot}): all expressed as % of total sample weight; OC: organic carbo



f_{OC}: fraction organic carbon content

Appendix F

Supplement to Chapter 3 – Tables 3.1 and 3.4: Weight distribution, elemental analysis, and organic carbon in grain size fractions.

Depth (ft)	Grain size fraction (mm)	wt %	OC %	C %	H %	N %
6-6.5	0.5-0.25	2.1	0.200	0.77	0.013	0.0013
	0.25-0.125	34	0.043	0.48	0.014	0.0019
	0.125-0.063	60	0.033	0.46	0.014	0.0013
	<0.063	4.0	0.058	0.83	0.012	0.0020
6.5-8	1-0.5	0.6	N/A	N/A	N/A	N/A
	0.5-0.25	12	0.012	0.16	0.009	0.0025
	0.25-0.125	73	0.021	0.25	0.010	0.0032
	0.125-0.063	13	0.027	0.48	0.011	0.0025
	<0.063	0.7	0.065	1.30	0.013	0.0019
14-16	1-0.5	28	0.190	0.85	0.046	0.0022
	0.5-0.25	48	0.140	0.63	0.050	0.0016
	0.25-0.125	14	0.230	0.87	0.063	0.0033
	0.125-0.063	4.8	0.400	1.60	0.071	0.0038
	<0.063	3.7	0.600	2.20	0.095	0.0100
28-30	1-0.5	10	0.017	0.22	0.024	0.0013
	0.5-0.25	63	0.017	0.21	0.028	0.0023
	0.25-0.125	21	0.024	0.40	0.040	0.0016
	0.125-0.063	4.9	0.069	0.74	0.036	0.0025
	<0.063	1.8	0.260	1.50	0.037	0.0023

Sample Code: same as in Chapter 3; wt %: weight fraction of subsample relative t composite; OC: organic carbon; C: total carbon; H: total hydrogen; N: total nitrog (C,H,N): all expressed as % of total sample weight

Appendix G

Collaborative Information provided by Dr. Lyon as a supplement to Chapter 3 – Ar attempt to further characterize the organic matter properties presented in Table 3.2 and 3.3.

MEMORANDUM
MANTECH ENVIRONMENTAL RESEARCH SERVICES CORP.
Environmental Science
In reply refer to: 99-WL?/v
To: Dr. Guy Sewell
From: William G. Lyon
Thru: Jim Seeley
Subject: SR #RE-0-109
Date: March 31, 1999

Results for SR #RE-0-109 , FTIR-Photoacoustic Spectra of Soil Samples fi NFL Tracer Test Area
Dear Guy:

The following results are based on samples received on 3/11/99 and on 3/2. from researchers at the University of Oklahoma (Professor David Sabatini and Hrissi Karapanagioti). Our basic strategy for detecting organic materials in quart sands by FTIR is to make a very careful comparison between spectra of as-is sam and spectra of chemically stripped samples. The chemical stripping is designe remove some portion of the organic constituents without greatly modifying mineral composition. Stripping methods are described in *RSKSOP-115* and - These methods, involving aqueous NaOH and concentrated H_2O_2, were applie the samples at the University of Oklahoma.

EXPERIMENTAL CONDITIONS

FTIR-PA spectra of the sediment samples were obtained in duplicate (denot and B) by co-addition of 256 scans at a resolution of 4 cm^{-1}. All spectra obtained on material initially dried at 60 C, and then purged in the photoacousti with cryogenically dried high purity helium gas. Noise curves were obtaine subtracting duplicate spectra, then multiplying the result by ½ 2, i.e., 0.707*(spec A - spectrum B). Ideally, these noise curves should be flat, and should display uniform Gaussian noise. Procedures for the use of the photoacoustic accessor for general QA/QC testing of the optical bench are detailed in *RSKSOP-187* and

QUARTZ BANDS IN SPECTRA OF AQUIFER MATERIAL

The spectra of the Canadian material contains many distinctive bands indicati -quartz, for example, the very sharp fundamental band at ca. 695 cm^{-1}, an

combination band at ca. 1870 cm^{-1}. The combination band at 1870 cm^{-1}, wl visible, is a particularly reliable indicator for -quartz, since there are hardly e bands in this region from organic compounds. Quartz also has a broad, very str Si-O stretching band in the region 1160-1050 cm^{-1}, as do many other silica Generally, when strong quartz bands are present, it is difficult to see traces of ot materials directly in the sediment spectra.

RESULTS FOR YOUR SAMPLES

The spectra of individual materials and also various comparison spectra displayed in a series of figures attached to this letter. Thirteen plots are included your samples. Our spectral file reference numbers indicated in boldface in the lis spectra given below.

Samples were delivered to the laboratory on March 11, 1999 by Ms. Hr Karapanagioti, who was also present during data acquisition. The first two spec pairs were obtained on the highest TOC sample (As-Is and Stripped) so that feasibility of the subtraction method could be assessed on the most favorable sam Unfortunately, these samples contained obvious signs of carbonate mineral conter evidenced by the combination bands observed near 2500 cm^{-1} and 2800 - 3000 cr These bands probably indicate the presence of hard-water evaporite minera caliche) on sand grain surfaces. The 2800 - 3000 cm^{-1} set of bands is especi troublesome because it coincides so completely with the region of aliphatic stretching, which is needed to corroborate the presence of organic matter in subtract spectra.

1. FTIR-PA spectrum A and noise for Canadian river alluvium, TO 0.40%. Data Files: **061-2a, -2b.spc**

2. FTIR-PA spectrum A and noise for Canadian river alluv Chemically stripped with NaOH(aq.) and H_2O_2. Data Files: **061-3b.spc**

The indication of carbonate minerals suggested that an HCl-wash of the sedim prior to other treatments might be beneficial[1]. Additionally, this highest TOC sa appeared to have a significant portion of its TOC present in the form of parti therefore, a density separation using a bromoform-carbon tetrachloride mi (following *RSKSOP-107*) was suggested as a means of providing a concentı

[1]Note that an HCl wash can remove lower molecular weight humic material, e.g., some fulvic a Acid washing also tends to alter the carboxylate groups on organic solids to carboxylic acid gro shifting the C-O stretch to higher values (more double bond character).

sample of organic matter[2]. These new samples were provided on 3/25/99. Spectr 6 demonstrates that the acid-treatment was effective in removing approximately t thirds of the carbonate from the highest TOC sample.

3. FTIR-PA spectrum A and noise for density separated organic parti from high TOC sample, files: **063-2a, -2b.spc**

4. FTIR-PA spectrum A and noise for Canadian river alluvium, TO 0.40%, pretreated with HCl, Data Files: **063-3a, -3b.spc**

5. FTIR-PA spectrum A and noise for Canadian river alluvi pretreated with HCl and chemically stripped, Data Files: **063-4 4b.spc**

1. Enlarged plot showing effect of acid treatment on spectrum of 0 TOC sample.

7. FTIR-PA spectrum A and noise for Canadian river alluvium, TO 0.20%, pretreated with HCl, Data Files: **066-2a, -2b.spc**

8. FTIR-PA spectrum A and noise for Canadian river alluv pretreated with HCl and chemically stripped, Data Files: **066-3 3b.spc**

9. FTIR-PA spectrum A and noise for Canadian river alluvium, TC 0.04%, pretreated with HCl, Data Files: **069-2a, -2b.spc**

10. FTIR-PA spectrum A and noise for Canadian river alluv pretreated with HCl and chemically stripped, Data Files: **069-3 3b.spc**

SPECTRA OF KNOWN STANDARDS

Two mineral spectra are also attached to this report to give you some idea o bands associated with the major minerals, quartz and calcite. These includ following:

11. FTIR-PA spectrum for -quartz (oil creek sand, -635 mesh)

2. FTIR-PA spectrum for $CaCO_3$ (optical grade calcite)

---

[2]Note that the dense mixture of bromoform and carbon tetrachloride (ca. 2.00 g cm^{-3}) can als dissolve loosely bound lipids from humic coatings and organic particles. This would decrease t size of the aliphatic C-H stretching bands in the 2800 - 3000 cm^{-1} range.

Additionally, the samples appear to have some clay (probably smectite-illite) perhaps some iron minerals present. The clay is visible spectroscopically mainly resolved broad band near 3600 cm^{-1}; other clay bands would overlap extensi with quartz bands, and be very hard to see. The iron mineral (hematite?) is obse only as a trace of reddish color, visible in some of the as-is samples, but not ir chemically stripped samples.

COMPARISON OF ORGANIC MATTER SPECTRA

In the following three spectra, comparisons are made between the partic organic matter, and other organic matter.

13. This figure shows the spectrum of separated organic part from the high TOC sample compared to the difference spect which represents, in part, a spectrum of the in-situ organic matt the high TOC sample. There are some similarities and differe Note that the separated organic particles are not entirely fre mineral matter as evidenced by the trace appearance of characteristic quartz combination bands, and the Si-O stretch band The particles show the larger set of aliphatic bands. These four b are assigned to asymmetric and symmetric H-C stretching assoc with methyl and methylene groups in aliphatic chains. The fact the methylene bands dominate indicates fairly long aliphatic ch The in-situ organic matter shows smaller aliphatic content.

The subtraction appears to have successfully removed both quartz calcite combination bands from the difference spectrum. The lea edge of the carbonyl-carboxylate region appears to have res bands near 1651 and 1556 cm^{-1} for the in-situ OM; whereas spectrum of the particles yields a single broad band peaking at Both spectra show a band-head peak near 1420. This would see indicate that the in-situ organic matter, following HCl treatment, higher proportion of its carbonyl contribution associated carboxylic acid. This band is probably also present in the spectru the particulate OM; however, it will require curve-fitting to resol This region of OM spectra is complex, involving overlapping b from carboxyl groups, asymmetric and symmetic carbo stretching, and aromatic ring deformations.

14. This figure compares subtraction spectra from samples TOC levels at 0.4 % and 0.2 %. There were difficulties decidi the subtraction factor for the lower TOC sample. With the subtra factor set at 0.35, the carbonate combination bands were rem precisely, and no traces of H-C stretch were detected; howeve quartz combination bands were under-subtracted. With the fact at 0.54, the quartz combination bands were approximately can

out, but the Si-O region and carbonate combination bands are cle
over-subtracted. The supposed bands resolved at 1696 and 1626 c
in the carbonyl-carboxylate region appear too narrow to be from (
and the lack of H-C stretching bands seems consistent with
negative finding. Therefore, the peculiar subtraction behavior for
0.2 % TOC sample is attributed to a mismatch in mineral conter
the as-is and stripped samples, probably induced by the processing.

15. This last figure compares the subtraction spectra obtained
samples with TOC levels at 0.4 % and 0.04 %. No org
matter was convincingly detected in the latter sample.

CONCLUSIONS

Spectra of natural organic matter were successfully obtained only for the sar
with the highest TOC value (0.40 %). The density-separated particulate org
matter yielded a high quality spectrum with very good signal to noise ratio, w
should be amenable to non-linear regression of the important bands. The sub
spectrum showing the in-situ organic matter in this high TOC sample is of l
quality, but could possibly be improved by increased purging of the sample with
helium, and by co-addition of a larger number of scans. Nevertheless, nonli
regression of this spectrum might yield an improved set of band positions, espec
for the carbonyl-carboxylate region.

Please let me know if you have any questions on these spectra or
interpretation.
spectra(15)
xc: D. Sabatini

REFERENCES

Lyon, W.G., and Rhodes, D.E., 1990, Density Separation of Solid Organic M
from Aquifer Sediments, *RSKSOP-107*.

Lyon, W.G., and Harvey, J.M., 1991 Destruction of Aquifer or Soil H
Materials by Hydrogen Peroxide, *RSKSOP-115*.

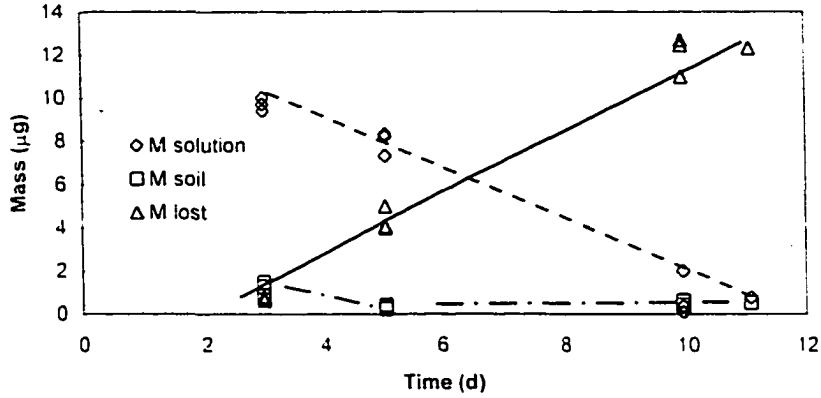
Lyon, W.G., and Staggs, R.L., 1993, Chemical Stripping of Organic Coatings
Aquifer Sands, *RSKSOP-129*.

Staggs, R.L., Lyon, W.G., and Glass, R.L., 1996, QC Procedures for the Di
FTS-45 Fourier Transform Infrared Spectrophotometer using the Hewlett-Pa
Vectra VL 5/100 and the Windows Supported Software, WIN-IR, *RSKSOP-187*.

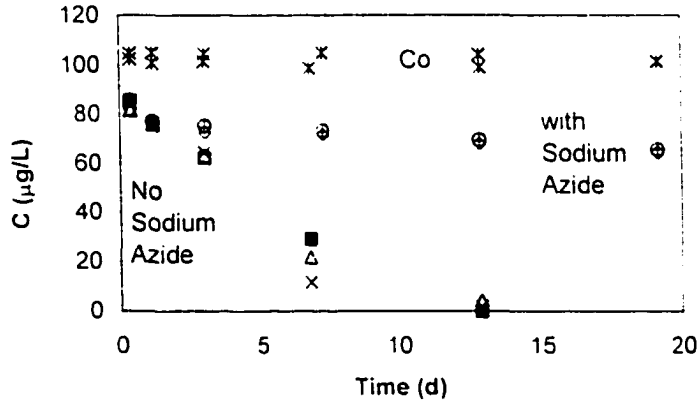
Lyon, W.G., Glass, R.L. and Staggs, R.L., 1996, Operation of the Digilab FT
Fourier Transform Infrared Spectrophotometer Using WIN-IR and the M
Accessory for Photoacoustic Spectra, *RSKSOP-188*.

Appendix H

Preliminary coupled sorption and biodegradation studies – Chapter 4



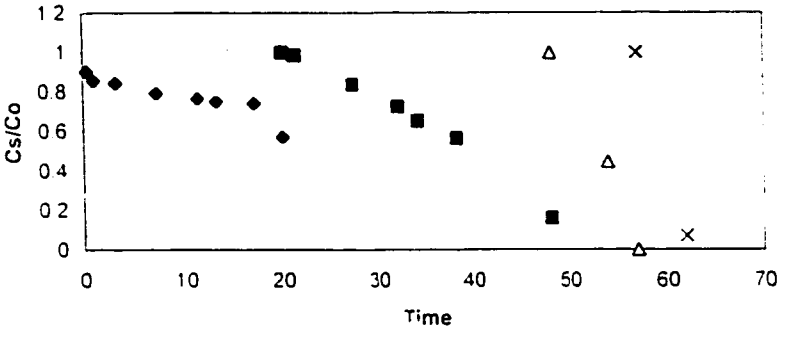
M solution: mass monitored through aqueous concentration measurements; M soil mass monitored through hot methanol extraction; M lost: Mass lost = Mass initial added – M solution – M soil.



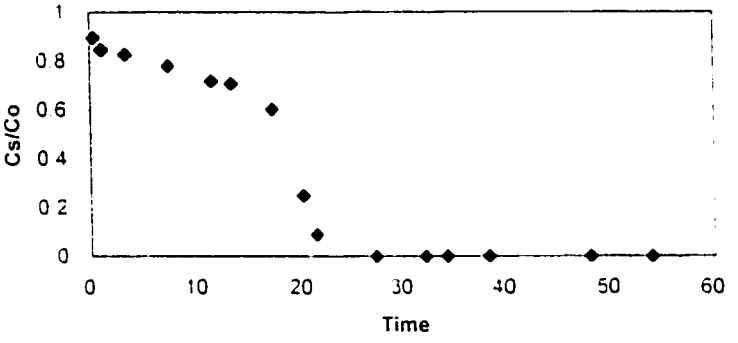
C_o: Blank concentration; Phenanthrene solution concentration in vials with sampl 6-6.5 ft (see Chapter 3) with soil and biocide (with sodium azide) and soil withou biocide (no sodium azide).

Preliminary coupled sorption and biodegradation studies – Chapter 4

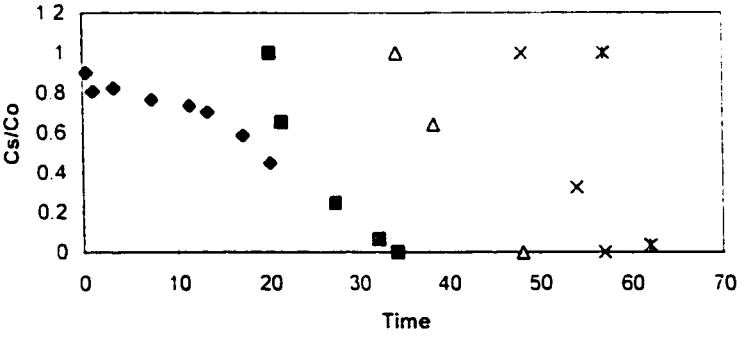
A



B



C



Triplicate samples with phenanthrene. Canadian River Alluvium and biocide; Degradation starts at ~17 days, A and C: several phenanthrene additions after phenanthrene aqueous concentration is depleted; B: phenanthrene is depleted belc the detection limit.

Appendix I

Collaborative information provided by Chris Gossard as a supplement to Chapter
Section 4.2.2

BACKGROUND

The literature review revealed a lack of models that couple both intraparticle diffus
with non-linear sorption and biological degradation. The model of Chung et
includes biodegradation in the external buffer solution but does not allow for r
linear sorption isotherms. Similarly, the model of Jäger considers non- linear sorp
but no degradation is incorporated into the model. This model also includes sev
options for grain sizes and types assuming a homogeneous distribution of the vari
grains. Our model incorporates the best characteristics from each of these two mo
by modifying Jäger's model to include biodegradation in the external solution.

MATHEMATICAL MODEL

In addition to those mentioned by Chung et al., two more simplifying assumpt
were made in the development of our model for intraparticle diffusion with non-li
sorption including biological degradation. For ease of implementation the follov
were assumed:

1 Biodegradation occurs only in the external buffer solution; microorganisms
excluded from the pore spaces of aggregates.
2 Biodegradation is negligible during the time required for the pollutant to dif
into or out of the aggregates.

The physical system consists of a homogeneous mixture of porous sphe
aggregates, each with varying diameters and properties, in a homogeneous bu
solution of constant volume. Initially, the pollutant may be entirely in the exte
solution, entirely inside the aggregates, or partitioned between both.
concentrations in the inner and outer fluids can be different, but must be unif
within each. The change of internal and external chemical concentrations with
are obtained from the mass balance equations of the chemical in the aggregates ar
the buffer solution.

The mass balance for the chemical inside the aggregates is written for the intrapar
concentration, $C(r, t)$ as,

$$\frac{\partial}{\partial t}\left(\varepsilon_j C_{jk} + \rho_j S_j[C_{jk}]\right) = \frac{D_{e,j}}{r^2}\frac{\partial}{\partial r}\left(r^2 \frac{\partial C_{jk}}{\partial r}\right) \tag{1}$$

where the subscripts j and k indicate grains of different type and radii respecti
The boundary conditions are

$$\left.\frac{\partial C_{jk}}{\partial r}\right|_{r=0} = 0 \tag{2}$$

$$-D_{e,j}\left.\frac{\partial C_{jk}}{\partial r}\right|_{r=R} = k_f (C_R - C_e) \tag{3}$$

and the initial condition is

$$C = C_{p0} \text{ at } t = 0 \tag{4}$$

Equations (1) and (2) are discretized using block centered differences and a weigh Euler time stepping scheme while Eq. (3) is discretized with a one-sided differe and explicit time stepping. For sorption the following three isotherms are considere linear.

$$S_i[C_{ik}] = K_d(C_{ik}) \tag{5}$$

Freundlich.

$$S_i[C_{ik}] = K_f(C_{ik})^{NF} \tag{6}$$

and Langmuir.

$$S_i[C_{ik}] = \frac{K_l(NF)(C_{ik})}{1 + NF(C_{ik})} \tag{7}$$

where K_d, K_f, and NF are the sorption coefficients and depend upon the chemical a soil characterisitics.

The non-linear sorption isotherms require an iterative solution for the chem distribution within the grains. The model uses Pickard iteration and linearizes sorption isotherm as

$$S_i^{t+1(\mu)} - S_i^{t+1(\mu-1)} = \frac{\partial S[C^{t+1(\mu-1)}]}{\partial C}(C_i^{t+1(\mu-1)} - C_i^{t+1(\mu-1)}) \tag{8}$$

where μ is the iteration index and t is the time level.

In this paper, we consider only first-order biodegradation in the external bu solution. The mass balance for the chemical outside the aggregates is written for external concentration, $C_e(t)$, as

$$\frac{\partial C_e}{\partial t} = -k_1 C_e + n_{ik} A_{ik} k_f (C_R - C_e) \tag{9}$$

with initial condition

$$C_e = C_{e0} \text{ at } t = 0 \tag{10}$$

and n_{ik} is the number of aggregates per unit volume of solution and A_{ik} is the sur area of the aggregate, both differ for each grain type and size. The coefficien mass transfer from aggregates to the external fluid, k_f, is related to the aggregate and must be empirically calibrated for a particular system.

SOLUTION METHOD

The external buffer solution concentration is coupled with the intrapar concentration through the boundary condition. This additional process was incl in Jäger's code by replacing the equation for the edge node of the soil particle w discrete version of Equation (3) as follows:

$$-D_{e,i}\frac{C_R^{t+1} - C_{R-1}^{t+1}}{\Delta r} = k_f(C_R^t - C_e^t) \tag{11}$$

where the superscript refers to the time stepping.

Additionally, the discrete form of Equation (9) was included inside the time iterat but outside of the non-linear sorption iteration loop.

NOMENCLATURE

A_{jk} surface area of aggregate (cm^2)
C concentration inside aggregates (mg/ml)
C_e concentration outside aggregates (mg/ml)
C_{e0} initial outside concentration (mg/ml)
C_{p0} initial inside concentration (mg/ml)
C_R boundary concentration of aggregate (mg/ml)
D_e effective diffusion coefficient in aggregate pores (cm^2/s)
k_1 first-order biodegradation rate (s^{-1})
k_f coefficient for mass transfer from aggregates to external fluid (cm/s)
K_d adsorption coefficient (cm^3/cm^3 of solid)
K_f first non-linear isotherm coefficient
M total mass of aggregates (mg)
n number of aggregates per unit volume of solution (cm^{-3})
NF second non-linear isotherm coefficient
r radial coordinate in the spherical aggregate (cm)
R radius of spherical aggregate (cm)
S sorbed concentration inside aggregate (mg/ml)
t current time level
t+1 future time level
V volume of the external buffer solution (ml)
v_p volume of an aggregate (cm^3)

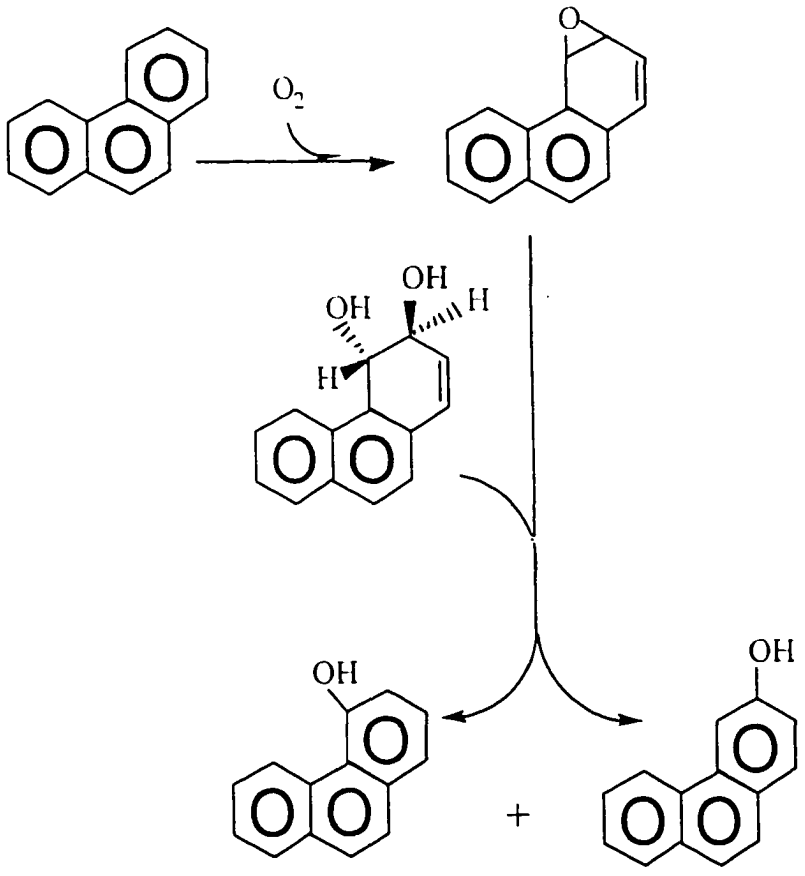
Greek letters

ε effective porosity of aggregates
ρ density of the aggregates (mg/ml)
μ iteration index

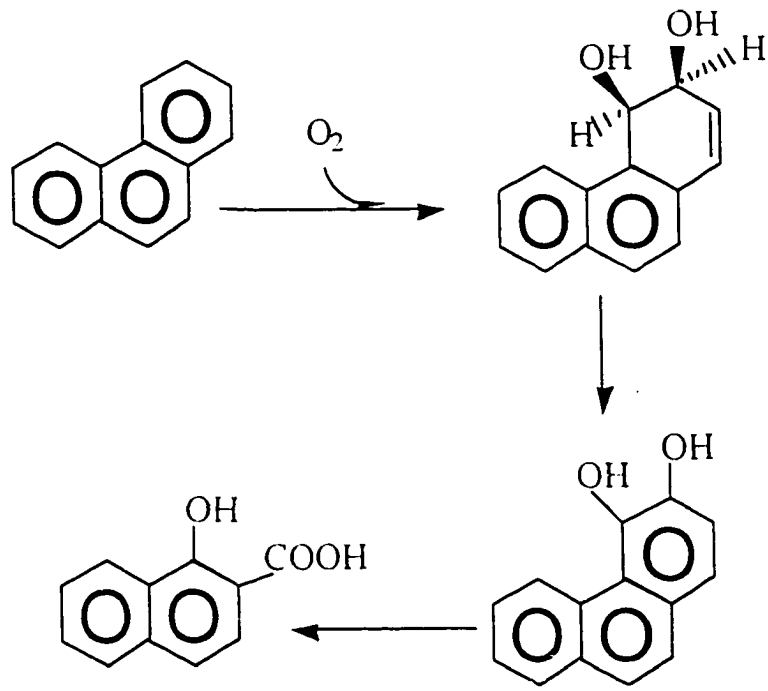
Appendix J

Collaborative information provided by Dr. Strevett as a supplement to Chapter
Section 4.3.2

The metabolic pathway commonly accepted for fungal organism *chrysosporium* is phenanthrene oxidized to phenanthrene-3,4-oxide then to phenanthrene-trans-3,4-dihydrodiol and possibly mineralized to CO_2 and other intermediates as follows (h the last step is 3-Phenanthrol or 4-Phenanthrol)[1]:



There was a 97% confidence that the fungal organism was *chrysosporium* and a 87 confidence that the synergistic bacteria was *Psuedomonas putida*. The metabolic pathway of bacteria[2]:



If indeed the fungal can grow on part phenanthrene and mineralize into the TCA cycle, and part degrade to an intermediate that the bacteria can use and produce 1H2N.

With the NA, a consortium grew. On MMS with phenanthrene, only two grew up were apparently synergistic and only the fungal colony out-complete the initial oxidation step (that is maybe why the bacteria did not grow alone -- weak enzyme structure).

[1] Sutherland, J., A. Selby, J. Freeman, F. Evans, and C. Cerniglia, 1991. Metaboli of phenanthrene by *Phanerochaete chrysosporium*, Appl. Environ. Microbiol., 57:3310-3316.

[2] Cerniglia, C., and M. Heitkamp, 1989. Microbial degradation of polycyclic aron hydrocarbon in aquatic environments. *In* Metabolism of Polycyclic Aromatic Hydrocarbons in the Aquatic Environment. Ed. by U. Varanasi. Boca Raton, FL, CRC Press, pp:41-68.

Appendix K

Supplement to Chapter 4 – Calculations proposed by Chung et al. (1993) discussec section 4.3.4

The use of a dimensionless group (φ) has been proposed as a criterion for determi the significance of intraparticle diffusion when both sorption and biodegrada occur simultaneously (Chung et al., 1993). This dimensionless group is defined

$$\varphi = a \{ (\varepsilon + K_d \rho) k_1 / D_e \}^{1/2}$$

where D_e is the effective diffusion coefficient of substrate in the grain internal por

TABLE Sorption Parameters Necessary for Estimating the Dimensionless Group φ

Sample Code	K_d (L/kg)	D_e (cm^2/h)	a (cm)	ε	ρ (g/cm^3)	k_1 (1/hr)	φ
Coaly	15,000	2.0E-06	0.0180	0.0084	2.6	0.04	500
Organic Coatings	26	5.8E-06	0.0044	0.0110	2.6	0.08	4.2
Mixture	140	6.5E-07	0.0027	0.0026	2.6	0.05	14

The sample code and variables are the same as in Chapter 4.
K_d : sorption distribution coefficient; D_e: effective diffusion coefficient of substra the grain internal pores; a: grain radius; ε: intraparticle porosity; ρ: grain density; k_1: first order rate coefficient for biodegradation reaction; φ: dimensio parameter

Comments

The previous table presents the parameters used to estimate the dimensionless g φ. The dimensionless group φ is two orders of magnitude higher for the sample organic matter dominated by coaly particles than the sample dominated by or coatings whereas the sample with mixed organic matter is in between. For the sa dominated by organic coatings the effective diffusion (D_e) has been modeled onl comparison purposes. This analysis demonstrates once again -- by the low φ val that diffusion in this sample can be ignored. On the contrary, the sample with POM biodegradation is very likely to be rate-limited by intraparticle diffusion.

Chung G.Y., McCoy B.J., and Scow K.M. (1993) "Criteria to Assess V Biodegradation is Kinetically Limited by Intraparticle Diffusion and Sorpt **Biotechol. Bioengineering**, V.41, pp. 625-632.

Appendix L

Independent research contacted on surfactant modified sorbents

Surfactant	Sorbent	Sorption plateau (g/g sorbent)
DOWFAX 8390	Alumina	0.060
STEOL CS330	Alumina	0.055
SMDNS	Alumina	0.020
AOT	Alumina	0.200 (precipitation wa observed)
HDTMA	Canadian River Alluvium	0.040

K_p: sorption partition coefficient measured after 48 hours of contact between chemical solution and sorbent.

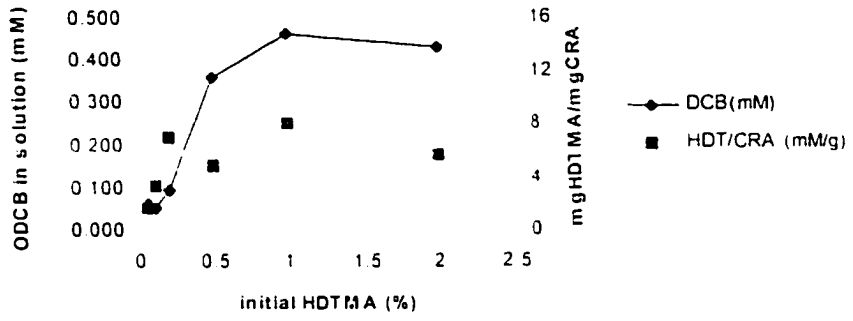
Chemical	CRA	HC	HZ	DA	LA	AA	SA
Benzene	0.2	N/A	N/A	N/A	N/A	N/A	N/A
Toluene	0.44	6.2	N/A	N/A	N/A	15.6	N/A
Ethyl-benzene	1.18	9	6.3	29.3	6.3	25.2	12.5
Di-chloro-benzene	3.28	27	50.8	58.6	34.9	51.3	25.2
Naphthalene	2.32	309	958	N/A	N/A	137.6	132

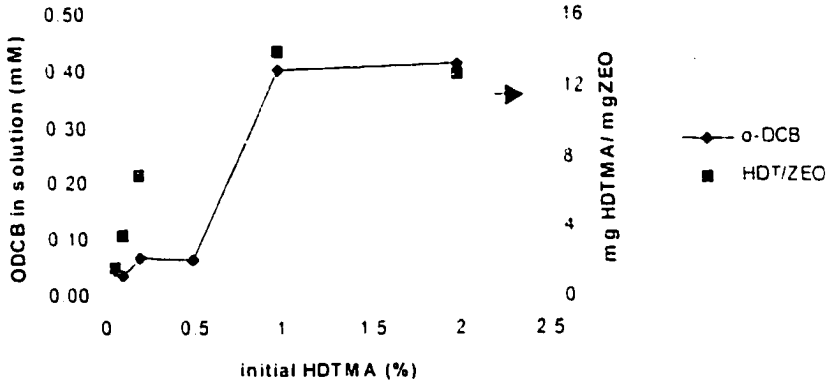
K_{oc}: organic carbon normalized sorption coefficient measured after 48 hours of contact between chemical solution and sorbent.

Chemical	CRA	HC	HZ	DA	LA	AA	SA
Benzene	50	N/A	N/A	N/A	N/A	N/A	N/A
Toluene	110	155	N/A	N/A	N/A	240	N/A
Ethyl-benzene	295	225	158	490	110	390	220
Di-chloro-benzene	820	675	1270	980	580	790	430
Naphthalene	580	7725	24000	N/A	N/A	2100	230

CRA: Canadian River Alluvium; HC: HDTMA modified Canadian River Alluvit HZ: HDTMA modified zeolite; DA: DOWFAX 8390 modified Alumina; LA: LUBRIZOL modified Alumina; AA: AOT modified Alumina; SA: STEOL CS 3. modified Alumina; N/A: not analyzed.

Surfactant modified sorbents





Di-chloro-benzene (log K_{ow} = 3.4)		
Media	Log K_{adm}	Log K_{oc}
HDTMA	4.4 (= log K_{mic})	-
CRA	-	2.9
HDTMA modified CRA	4.8	2.2
HDTMA modified Zeolite	4.7	2.0

CRA: Canadian River Alluvium; K_{ow}: octanol water partition coefficient; K_{adm}: admicelle partition coefficient; K_{mic}: micelle partition coefficient; K_{oc}: sorption partition coefficient; All measured after 48 hours of contact between chemical solution and sorbent.